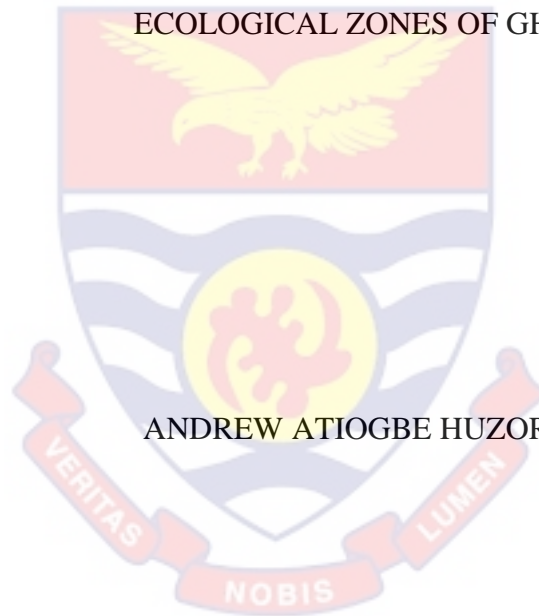


UNIVERSITY OF CAPE COAST

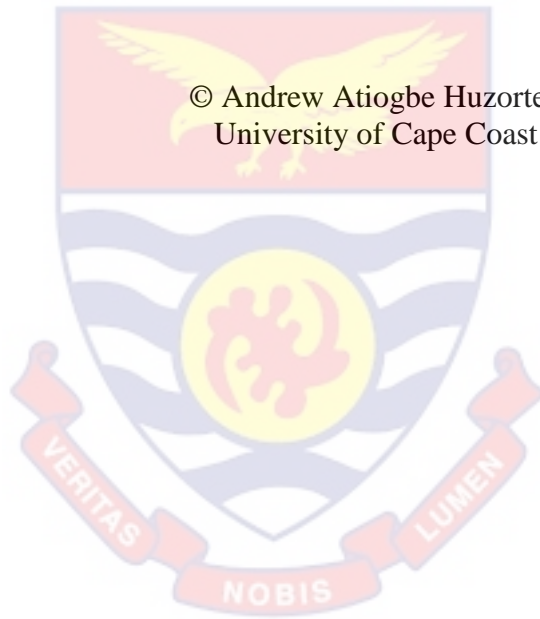
OPTICAL SPECTROSCOPIC ANALYSIS OF HONEY FROM AGRO-
ECOLOGICAL ZONES OF GHANA



ANDREW ATIIOGBE HUZORTEY

2024

© Andrew Atiogbe Huzortey
University of Cape Coast



UNIVERSITY OF CAPE COAST

OPTICAL SPECTROSCOPIC ANALYSIS OF HONEY FROM AGRO-
ECOLOGICAL ZONES OF GHANA

BY

ANDREW ATIOTGBE HUZORTEY

Thesis submitted to the Department of Physics of the School of Physical
Sciences, College of Agriculture and Natural Sciences, University of Cape
Coast, in partial fulfilment of the requirements for the award of Doctor of
Philosophy Degree in Physics

NOVEMBER 2024

DECLARATION

Candidate's Declaration

I hereby declare that this thesis is the result of my own original research and that no part of it has been presented for another degree in this university or elsewhere.

Candidates' Signature Date

Name: Andrew Atiogbe Huzortey

Supervisors' Declaration

We hereby declare that the preparation and presentation of the thesis were supervised in accordance with the guidelines on supervision of thesis laid down by the University of Cape Coast.

Principal Supervisor's Signature: Date:

Name: Prof. Benjamin Anderson

Co-Supervisor's Signature: Date:

Name: Dr Alfred Owusu

ABSTRACT

This study investigated the optical spectroscopic properties of honey produced in Ghana's agro-ecological zones using Raman, Laser-Induced Fluorescence (LIF), and UV-Vis Transmission spectroscopic techniques. Various Multivariate Data Analysis (MDA) methods were applied to the spectroscopic data. UV-Vis Transmission and LIF spectroscopy identified phytochemical compounds, while Raman spectroscopy identified the sugar composition in the honey. The optical measurements revealed that honey types originating from the different agro-ecological zones did not necessarily possess the same spectral properties. The multivariate analysis revealed distinct groupings among the honey samples, where each group shared common constituents and exhibited unique qualities. These groupings were not determined by the agro-ecological zones, but rather by the spectral similarity relating to the specific properties and composition of the honey samples. Further, correlations were established between the LIF spectral parameters and physicochemical properties, including colour and 5-hydroxymethylfurfural (HMF) content, allowing for the prediction of honey freshness with high accuracy. The research also found specific excitation sources and sample pretreatment that effectively controlled fluorescence interference in the Raman spectral measurement of honey. Overall, the various analysis employed in this study has contributed to a better understanding of the optical spectroscopic properties of honey from the agro-ecological zones and their help for determining its phytochemical constituents and sugar composition. The study also offers potential applications for authentication, freshness prediction, and quality control that can be implemented for the honey industry in Ghana.

KEY WORDS

Agro-ecological zones

Honey

Laser Induced Fluorescence Spectroscopy

Multivariate Data Analysis

Raman Spectroscopy

UV-Vis Transmission spectroscopy

ACKNOWLEDGEMENTS

I am grateful to my supervisors, Prof. Benjamin Anderson, Dr Alfred Owusu and their families. I also appreciate the International Science Programme (ISP), Uppsala University, Sweden, for supporting me financially through the African Spectral and Imaging Network (AFSIN). I am grateful to The World Academy of Sciences (TWAS) of the International Centre for Theoretical Physics (ICTP), Italy, for sponsoring my Research and Advance Training in Raman spectroscopy at Shahid Behesti University, Iran. I am also thankful to DRIC-UCC for the research grant which birthed this honey project. I thank all the Department of Physics and Conservation Biology and Entomology faculty and staff as well as professors, fellow students and members of AFSIN and the Laser and Fibre Optics Centre (LAFOC), UCC.

I wish to thank Prof. P. D. Sahare, Dr Amitanshu Pattanaik, Dr Martina Saran, Dr Sudhisht Srivistava, Dr Surender Kumar, Dr Anju Bala and Dr Vishnu Chauhan of the University of Delhi. Not forgetting Prof. Tavassoli, Mr Sayeed Abdee, Dr and Mrs Khadem, Dr Ali Safi, Dr Zeinab Ebrahimpour, Mr Abbas Aeffi, Ms Maryam Ardekani, Ms Parisa Noorbakhsh, Mr Ali Mohamed, Mrs Mardiyah Honiyeh, of Teksan company. Also, I wish to express my profound gratitude to Prof. Y. A. Ankomah, Dr Marian Baah, Dr Shemira Yunus, Mr Philip Odonkor, Mr Rabbi Boateng, Ms Esi Nyarko, Ms Georgina Fianoo, Dr Anita Antwiwaa, Ms Hannah Mokani, Mrs Mary Larweh, Ms Sarah Frempong, Ms Sarah Segbenu, Mr Isaac Asante, Ms Ruth Kwofie, Mr Stephen Akuoko, Ms Felicia Sagoe, Mr Samuel Anlimah, Ms Abigail Nyarko, Ms Selina Mensah, Mr and Mrs Dzah, Mr Laud Koomson, Dr Raphael Owusu, SMOBA colleagues and countless others who have all helped me in diverse ways to come this far.

DEDICATION

To the Huzortey family

TABLE OF CONTENTS

	Page
DECLARATION	ii
ABSTRACT	iii
KEY WORDS	iv
ACKNOWLEDGEMENTS	v
DEDICATION	vi
LIST OF TABLES	xii
LIST OF FIGURES	xiv
LIST OF ABBREVIATIONS	xxiv
CHAPTER ONE: INTRODUCTION	
Background to the Study	1
Statement of the Problem	5
Purpose of the Study	7
Research Objectives	7
Significance of the Study	8
Delimitation	8
Limitations	9
Organisation of Study	9
CHAPTER TWO: LITERATURE REVIEW	
Introduction	10
Honey	10

Composition and Importance of Bee Honey	11
Assessment of Honey	12
Honey Production and Assessment in Ghana	14
Optical Spectroscopy	16
Optical Radiation Interaction with Matter	18
Optical Spectroscopy Analysis of Honey	23
Optical Transmission Spectroscopy	24
Fluorescence Spectroscopy	26
Raman Spectroscopy	29
Other Spectroscopic Methods for the Study of Honey	38
Optical Spectra Data Analysis	39
Spectral Preprocessing	39
SNV Normalisation	39
Spectral Deconvolution	40
Univariate Spectral Data Analysis	40
Multivariate Data Analysis	40
Principal Component Analysis	41
K-Means Clustering Analysis	42
Chapter Summary	44
CHAPTER THREE: METHODOLOGY	
Introduction	45

Honey Samples	45
Other Samples	48
Sample Preparation Procedure for Raman Spectroscopy Measurements	49
Instrumentation, Setups and Spectral Measurements	50
Raman Spectral Measurements	50
UV-Vis Transmission Measurements	52
Laser-Induced Fluorescence Measurements	53
Other Measurements and Related Experimental Instruments Used	55
Brix and Moisture Content Measurements	55
Colour Measurement	56
HMF Content Measurements with HPLC	56
Data Analysis	57
Spectral Preprocessing	58
Spectral Normalisation	58
Spectral Deconvolution	58
Spectral Baseline Correction	58
Multivariate Methods	61
Principal Component Analysis	62
K-means Clustering Analysis	62
Additional Statistical Analysis	63
Chapter Summary	63

CHAPTER FOUR: RESULTS AND DISCUSSION

Introduction	65
Laser-Induced Fluorescence Spectra	65
Principal Component Analysis of the 445 nm Fluorescence Spectra	67
Deconvoluted Laser Induced Fluorescence Spectra	71
Correlation of Deconvoluted LIF Spectra with Brix, Moisture and Colour of Honey	74
LIF Monitoring of Honey Quality via 5-Hydroxymethylfufural (HMF)	75
LIF Spectra of Harvested Honey under Different Conditions (Heating, Ageing, Water and Sugar Adulteration)	78
Sugar Adulteration	82
532 nm and 785 nm Excited Raman Spectra	84
532 nm Excited Raman Spectra of Different Pretreatments applied to Honey Samples	85
Comparison of the Preprocessed 532 nm and 785 nm Excited Raman Spectra of Honey and Molecular Assignment	88
532 nm Excited Raman Spectra Compared for Honey Samples on Different Types of Substrate	92
785 nm Excited Raman Spectra Compared for Honey on a Glass Slide and Honey in Vial	93
Principal Components and K-means Clusters of the 785 nm Excited Raman Spectra	94
UV-Vis Transmission Spectra	98

Principal Components and K-means Clusters of the Transmission Spectra	99
Chapter Summary	104
CHAPTER FIVE: SUMMARY, CONCLUSIONS, AND RECOMMENDATIONS	
Overview	106
Summary	106
Conclusions	109
Recommendations	111
REFERENCES	113
APPENDICES	138
APPENDIX A: CHROMATOGRAM OF HMF STANDARD AND CALIBRATION REPORTS	138
APPENDIX B: HMF CHROMATOGRAM OF ALL SAMPLES	140

LIST OF TABLES

	Page
1 Timescale for Various Energy Transitions in the Optical Domain	22
2 Molecular Constituents of Honey and their Absorption Range in the Optical Region of the EM Spectrum	25
3 Fluorophores in Honey with their Absorption and Corresponding Emission Wavelength in the Optical Region of the EM Spectrum	28
4 Raman Spectra Bands of Kinds of Honey Obtained using 532 nm Laser Compared with 785 nm Laser and that in Literature (A= (Goodacre et al., 2002), B= (Anjos et al., 2018), C= (Pierna et al., 2011) and D= (S. Li et al., 2012))	32
5 Names and Locations of Honey Samples Collected from Apiaries in some Parts of the Central Region and Accra	47
6 The Honeys Samples Collected from the Different Agro-Ecological Zones of Ghana, Indicating their Host Plant, Obtained from the Department of Conservation Biology and Entomology, UCC	48
7 PCA Loading Ranges and Peak Centres	69
8 Spectral Parameters from the Five Bands of the Deconvoluted LIF Spectra of the Samples	73
9 The P-values Obtained by Correlating Deconvoluted LIF Spectral Parameters with Measured HMF of Samples	76

- 10 Raman Spectra Bands of Honey Obtained using a 532 nm Laser Compared with a 785 nm Laser, and that in Literature (A (Goodacre et al., 2002), B (Anjos et al., 2018), C (Pierna et al., 2011) and D (S. Li et al., 2012)) 91
- 11 Honey Classification Based on Transmission Spectra Showing the Potential Absorption Species in the Four Clusters: Each Cluster is Composed of the Honey Samples Established by their Sample Code 102

LIST OF FIGURES

	Page	
1	Global Trends in the Biophotonics Market Growth Rate as an Example for Light-Based Technologies (Mordor Intelligence, 2022)	14
2	EM Spectrum of Different Types of Radiations and their Respective Energies (Frequency, Wavelength) Ranges (Vitha, 2018)	16
3	Types of EM Radiations and Corresponding Effects on Atoms and Molecules (Banwell & McCash, 2017)	17
4	Various Phenomena Occurring during the Interaction of Optical Radiation with a Sample (Narang & Pubby, 2017)	18
5	Jablonski Diagram Describing the Energy Transition Process Leading to Scattering and Emission Based on Different Types of Optical Radiation Involved (Efremenko & Kokhanovsky, 2021)	19
6	Energy Transition Process for Fluorescence and Raman Scattering Phenomenon (Masilamani et al., 2017)	21
7	The Major Optical Spectroscopy Methods used for Honey Analysis According to Cozzolino et al. (2011)	24

8	Jablonski Diagram Representing Quantum Energy Transitions for Rayleigh and Raman Scattering (Ding et al., 2022)	31
9	The Map of the Study Area shows the Agro-Ecological Zones of Ghana, where the Honey Samples were obtained. Samples are Coded, as shown in Parenthesis for each Agro-Ecological Zone, for Identification (FAO, 2005)	46
10	Harvested Honey Samples (A) in the Honeycomb, (B) being Drained and (C) Bottled for the Study	46
11	Honey Samples from Different Agro-Ecological Zone Collected into Eppendorf Tubes provided by the Conservation Biology and Entomology Department of the University of Cape Coast	47
12	Sample Preparation Procedure of Honey with Charcoal to avoid Fluorescence Contamination for Raman Spectral Analysis when using 532 nm Laser Excitation	50
13	Benchtop Raman Microscope used for the Raman Spectra Measurement of Honey Samples in this Study	51
14	Experimental Set-up for Optical Transmission Measurement of Honey Samples	52
15	Experimental Set-up for Laser Induced Fluorescence Measurement of Honey Samples	53

- 16 The Digital Refractometer used in Measuring the Brix and Moisture Levels in the Honey Samples 56
- 17 Raman Signal Recovery Processes using SDT-RIA, (A) is the Simulated Raman Spectra and its Second Derivative, (B) Shows the Most Intense Peak Fitted in the Second Derivative Spectrum, (C) Shows how SDT-RIA Estimates the Background, and (D) Shows how Accurately the Recovered Signal Compares with the Original Spectrum having no Baseline. 59
- 18 Baseline Correction for 532 nm Excited Raman Spectra of Charcoal Treated Honey. (A) Experimentally Measured Raman Spectra of the Honey Contaminated by Fluorescence Baseline. (B) Second Derivative and Fitting of the of the Contaminated Spectra to obtain Peak Parameters for Baseline Correction. (C) Estimated Baseline for the Contaminated Spectra Based on Parameters of the Fitting. (D) Recovered Spectra after the Baseline is Subtracted from the Experimentally Measured Spectra. 60
- 19 Baseline Correction for 785 nm Excited Raman Spectra of Charcoal Treated Honey. (A) Experimentally Measured Raman Spectra of the Honey Contaminated by Fluorescence Baseline. (B) Second Derivative and Fitting of the Contaminated Spectra to Obtain Peak Parameters for Baseline Correction. (C) Estimated Baseline for the 61

- Contaminated Spectra Based on Parameters of the Fitting.
(D) Recovered Spectra after the Baseline is Subtracted from the Experimentally Measured Spectra.
- 20 SNV Normalised and Averaged Fluorescence Spectra of Honey Samples Collected from the Various Agro-Ecological Zones of Ghana (Sudan Savana (SS), Guinea Savana (GS), Transition, Zone (TS), Semi-Deciduous Forest (SD), Moist Evergreen (ME) and Coastal Savana (CS)) Used in the Study. The Number of Honey Samples from Each Agro-Ecological Zone Is Stated in the Legend. 66
- 21 Principal Component Analysis of Fluorescence Spectra of Honey Samples Showing the Variance Plot (A), Score Plot for PC2 Against PC1 of Samples from Different Agro-Ecological Zones with the Respective Number of Samples from Each Agro-Ecological Zone Described in the Legend (B), and the Loadings Plot for PC1-PC3 (C-E) 68
- 22 PCA Biplot Showing PC1 and PC2 Score Distribution with Loading Coefficients of Identified Fluorophores in Honey 70
- 23 Deconvoluted SNV Normalised LIF Spectra of One of the Honey Samples Showing Peaks of Possible Emissions from Fluorophores, with An Inset Demarcating the Peak Parameters (A = Intensity, B = Full Width at Half Maximum, C =Centre Wavelength) 72

- 24 Correlation Coefficient (R²) and Significance (P-Value) for the Correlation Between Physicochemical Parameters; Brix, Moisture, Color, and Deconvoluted LIF Spectral Parameters shown by a Colour Map. P1, P2, P3, P4, and P5 Represent Each Deconvoluted Peak, While the Alphabets a, b, c and d Represent each Peak's Intensity, Wavelength, Width and Area, Respectively. 74
- 25 Normalised LIF Spectra of Honey Samples Selected from Different Years to Study their HMF. Each Spectrum Is Colour Mapped in Order of the HMF Value, as Indicated in the Legend 75
- 26 Correlation between (A) Deconvoluted LIF Peak 1a Intensity with HPLC Measured HMF for Samples with HMF Concentration below 40 mg/ kg and (B) HPLC Measured HMF with Predicted HMF by the Peak 1a 77
- 27 LIF Spectra of Two Freshly Harvested Honey Samples used for Ageing Studies 78
- 28 LIF Spectra of Honey Samples Measured at Different Times from the Harvesting Period to 3 Years 79
- 29 LIF Spectra of Honey Heated in Different Methods 80
- 30 LIF Spectra of Fresh Honey, Water-Diluted Honey Samples and Distilled Water for Comparison 81

31	Spectra of Selected Honey Samples (H1 and H4) Compared with Sugar Caramel as a Suspected Adulterant	82
32	LIF Spectra of Two Harvested Honey Samples (H1 and H4) Adulterated with 10, 20, 30 and 50% Sugar Caramel	83
33	The Plot of Peak Intensities against the Honey Level of Adulteration Showing the Rate of Change in Spectra of Honey Adulterated with Sugar Caramel.	84
34	Raman Spectra of Raw Honey Samples Acquired using Different Laser Excitation Sources of Wavelengths (A) 532 nm and (B) 785 nm.	85
35	532 Excited Raman Spectra obtained from (A) Raw, (B) Water Dilution, (C) Heated and (D) Activated Charcoal-Treated Honey with Computed Signal-to-Fluorescence Ratio (SFR) Values shown in the Legend	86
36	Comparison of Baseline Preprocessed 532 nm Excited Raman Spectra of Raw and Pretreated Honey Samples	87
37	Raman Spectra of Honey Samples Measured Under Different Conditions: (A) Honey Subjected to Activated Charcoal Pretreatment, measured with a 532 nm Laser Excitation, and (B) Honey Without Pretreatment, Measured with a 785 nm Laser Excitation.	88

- 38 Comparison of Raman Spectra of Honey on Glass, Silicone, and Back-Coated Mirror Surface Substrate 92
- 39 Raman Spectra of the Honey Sample Measured on a Glass Slide Compared with a Plastic Vial 93
- 40 The 785 nm Excited Normalised Raman Spectra of All the Honey Samples from the Different Agro-Ecological Zones of Ghana. (Sudan Savana (SS), Guinea Savana (GS), Transition, Zone (TS), Semi-Deciduous Forest (SD), Moist Evergreen (ME) and Coastal Savana (CS)) Used in the Study. The Number of Honey Samples from Each Agro-Ecological Zone Is Stated in the Legend. 94
- 41 PCA- Biplot Showing Scores Distribution of Samples in PC1 and PC2 Axis with Respective Loadings Influencing the Sample Distribution Indicated by the Wavelength and Associated Constituent from Literature 95
- 42 The Evaluated K-means Clustering using (A) The Silhouette and (B) The Davies-Bouldin Method of Scores from the Principal Component Analysis of the Raman Spectra from the Honey Sample to Select the Optimal Number of Classes Existing among the Samples from Different Agro-Ecological Zones 96

- 43 Groups of Honey Identified using K-Means Clustering Analysis on the PC Scores and their Related Raman Spectra for K=2 (a-b) and K=3 (c-d) 97
- 44 SNV Normalised Optical Transmission Spectra of all Honey Samples from the Six Agro-Ecological Zones of Ghana: Sudan Savannah (SS=2), Guinea Savannah (GS=7), Transition Zone (TR=6), Semi-Deciduous Forest (SD=6), Moist Evergreen Forest (ME=2) and Coastal Savannah (CS=2) 98
- 45 The Variance and (B) the Loadings Plots from the Principal Component Analysis of the Normalised Transmission Spectra of the Honey Samples. The Arrow in the Variance Plot Indicates the Selected Number of Components by the Elbow Method 100
- 46 The Evaluated K-Means Clustering using (A) The Silhouette and (B) The Davies-Bouldin Method of Scores from the Principal Component Analysis of the Transmission Spectra from the Honey Sample to select the Optimal Number of Classes existing among the Samples from Different Agro-Ecological Zones 100
- 47 Optical Transmission Signals Depicting the Four Classes of Honey, based on the K-Means Clustering Analysis. Cluster 1: 350 nm, Cluster 2: 430 nm, Cluster 3: 500 nm, 101

	and Cluster 4: 600 nm can be Identified by the Wavelength At which Transmission begins to occur for most of the Samples in each Group	
48	Matrix Plot Comparing Cluster Pattern for Different Principal Component (PC) Score Plot Combinations. the Matrix Plot's Diagonal shows each Cluster's Score Distribution as a Histogram. the Four Groups are Better Separated along the First Principal Component (PC1).	103
49	Chromatogram of HMF Standard	138
50	Calibration Curve obtained for different Concentrations HMF Standard	139
51	Chromatogram of Honey Sample S1 for HMF Determination	140
52	Chromatogram of Honey Sample S2 for HMF Determination	141
53	Chromatogram of Honey Sample S3 for HMF Determination	142
54	Chromatogram of Honey Sample S4 for HMF Determination	143
55	Chromatogram of Honey Sample S5 for HMF Determination	144

56	Chromatogram of Honey Sample S6 for HMF Determination	145
57	Chromatogram of Honey Sample S7 for HMF Determination	146
58	Chromatogram of Honey Sample S8 for HMF Determination	147
59	Chromatogram of Honey Sample S9 for HMF Determination	148
60	Chromatogram of Honey Sample S10 for HMF Determination	149
61	Chromatogram of Honey Sample S11 for HMF Determination	150
62	Chromatogram of Honey Sample S12 for HMF Determination	151
63	Chromatogram of Honey Sample S13 for HMF Determination	152
64	Chromatogram of Honey Sample S14 for HMF Determination	153
65	Chromatogram of Honey Sample S15 for HMF Determination	154

LIST OF ABBREVIATIONS

AEZ	Agro-ecological zones
ANOVA	Analysis of Variance
CSIR	Centre for Scientific and Industrial Research
CV	Coefficient of Variation
EM	Electromagnetic
FDA	Food and Drugs Authority
FTIR	Fourier Transform Infrared
GC	Gas Chromatography
GSA	Ghana Standards Authority
HMF	Hydroxy Methyl Furfural
HPLC	High Performance Liquid Chromatography
IR	Infrared
KCA	K Means Clustering Analysis
LIF	Laser Induced Fluorescence
LIBS	Laser Induced Breakdown Spectroscopy
LOOCV	Leave One Out Cross Validation
MIR	Mid-Infrared
MS	Mass spectroscopy
NIR	Near-Infrared
OTS	Optical Transmission Spectroscopy
OS	Optical Spectroscopy
OST	Optical Spectroscopy Techniques
PCA	Principal Component Analysis
R ²	Correlation Coefficient

RS	Raman Spectroscopy
SDT-RIA	Second Derivative Technique Range Independent Algorithm
SFR	Signal to Fluorescence Ratio
SNV	Standard Normal Variate
UCC	University of Cape Coast
UV	Ultraviolet
VIS	Visible

CHAPTER ONE

INTRODUCTION

There is significant interest in the use of Optical Spectroscopy (OS) techniques for biological sample analysis due to the non-destructive nature, high analytical efficiency, relatively low cost, and potential to be translated into portable devices. A biological sample like honey is a popular natural food produced by bees, which varies in composition based on factors such as botanical source, geographic location, harvesting methods, etc. These factors sometimes affect the type and quality of honey. In Ghana, a region in tropical Africa with rich biodiversity, honey holds a special place in dietary and medicinal practices. The diverse flora of the region imparts distinct characteristics to the honey produced, making it an interesting subject for study. Even though, previous research has explored various analytical techniques to study honey, the potential of OS, which is based on light-matter interaction, remains relatively unexploited in the context analysing honey from Ghana. This study aims to use OS to analyse honey from various Agro-Ecological Zones (AEZ) in Ghana to reveal the uniqueness and qualities of these honey and potentially enhance the value of this essential natural product in the region.

Background to the Study

There is growing interest in applying light and light-based technologies to solve everyday problems. These technologies are present in large-scale devices such as satellites and simple ones such as phones and watches. Nowadays, almost every field of study employs light-based technology. Hence, whether it is archeological investigation, space exploration, environmental monitoring,

clinical or medical diagnosis, cosmetic therapy or agricultural innovations, light-based technologies remain paramount (Chen & Segev, 2021; Forbes, 2015).

Applying light-based technology to study samples requires employing one or multiple optical techniques. These techniques, including reflection, refraction, scattering, polarisation, and transmission, can determine a sample's constituents, characteristics, and other properties to help draw qualitative and quantitative conclusions about the sample or its environment. The qualitative or quantitative study of these phenomena due to light energy and its interaction with matter is called spectroscopy (Demtröder, 1982; Svanberg, 2004). Spectroscopy, therefore, enables the charting of light energy's interaction with matter. Light energy herein refers to the various forms of Electromagnetic (EM) radiation (i.e., Gamma rays to Radio waves). At the same time, matter generally includes the subjects of investigation, such as solids, liquid/gels, gas or plasma and, in this case, honey. Light-matter interaction using radiations chosen within the optical window of the electromagnetic spectrum, specifically Ultraviolet, Visible and Near-Infrared (UV-Vis-NIR), is termed optical spectroscopy (Balas, 2009; Rossman, 2014; Svanberg, 2004).

Optical spectroscopy is becoming preferable for several reasons. Firstly, light energies in the optical domain are non-ionising compared to their counterparts, such as gamma-rays and x-rays (Balas, 2009). These characteristics make OS techniques a relatively safer option. Secondly, the setup requirement for optical spectroscopy is rapidly evolving to miniature instrumentation deployed as handheld devices (Petersen et al., 2013). Most of these instruments nowadays are relatively low cost, with commonly available

components, some of which are also salvageable from other appliances and devices or even 3D printed (Lu et al., 2020; Manefjord et al., 2022; Owusu et al., 2016; Sigernes et al., 2018). Thirdly, the OS techniques can rapidly provide data as single data points, an array of data points forming a line spectrum or a stack of line arrays forming matrices as seen in images. These various data forms, even as large datasets, can be used in Machine Learning, Deep Learning and Artificial Intelligence (AI) applications (Bishop & Nasrabadi, 2006; Zhou et al., 2019). Fourthly, light-based methods can provide multi-component information from samples just by a single measurement compared to most chemical-based processes, which determine one component at a time (Demtröder, 1982; Svanberg, 2004). In this vein, light-based techniques that apply optical spectroscopy are fast becoming a method of choice also in the agro-food industry, honey in particular (Naila et al., 2018; Noviyanto et al., 2015).

Honey is a well-known valuable food product for health, nutrition, economic and religious purposes (Bogdanov, 2015). Honey's nutritional constituents comprise sugars (70-95%), water (up to 25% or less) and hundreds of other vitamins, phytochemicals and substances (Codex Alimentarius, 2001; Crittenden, 2011). Honey is used in many situations as a natural sweetener in foods, providing vital nutrients to the body (Corvucci et al., 2015; Oddo et al., 1995; Ulloa et al., 2013). It also has other benefits in pharmaceuticals, wound healing therapeutics and cosmetic products (Alvarez-Suarez et al., 2010; Bogdanov et al., 2008; Corvucci et al., 2015; Mahmoodi-Khaledi et al., 2017; Oddo et al., 1995; Ruoff et al., 2005; Tahir et al., 2019).

The efficacy of honey fits for specific purposes depends on the geographic, botanical and entomological origin of the honey (Corvucci et al., 2015; Mahmoodi-Khaledi et al., 2017; Oroian & Ropciuc, 2018; Pierna et al., 2011; Ulloa et al., 2013). Other factors, such as age, storage conditions and harvesting season, also impact the quality of honey and its constituents (Akpabli-Tsigbe, 2015; Bogdanov et al., 1999). Therefore, every honey may appear to have unique properties at any time, which can vary from place to place. Consequently, employing low-cost but rapid techniques to help study honey from any jurisdiction is indispensable. A thorough study of honey can help their valorisation and ensure continuous monitoring to maintain high-quality standards in the industry. Additionally, it could mitigate some of the sophisticated fraudulent schemes culpable of tarnishing the reputation and integrity of the local honey industry.

Light-based techniques, especially optical spectroscopy, have helped evaluate honey constituents, established quality features and detected fraudulent schemes in the honey industry. Recent reports describe some OS techniques currently applied for honey analysis (Naila et al., 2018; Pita-Calvo et al., 2017). Some methods include Fourier Transform Infra-Red (FTIR), Raman, Fluorescence, Diffuse Reflectance, Polarisation, and Absorbance spectroscopy. Admittedly, each spectroscopic technique has the kind of information they provide about a sample and, thus, could have specific applications in honey analysis.

Among the various spectroscopic techniques, FTIR is the most extensively used technique for studying molecular constituents of honey (Cozzolino et al., 2011; Tahir et al., 2017; Vlaeva et al., 2017). Similar to FTIR,

Raman spectroscopy is another standard OS technique used for studies on honey. Raman spectroscopy gives information about honey's sugar composition, which is complementary to FTIR. Fluorescence spectroscopy is another commonly used OST to provide information about the numerous intrinsic fluorophores in honey (Lakowicz, 2006). Absorbance and Transmission spectroscopy gives similar information as fluorescence does, albeit over a broader range of the EM spectrum, by providing spectral signatures or fingerprints unique for every sample representing honey's general biochemical composition.

Recently, elemental analysis using Laser-Induced Breakdown Spectroscopy (LIBS) is also becoming common (Bilge et al., 2016; Peng et al., 2020; Stefas et al., 2020, 2021, 2022). All these OSTs could play an integral role in analysing honey produced in Ghana to help improve the current state of the honey industry.

Statement of the Problem

Ghana ranks 125 in the world in the export of honey, generating an income of about \$1000 while ranking 118 for import at the expense of about \$113,000 more than ten times the amount exported (Workman, 2020). Given Ghana's rich floral diversity, immense benefits could be reaped in by the honey industry if locally-produced honey is well-studied for its unique properties and functions. So far, studies on honey from Ghana have explored botanical and geographical identification using Melissopalynology (Besah-Adanu et al., 2019; Letsyo & Ameka, 2019). Some studies have also used High-Performance Liquid Chromatography (HPLC) and other chemical analysis methods to investigate molecular constituents of honey for quality assessment (Bentum et

al., 2022; Letsyo et al., 2017). Other studies have also reported measurement of various physicochemical parameters such as diastase, pH, acidity, and colour (Adadi & Obeng, 2017; Adjaloo et al., 2017; Akpabli-Tsigbe, 2015; Ankrah, 1998; Bentum et al., 2022; Combey et al., 2021; Klutse et al., 2021; Letsyo et al., 2017; Letsyo & Ameka, 2019; Yeboah-Gyan & Marfo, 2015). However, the methods employed in these studies are laborious, time-consuming, relatively expensive, destructive to the sample and sometimes hazardous to the researcher.

Optical spectroscopic techniques have been shown to overcome many of the shortfalls associated with conventional methods (Naila et al., 2018). For instance, infra-red and Raman spectroscopy have been used to obtain information about the reducing sugars in honey (Batsoulis et al., 2005; Šugar & Bouř, 2016). Likewise, fluorescence, absorption, reflectance and transmission spectroscopy have provided nutritional information of honey (Almaleeh et al., 2017; Frausto-Reyes et al., 2017; Parri et al., 2020; Ruoff et al., 2005). Physicochemical parameters of honey for quality analysis, such as pH, HMF, etc., can be related to the spectral bands obtained from these optical techniques (Anjos et al., 2018; Escuredo et al., 2021; Mashhadi et al., 2020; Mehryar et al., 2013; Tahir et al., 2017).

However, not much has been studied on honey's specific qualities from Ghana's AEZ employing OS techniques. Considering the simplicity, safety, rapidity, and cost-effectiveness, among other benefits, using optical spectroscopy to study honey produced in Ghana is needed to help complement existing methods to improve its status on the local and global market.

Purpose of the Study

This study aims to quantitatively and qualitatively explore the OS properties of honey produced in Ghana's AEZ using three OS techniques to better understand the properties of honey for value addition. The optical spectroscopy techniques will help provide knowledge about some underlying biochemical and physicochemical properties of honey. This study is being conducted to obtain baseline OS data of honey produced in Ghana, which will help regulatory bodies and guide future studies. It will offer a way to compare honey from Ghana to those from other parts of the world.

Research Objectives

The aim of the study will be achieved with the following research objectives:

1. To measure the optical spectra of raw honey from agro-ecological zones using Laser Induced Fluorescence (LIF) spectroscopy, Ultra Violet – Visible (UV-Vis) Transmission Spectroscopy and Raman spectroscopy.
2. To use Multivariate Data Analysis techniques; Principal Component Analysis, Cluster analysis, to analyse the measured optical spectra of the honey samples.
3. To measure some physicochemical properties and conditions of the honey samples and compare with their spectral properties as an alternate technique for quality analysis. The conditions include ageing, water dilution, heating, and sugar caramel adulteration. The physicochemical parameters include colour, moisture Brix, and 5-Hydroxymethylfurfural (HMF).

4. To measure the effectiveness of the excitation source, sample preparation method, substrate type and sample container in Raman spectral measurement of honey samples.

Significance of the Study

Studies on the specific qualities of honey from Ghana have not employed optical spectroscopic techniques. This research would show how the various optical spectroscopic techniques could help project the properties of local honey from Ghana for their valorisation. It would offer rapid, non-destructive and cost-effective alternatives for proper labelling and promotion of appropriate usage of honey. Regulatory bodies and research institutes such as Food and Drugs Authority (FDA), the Centre for Scientific and Industrial Research (CSIR) and the Ghana Standards Authority (GSA) would find the spectroscopic techniques helpful in monitoring honey quality and curbing fraudulent activities on honey in the markets. Additionally, for the first time, the study highlights the optical properties of honey from AEZ of Ghana, potentially providing baseline data on local honey for future studies.

Delimitation

The study focused mainly on three spectroscopic techniques; UV-Vis Transmission spectroscopy, Laser-Induced Fluorescence spectroscopy and Raman spectroscopy out of the numerous spectroscopic techniques. Also, of the several applications of each of the optical spectroscopic techniques to honey, this study focused on using these techniques to determine the molecular constituents of honey produced in Ghana and relating them to selected

physicochemical parameters (Brix, HMF, Moisture, Colour) and conditions (Ageing, Water dilution, heating, and Sugar Caramel Adulteration).

Limitations

The study was limited to available optical spectroscopic instruments. Also, the study was capable of performing only a few physicochemical measurements due to the low volume of honey obtained from the various apiaries.

Organisation of Study

This study is structured into five chapters. Chapter one gives an overview of the use of light-based technologies in the study of honey and the need to employ the same for the study of honey produced in Ghana with the stated objectives. Chapter two is the review of related literature on optical spectroscopy techniques and the sampled honey. The basis of the various spectroscopic phenomena and methods employed for analysis is also reviewed in chapter two. Chapter three details the experimental methods employed in studying the honey sampled and the data analysis techniques used. In chapter four, the results obtained from all the measurements are reported and discussed by linking them to the literature. Finally, chapter five summarises critical findings, the conclusions and recommendations for future work.

CHAPTER TWO

LITERATURE REVIEW

Introduction

This chapter describes in detail the major themes of the study, which are honey, optical spectroscopy and multivariate data analysis. Previous studies on using various optical spectroscopy techniques in the study of honey are discussed to highlight the gaps that this study attempts to resolve.

Honey

Honey is a very well-known high value sweet natural food produced by honey bees. The internationally accepted definition for honey is provided by Codex Alimentations (2001), which states that "honey is a natural sweet substance produced by honey bees (*Apis mellifera* and *Melliponini*), from the nectars of plant flowers and honeydew" (Codex Alimentarius, 2001). Generally, honey bees are known to produce honey from the nectar and secretions of plants (blossom or floral honey) or from excretions of some insects (honeydew honey). These nectars and secretions are transformed in the guts of the bees and then stored in honeycombs in the hives to ripen for their consumption at a later time.

The floral honey are very common (El Sohaimy et al., 2015). Blended or compound Honey is obtained from a mixture of blossom/floral and honeydew. Floral Honey is further classified into monofloral (or unifloral) honey and multifloral (or polyfloral) honey. Monofloral or unifloral honey has pollen from majorly one type of plant vegetation (usually > 45 %). Some examples are Sunflower, Manuka, Astragalus, etc. Multifloral or polyfloral honey has mixture of different proportions of pollen from several different

plants. Unifloral honey are rare in tropical areas because of the large number of floral sources bees are capable of visiting for a small geographical area during the flowering period of plants. Therefore, precisely identifying the discrimination points between multifloral and unifloral honey can take time and effort. However, microscopy analysis can be used to determine the pollen content of honey and the proportions of their blends to assist with indicating their botanical origin (Agashe & Caulton, 2019). Also, specific physicochemical properties and molecular analysis can be used to confirm the results of the microscopy analysis (Letsyo & Ameka, 2019; Ruoff et al., 2005).

Composition and Importance of Bee Honey

Bee honey compositions depend primarily on its floral/botanical origin (Soria et al., 2004). These honey constituents are predominantly informed by the plant's sources from which bees forage. The major component of honey, which is sugar (70 to 85%) and water (15 to 25%), is obtained from the nectars fed on by the bees (Alvarez-Suarez et al., 2010). Honey is, therefore, made of mainly carbohydrates. It contains more than 22 different types of both complex and simple sugars such as sucrose, fructose, and glucose are more abundant. Moisture (or water) is the second-highest content in honey. Moisture regulates spoilage and protects against granulation. Honey can be preserved longer when moisture content is low thus limiting microbiological activity (Bogdanov, 2009).

In addition to water and sugar, honey contains several other food substances in minor quantities (Bogdanov, 2015; Tahir et al., 2019). These food substances include protein, organic acids, amino acids, vitamins, minerals, ash,

enzymes, and phenolic compounds (Bogdanov et al., 2008; Parri et al., 2020; Pyrzynska & Biesaga, 2009). These food substances are predominant in the nectars of flowering plants. Hence, because the process bees employ in making honey is natural, the integrity of these food substances is maintained and made available in an almost unaltered state to function to the fullest when eaten. These plant-based food substances are vital roles for good health. Therefore, honey can exhibit many properties; antitumor, antioxidant, and anti-inflammatory. Other properties include antimicrobial, parasitocidal, anticoagulant, antidiabetic, and lipid-lowering properties (Carter et al., 2016; Hegazi et al., 2021; Leyva-Jimenez et al., 2019; Mahmoodi-Khaledi et al., 2017). The proportions of sugar, water, and other food substances are affected by the floral type and geographical location (El Sohaimy et al., 2015). The presence and levels of various phenolic compounds serve as indicators of the type and quality of honey, as phenolic acids and flavonoids are natural chemical markers associated with specific floral origins (Pyrzynska & Biesaga, 2009).

Assessment of Honey

Honey is assessed to determine its authenticity, quality, and functional properties. The entomological, botanical, and geographical origins are usually interesting for honey authentication. Melissopalynology is commonly for determining the geographical and botanical origin of Honey (Corvucci et al., 2015; Oddo et al., 1995; Ponnuchamy et al., 2014). For quality assessment, physicochemical parameters are judged against standards set by the international honey commission and other regions and governmental regulatory bodies (Bogdanov, 2009). Physicochemical parameters usually measured in honey are moisture, electrical conductivity, ash content, free acidity,

hydroxymethyl furfural, diastase activity, apparent reducing sugars, sugars (glucose, sucrose, fructose, etc.), insoluble matter, invertase activity, proline and specific rotation (Mahmoodi-Khaledi et al., 2017; Oddo et al., 1995; El Sohaimy et al., 2015). For functional properties, honey is tested for its biological activities, such as antibacterial, antioxidant, antitumor, anti-inflammatory, and antiviral capabilities (Bogdanov, 2015; Leyva-Jimenez et al., 2019).

The molecular and elemental composition of honey also can be studied to help with its authentication, quality and functional assessment. Different types of analytical techniques such as isotopic, Atomic Absorption Spectroscopy (AAS), Neutron Activation Analysis (NAA), Inductively Coupled Plasma Atomic/Optical Emission Mass Spectroscopy (ICP-AES, ICP-OES, ICPMS), etc., are some of the conventional methods used for the elemental analysis of honey. While chromatographic and several other chemical-based methods are utilised for the molecular assessment of Honey (Aghamirlou et al., 2015; Arida et al., 2012). High-Performance Liquid Chromatography (HPLC) and Gas Chromatography/Mass Spectrometry (GC/MS) are the most widely used methods to assess the molecular composition of honey, which can also be used to assist authentication and quality analysis (Arida et al., 2012). The HPLC and GC/MS techniques are exact methodologies; they are the gold standard in determining honey's molecular composition. Unfortunately, HPLC and GC/MS techniques are generally time-consuming, complex, and labour-intensive or require specialised personnel to interpret the results. In addition, the HPLC, as mentioned earlier, and GC/MS analytical techniques require a lot of sample pre-treatment. However, demand for honey has surged globally, making honey a big business in the agro-food

industry (García, 2018; Wu et al., 2015). This situation leads to challenges for the honey industry to deliver good quality honey products. Hence, scientists and regulatory bodies continue their quest for novel, simplified, highly responsive, and cost-effective techniques to analyse the molecular composition of honey. According to Naila et al. (2018), there is a heightened interest in Light-based methods for the molecular analysis of Honey (Naila et al., 2018). Light-based methods are very safe and common. Nonetheless, most developing countries have yet to use optical spectroscopy for its practical applications (Figure 1).

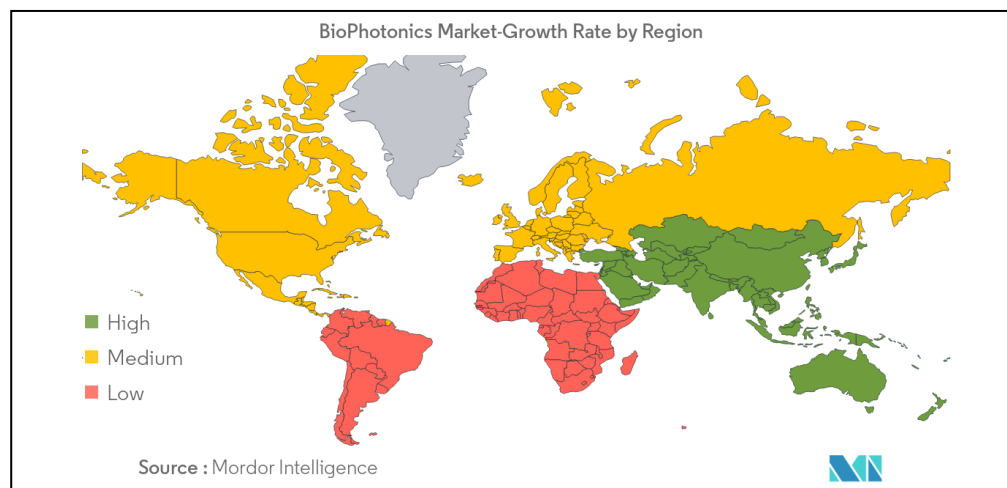


Figure 1: Global trends in the biophotonics market growth rate as an example for light-based technologies (Mordor Intelligence, 2022)

Honey Production and Assessment in Ghana

Honey is mainly obtained in Ghana in two ways: Apiary honey and Forest honey (Akpabli-Tsigbe, 2015; Klutse et al., 2021). The bees freely forage on multiple plant sources to make honey in both methods. At specific times in the year, honey is thought to be ripe/ mature before harvesting, usually during the peak of the dry season, just before the arrival of the dry harmattan wind. Typically, in the latter part of October and may continue until June before the onset of the wet season (TECA, 2022). However, some areas with plants such

as coconut that flower all year round can have honey throughout the year. The significant types of bee species from which honey is obtained in Ghana sting at the slightest provocation; hence, harvesting is usually conducted at night. At night time, the bees are known to be less active. Also, the bee smoker is used intensively during harvesting to dispel the bees from the hive, enable easy access to their combs, and daze them to forestall any attack. The post-harvest process involves honey extraction from honeycombs, straining the honeycombs to remove debris and packaging. The main extraction methods are hand-squeezing, solar, and cold extraction methods. From one honey producer to another, the variations in the foraging behaviour, harvesting season, harvesting procedure, and post-harvest activities such as extraction, straining, and packaging may complicate honey authentication and influence the variation in the molecular composition of the honey, thus requiring regular assessment. However, the evaluation of Honey from Ghana still relies on conventional methods. (Adadi & Obeng, 2017; Akpabli-Tsigbe, 2015; Ankrah, 1998; Bentum et al., 2022; Klutse et al., 2021; Letsyo et al., 2017; Letsyo & Ameka, 2019; Yeboah-Gyan & Marfo, 2015). While all of these studies have been towards assessing honey for its molecular composition authenticity, quality, or quality characteristics, studies have yet to focus on the optical spectroscopy analysis of Honey from Ghana. However, the advantages of optical spectroscopy techniques show they could play an integral role in studying honey, especially for developing countries in the tropics, like Ghana, whose ecological makeup is very viable for honey production.

Optical Spectroscopy

Optical spectroscopy deals with radiations in the optical region of the EM spectrum interaction with matter. The EM spectrum comprises EM radiations of different energies according to Equation (1).

$$\text{Energy, } E = hf = \frac{hc}{\lambda} \quad (1)$$

Where h is Planck's constant (6.63×10^{-34} Js), f is frequency, λ is the wavelength, and c is the speed of light (3.0×10^8 ms⁻¹). The EM radiations are arranged in order of the magnitude of their energy to form the EM spectrum (Figure 2). The optical region of the EM spectrum occupies energy ranges between 100 nm to 0.33 mm (Rossman, 2014).

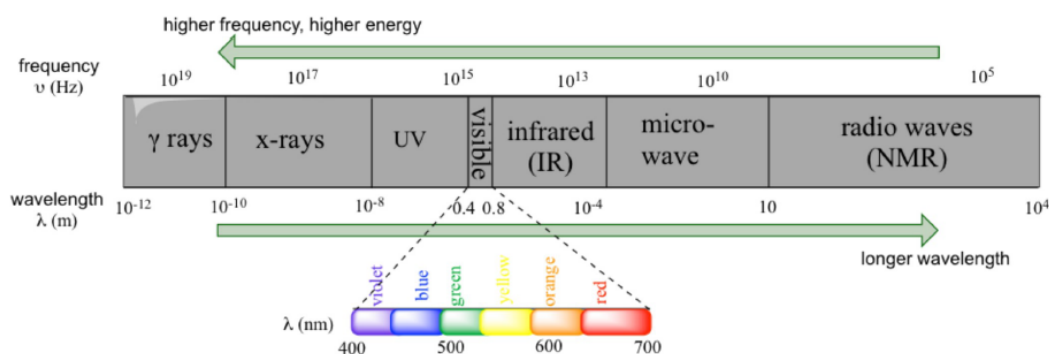


Figure 2: EM (EM) spectrum of different types of radiations and their respective energy (Frequency, Wavelength) ranges (Vitha, 2018)

The optical radiations include Ultraviolet (UV), Visible, and Infra-Red (IR) radiations. Radiation within the UV region is subdivided into UVA, UVB, and UVC, in the ranges 315 – 400 nm, 280 -315 nm, and 100 -280 nm, respectively. The visible range also is between 400 – 700 nm (Violet, Indigo, Blue, Green, Yellow, Orange, and Red). Infra-Red (IR) Radiations range from 2.5 – 15.38 μ m (4000 to 650 cm⁻¹). It can be divided into Near Infra-Red (NIR:

0.8-2.5 μm), Mid Infra-Red (MIR: 125000 to 4000 cm^{-1}), and Far Infra-Red (FIR: 2 cm to 1 mm). The FIR region, which falls between the Mid IR and microwaves, has radiation referred to as millimetre wave (MMW: 2 cm to 1 mm) radiation, and from 1 to 0.33 mm is called submillimeter (sub-MMW or sub-mm: 1 to 0.33 mm) radiation. Radiation with shorter wavelengths, therefore higher energy, is called terahertz (THz) radiation because the frequency of these waves is on the order of 10^{12} Hz (extending from 30 THz down to about 200 GHz) (Butcher et al., 2016; Svanberg, 2004; Vitha, 2018)

Optical radiation interaction with matter cause changes in electron distribution or increases the amplitude of bond vibrations in a sample (Figure 3). The changes in the electron distribution and bond vibrations help obtain molecular information about a sample (Svanberg, 2004).

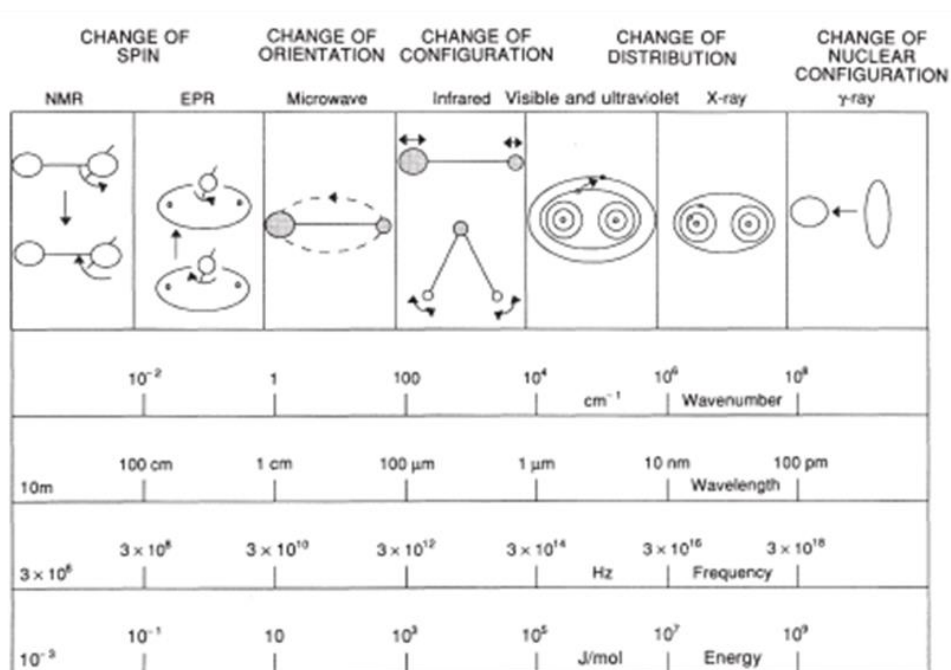


Figure 3: Types of EM radiations and corresponding effects on atoms and molecules (Banwell & McCash, 2017)

Optical Radiation Interaction with Matter

When optical radiation interacts with a sample, the radiation is either absorbed, reflected, transmitted, or scattered depending on the specific attributes of the sample type. (Figure 4). Therefore, optical spectroscopy could be used for qualitative (what is in the sample) and quantitative (how much of it is present) assessments of samples.

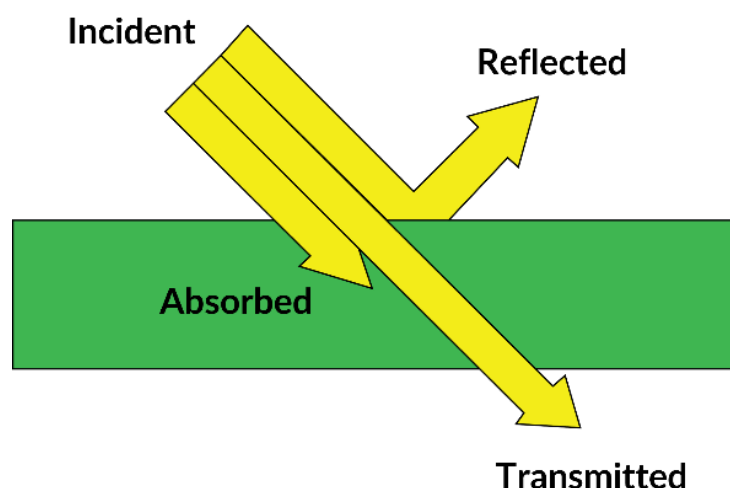


Figure 4: Various phenomena occurring during the interaction of optical radiation with a sample (Narang & Pubby, 2017)

The general conservation of energy requires that the energy of the incident radiation (I) will be equal to the sum of part of the radiation that is reflected (R), Transmitted (T), and absorbed (A), as shown in Equation (2).

$$I = R + T + A \quad (2)$$

Measuring the optical radiation interactions on a sample determines the various optical spectroscopic techniques, such as absorbance, reflectance, Transmission, etc. The absorption further leads to emission and scattering phenomena explained by the fact that atoms and molecules exist in different

states with different quantised energy in any sample. However, as demonstrated by Boltzmann distribution, most molecules and atoms exist in the lowest electronic and vibrational states. The energy of the molecules is a combination of the electronic, rotation, and vibration energy (Equation 3) (Vitha, 2018).

$$E_{molecule} = E_{vibration} + E_{rotation} + E_{electronic} \quad (3)$$

Therefore, when optical radiation with energy (E) is incident on a sample, the energy is absorbed provided it matches with the energy difference (ΔE) between two quantum states (E_1 and E_2) of the molecules of the sample. The absorbed energy ($E_{molecule}$) leads to vibrational, rotational or electronic transition (Figure 5).

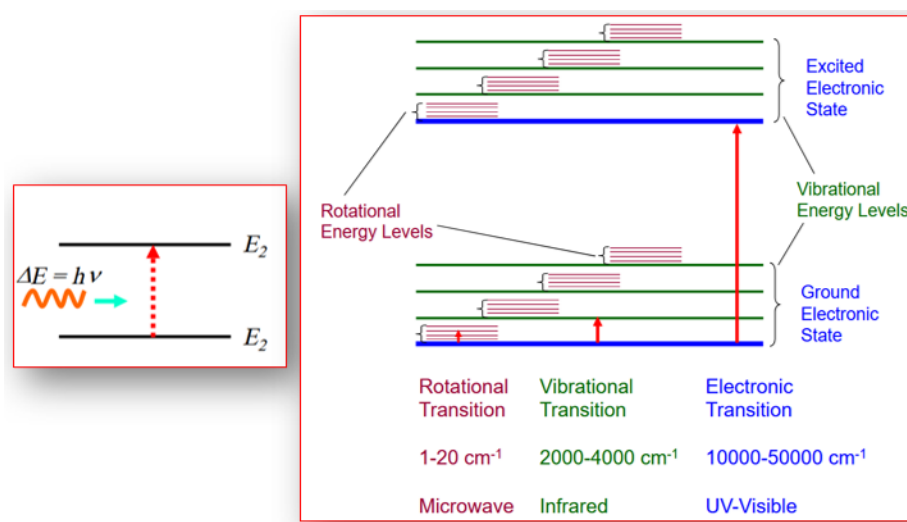


Figure 5: Jablonski diagram describing the energy transition process leading to scattering and emission based on different types of optical radiations involved (Efremenko & Kokhanovsky, 2021).

Absorption occurs as a transition from a lower energy level to a higher energy level of an atom or molecule of the sample. Measuring the concentration of an absorbing species in a sample is accomplished by applying the Beer-Lambert Law (Equation 4):

$$A = \epsilon cl \quad (4)$$

Where l is path length, ϵ is the molar extinction coefficient, and c is concentration of the absorbing species.

Absorbed radiations in the Infrared cause vibrational and rotational transitions, whereas radiations in the UV-Visible domain cause electronic transitions. An absorption spectrum that depends on the energy level structure of an atom or molecule can be obtained by charting the absorption of the respective optical radiation which is wavelength dependent. The spectrum and absorption spectra are useful for identifying compounds.

Typically, radiations in the UV and visible regions have the same effect on matter, causing electron promotion to higher energy orbitals. A sample that absorbs visible or UV radiation obtains an energy that temporally destabilises the atoms and molecules, causing a redistribution of the electrons from the lowest to the higher energy states. In the higher energy states, electrons are distributed in orbitals with the valence electrons, populated by π -electrons, bonding (σ) electrons, and lone pair electrons (n-orbitals). UV-Visible radiation, that, causes a redistribution among electrons in the valence orbitals but the molecule, however, remains intact except for higher energies in the UV (UV B and UVC) which can cause the breaking of bonds (Bakar et al., 2016; Borowicz et al., 2012; Sackey et al., 2015; Chen et al., 2013).

Also, IR radiation absorbed by a sample increases the amplitude of bond vibrations. The bonds in molecules are in constant vibration and stretching with characteristic frequencies. EM radiations in the IR range of the spectrum coincide with these characteristic frequencies of the bonds cause further

stretching and bending. The fundamental frequencies of the molecules or their overtones can be determined to provide chemical information resulting from the overlap of fundamental frequencies present in the Near IR (Stuart, 2004; Vitha, 2018).

The shift from a higher energy level to a lower one can result in emission when energy is transferred to the radiation field, or it can undergo non-radiative decay without emitting radiation (Figure 6). The non-radiative processes include heating and other internal conversion mechanisms. In the case of molecules, the transition is referred to as fluorescence when it occurs between states of the same spin, and phosphorescence when the transition happens between states of different spins. At low concentrations, the emission intensity of a substance displaying fluorescence or phosphorescence is directly proportional to the concentration of the analyte, which aids in quantifying the emitting species.

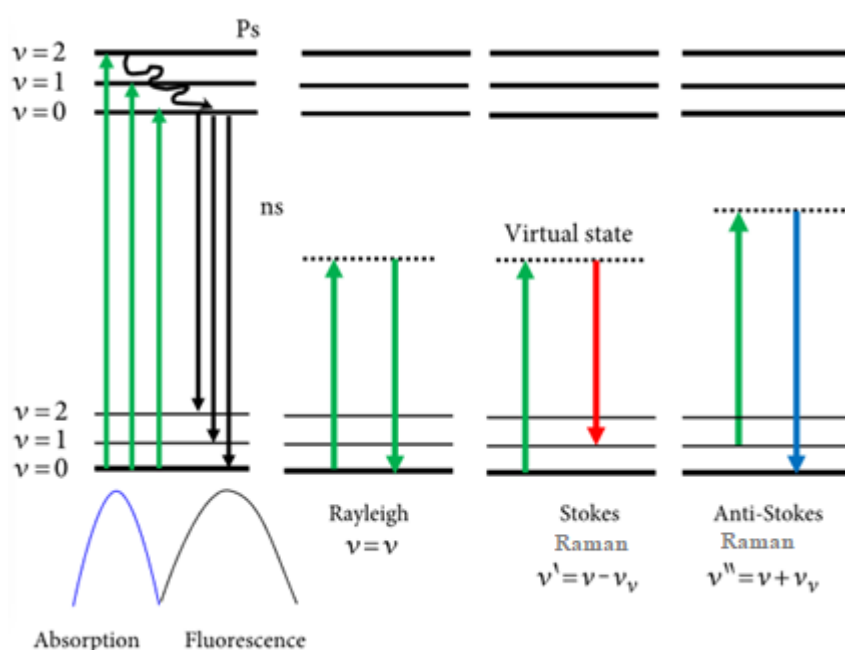


Figure 6: Energy transition process for Fluorescence and Raman scattering phenomenon (Masilamani et al., 2017)

Redirection of light due to its interaction with matter is called scattering. It may or may not occur with the transfer of energy, i.e., the scattered radiation has a slightly different or the same wavelength. The phenomenon of light being dispersed at the identical wavelength as the incoming light is known as Rayleigh scattering. Conversely, when light is scattered due to phonon vibrations, it is referred to as Brillouin scattering, which typically exhibits a spectral shift of 0.1 to 1 cm^{-1} from the incident light. The light scattered due to molecules' vibrations or optical phonons in solids is called Raman scattering, typically shifted by as much as 4000 cm^{-1} from the incident light. The Perrin Jablonski diagram also allows discussion timescales associated with the different transition processes (Table 1).

Table 1: Timescale for various energy transitions in the optical domain

Transition	Timescale (s)
Absorption	Femtoseconds (10^{-15})
Raman Scattering	Nanoseconds (10^{-9})
Fluorescence	Sub-nanoseconds to sub-microseconds (10^{-10} to 10^{-7})
Phosphorescence	Microseconds to seconds (10^{-6} to 10^0)

Source: (Vitha, 2018)

There are many applications of optical spectroscopy for molecular analysis because it is a safe and non-destructive method. Also, optical spectroscopy measurements require relatively inexpensive sources for their generation, cheaper detectors, and straightforward mathematical methods for analysis (Svanberg, 2004).

Optical Spectroscopy Analysis of Honey

The optical spectrum-based food analysis approach provides non-invasive, non-destructive, fast, and fully automatic methods with minimum or no sample preparation. This approach helps to overcome the drawbacks of conventional chemical processes, which are time-consuming, laborious, and require complex sample preparations.

The advantages of the optical spectroscopy techniques (visible, near and middle infrared, fluorescent) concerning other methods are the non-invasive approach and relatively easy and quick data acquisition. Optical spectroscopy analysis has been used in many studies for geographical and botanical discrimination, to identify adulteration, and correlation with physicochemical parameters of honey such as moisture, pH, diastase, acidity, etc. (Escuredo et al., 2021; Leme et al., 2018; Tahir et al., 2017). Studies on honey with light have been recent, mainly in the last two decades. According to Cozzolino et al. (2011), the principal optical spectroscopy methods used for honey analysis are summarised in Figure 7 (Cozzolino et al., 2011). In Figure 7, Infrared spectroscopy methods (FT/ NIR, MIR, NIR) are the most dominant, followed by Raman, Fluorescence, and UV-VIS-NIR spectroscopy. This study focuses on UV-Vis-NIR in transmission mode, fluorescence, and Raman spectroscopy for assessing honey.

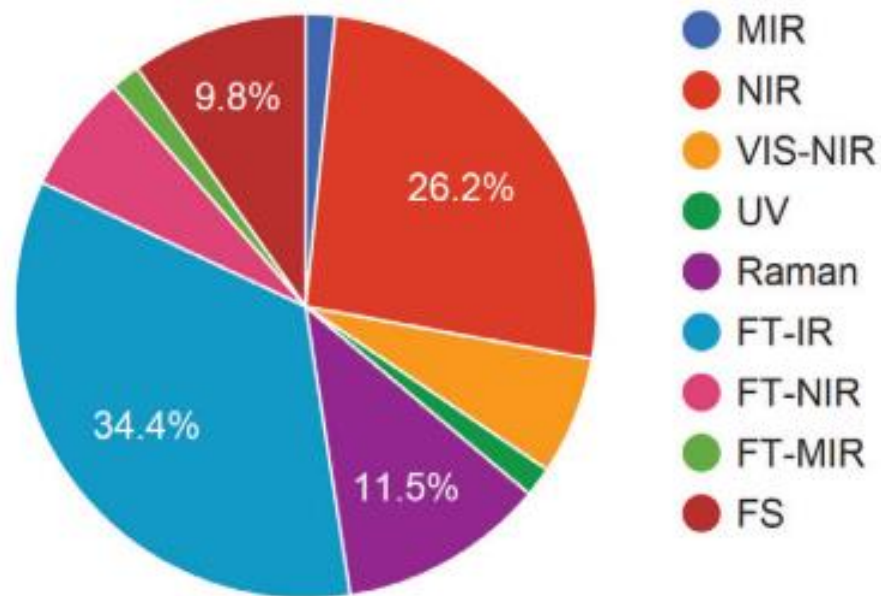


Figure 7: The major optical spectroscopy methods used for honey analysis according to Cozzolino et al. (2011)

Optical Transmission Spectroscopy

Optical Transmission Spectroscopy (OTS) or UV-Visible spectroscopy in transmission mode is one of the simplest optical spectroscopic methods currently being used in various studies on Honey (Bergamo et al., 2020; Frausto-Reyes et al., 2017; Huang et al., 2019; Li & Yang, 2012; Tsankova & Lekova, 2015 ; Vlaeva et al., 2017; Zhao et al., 2011). In Transmission spectroscopy, the transmittance (T) is expressed as the ratio of transmitted light intensity (I_t) to the incident light I_o (Equation 5). Transmission and absorption (A) spectroscopy give complementary information and can be used interchangeably (Equation 6):

$$T = \left(I_t / I_o \right) \quad (5)$$

$$A = \text{Log}_{10} \left(1/T \right) \quad (6)$$

The OTS spectra provide signatures/fingerprints unique for every honey sample, revealing the general biochemical composition within the absorption range on molecules in the optical region (Table 2).

Table 2: Molecular constituents of honey and their absorption range in the optical region of the EM spectrum

Compound	Absorption (nm)
Phenolic Compounds (Benzoic Acid)	240 – 265
Phenolic Compounds (Gallic acid, Tryptophan, 4-hydroxybenzoic, caffeic, vanillic, ferulic/ chlorogenic acid, syringic acid, p-coumaric acid)	280 – 320
Aromatic amino acids	260 – 285
Flavonoids Compounds (Chlorogenic acid, O-Coumaric acid, Quercetin)	310 – 360
Folic Acid (Vitamins B9), Vitamin B6	330 -340
Maillard reaction products (HMF and Furosine)	360 – 435
Riboflavin (Vitamin B2)	400 – 510
Carotenoids	400 – 500
Chlorophyll	600 – 700

Source: (Mashhadi et al., 2022; Parri et al., 2020)

OTS method is non-destructive, relatively cheap, safe, reproducible, rapid, and requires little or no sample preparation. Some studies on honey have employed the OTS technique for geographical and botanical origin characterisation, cheap honey sensor development, rapid adulteration quantification and determination of diastase activity (Almaleeh et al., 2017; Bergamo et al., 2020; Ferreiro-González et al., 2018; Frausto-Reyes et al., 2017; Huang et al., 2019; Li & Yang, 2012; Tsankova & Lekova, 2015; Ulloa et al., 2013; Zhao et al., 2011).

Fluorescence Spectroscopy

Another commonly used optical spectroscopic method for studying honey is the Fluorescence Spectroscopy (FS) technique. FS technique has widely been used to assess botanical and geographical origin and also for the discrimination between genuine and adulterated Honey (Karoui et al., 2007; Lenhardt et al., 2014; Ruoff et al., 2005). The principal advantages of fluorescence spectroscopy are its rapidity and sensitivity. It is 100–1000 times more sensitive than other spectrophotometric techniques.

Fluorescence occurs when a molecule in an excited state returns to a lower-energy electronic state by emitting a photon. The fraction of molecules in the excited state that returns to the ground state by fluorescence is known as the fluorescent quantum yield, Φ_f . The intensity of fluorescence emission, F_I , is proportional to the amount of radiation absorbed by the sample ($F_o - F_T$) and the fluorescence quantum yield (Φ_f). Therefore;

$$F_I = k\Phi_f(F_o - F_T) \quad (6)$$

Φ_f ranges from 1 (i.e. when every molecule in an excited state undergoes fluorescence) to 0 (i.e. when fluorescence does not occur respectively). k is also the constant that accounts for the efficiency of collecting and detecting fluorescent emissions.

Fluorescence spectroscopy provides information on the presence and proportions of fluorescent molecules in honey. The concentration fC of the fluorescing species is obtained if the equation Beer's law, $\frac{F_T}{F_o} = 10^{-\epsilon bC}$, is solved for F_T in Equation (7):

$$F_I = k\Phi_f F_o(1 - 10^{-\varepsilon bC}) \quad (7)$$

Thus, when $\varepsilon bC < 0.01$ the intensity of fluorescence increases with the concentration of the fluorescing species, as shown in Equation (8):

$$F_I = 2.303k\Phi_f \varepsilon bCF_o \quad (8)$$

The concentrations of these fluorophores vary depending on the honey's geographical and floral origin (Karoui et al., 2007; Becker et al., 2003; Ruoff et al., 2005). Honey contains fluorophores, which are also known as endogenous or intrinsic fluorophores. These include various amino acids such as tyrosine, phenylalanine, and tryptophan, as well as proteins, polyphenols, flavonoids, some vitamins (A, B, and E), Maillard products like hydroxymethylfurfural, furosine, and advanced glycation end products, as well as chlorophyll a and hematoporphyrins as shown in Table 3 (Cuss & Guéguen, 2015; Becker et al., 2003; Bong et al., 2016; Flanjak et al., 2022; Karoui et al., 2007; Parri et al., 2020; Strelec et al., 2017; Ye et al., 2011).

Table 3: Fluorophores in Honey with their absorption and corresponding emission wavelength in the optical region of the EM spectrum

Compound	Absorption (nm)	Emission (nm)
Phenolic Compounds (Benzoic Acid)	240 – 265	370 – 495
Phenolic Compounds (Gallic acid, Tryptophan, 4-hydroxybenzoic, caffeic, vanillic, ferulic/ chlorogenic acid, syringic acid, p-coumaric acid)	280 – 320	390 – 470
Aromatic amino acids	260 – 285	320 – 470
Flavonoids Compounds (Chlorogenic acid, O-Coumaric acid, Quercetin)	310 – 360	370 – 470
Folic Acid (Vitamins B9), Vitamin B6	330 -340	450
Maillard reaction products (HMF and Furosine)	360 – 435	440 – 520
Riboflavin (Vitamin B2)	400 – 510	480 – 750
Carotenoids	400 – 500	520 – 570
Chlorophyll	600 – 700	670 – 790

Source (Mashhadi et al., 2022; Parri et al., 2020)

Fluorescence spectroscopy study of honey can be achieved in the front-face (0°) or right-angle fluorescence (90°) in the experimental configurations. Front-face fluorescence spectroscopy provides information on auto-fluorescent molecules predominantly acquired from the surface of honey. In contrast, right-angle fluorescence spectroscopy assesses autofluorescence throughout the transparent or semi-transparent honey samples, offering a comprehensive analysis of the entire sample volume. Nevertheless, the right-angle fluorescence method may suffer an inner filter effect and fluorescence quenching. A recent study by Mashhadi et al (2022) demonstrated that using 60-degree detection reduces the incidence of inner filter effects, fluorescence quenching and even multiple scattering of the photons (Mashhadi et al., 2020, 2022).

Again, due to the numerous fluorophores in honey, their fluorescence signals overlap, making it sometimes impossible to measure a single compound's concentration. Consequently, the fluorescence measurement of

honey produces intricate spectral patterns that can serve as distinct spectral fingerprints for each sample. These patterns arise from the presence of different endogenous fluorophores and their absorbing and quenching species. Through fluorescence analysis, it is possible to identify individual molecular species in honey by measuring emission spectra at specific excitation wavelengths, or conversely, by selecting excitation wavelengths to observe the emission spectra (Karoui et al., 2007). Also, the Fluorescence Excitation-Emission Matrix (FEEM) is another approach widely used to identify individual molecular species in Honey (Antônio et al., 2022; Lenhardt et al., 2015). FEEM resolves challenges associated with overlapping spectral profiles resulting from the presence of multiple fluorophores. This is achieved by presenting both excitation and emission spectra in three-dimensional plots, effectively mitigating spectral overlap issues. This data can be analysed with multivariate statistical methods to characterise honey samples. Mathematical methods using spectral deconvolution can also resolve the overlapping fluorescence spectra to identify individual molecular species in honey (Parri et al., 2020).

Raman Spectroscopy

Raman spectroscopy is another common vibrational technique used for studies on honey. Raman spectroscopy offers the characteristic spectral patterns, often referred to as "fingerprints," of the molecular constituents present in honey. These patterns enable the acquisition of qualitative and quantitative information about the honey sample (Pelletier, 2003; Šugar & Bouř, 2016). Over the past two decades, the utilization of Raman spectroscopy has become increasingly prominent in honey analysis (Batsoulis et al., 2005; Corvucci et al., 2015; De Oliveira et al., 2002; Frausto-Reyes et al., 2017; Goodacre et al., 2002;

Grazia Mignani et al., 2016a; S. Li et al., 2012; Oroian et al., 2018; Oroian & Ropciuc, 2018; Özbalci et al., 2013; Paradkar & Irudayaraj, 2002; Pelletier, 2003; Pierna et al., 2011; Raduan et al., 2014, 2017; Salvador et al., 2019; Šugar & Bouř, 2016; Tahir et al., 2017). Analysis of the Raman spectra of honey can be relied on for botanical, geographical, and entomological differentiation of honey. Studies used Raman spectroscopy to determine botanical origins (Corvucci et al., 2015), geographical origins (Pierna et al., 2011), adulteration (Oroian et al., 2018; Paradkar & Irudayaraj, 2002), and phenolic compounds (Tahir et al., 2017).

The Raman effect is observed on a molecule subjected to EM radiation. The EM radiation's electric field (E) induces the molecule's electric dipole moment (μ). The extent of polarisation is given by the induced dipole moment in Equation (9) as

$$\mu = \alpha E \quad (9)$$

Where α is the polarizability tensor, and the electric field is given by $E = E_o \sin(2\pi\nu t)$ hence Equation (9) becomes

$$\mu = \alpha E_o \sin(2\pi\nu t) \quad (10)$$

The polarizability term α changes depending on if the molecule undergoes rotation ($\alpha = \alpha_o + \gamma \sin 2\pi\nu_{rot} t$) or vibration ($\alpha = \alpha_o + \beta \sin 2\pi\nu_{vib} t$), thus using the trigonometry relation, $\sin A \sin B = \frac{1}{2} [\cos(A - B) - \cos(A + B)]$ to expand Equation (10), into

$$\mu = \alpha_o E_o \sin(2\pi\nu t) + \frac{1}{2} \beta \alpha_o [\cos 2\pi(\nu - \nu_{vib})t - \cos 2\pi(\nu + \nu_{vib})t] \quad (11)$$

for vibrational motion, and

$$\mu = \alpha_o E_o \sin(2\pi\nu t) + \frac{1}{2} \gamma \alpha_o [\cos 2\pi(\nu - 2\nu_{rot})t - \cos 2\pi(\nu + 2\nu_{rot})t] \quad (12)$$

for rotational motion. In this case, variation occurs at twice the rotational frequency, ν_{rot} . This is because the polarizability is the same for opposite directions of the field. The equations show that for either vibrational or rotational motion, the oscillating dipole has three frequency components, ν the Rayleigh line, $\nu + \nu_{vib}$, the Anti Stokes Raman line, and $\nu - \nu_{vib}$ is the Stokes Raman line (Figure 8). The Raman Effect occurs only when the polarizability changes ($\alpha_l \neq 0$), whereas the polarizability remains unchanged for Rayleigh scattering ($\alpha_l = 0$).

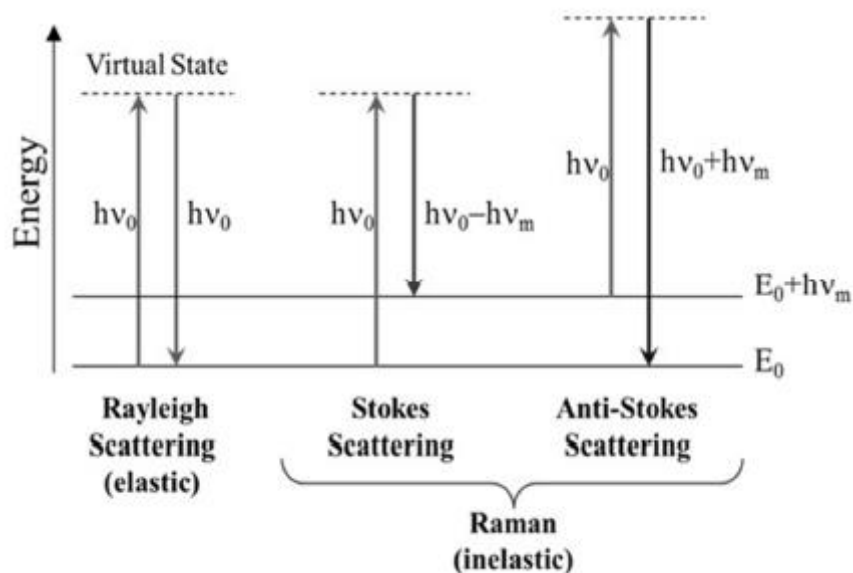


Figure 8: Jablonski Diagram representing Quantum Energy Transitions for Rayleigh and Raman Scattering (Ding et al., 2022)

The Raman spectrum of a sample is obtained as peaks with different intensities spread over a wavelength scale. Each peak in the Raman spectrum corresponds to the vibrational modes of a molecule. Raman spectroscopy

mainly provides the vibrational modes of various sugar molecules, i.e. glucose, fructose, sucrose, etc., and water in Honey (Artlett & Pask, 2015; Batsoulis et al., 2005; Casella et al., 2013; Damto, 2019; Mabrouk et al., 2013). The vibrational modes of each of these sugars in honey are shown in Table 4.

Table 4: Raman spectra bands of kinds of honey obtained using 532 nm laser compared with 785 nm laser and that in literature (A (Goodacre et al., 2002), B (Anjos et al., 2018), C (Pierna et al., 2011) and D (Li et al., 2012))

A	Raman band (cm ⁻¹)			Type of vibration	Primary Sugar
	B	C	D		
430	421.5	424	425	C-C-O and C-C-C bending	Fructose Glucose
460	-	449	-	Skeletal Vibration	Maltose Sucrose
523	520.8	519	517	C-C-O and C-C-C deformation	Glucose Fructose
631	625.7	630	629	Ring deformation	Fructose Sucrose
709	705.4	708	705	C-O and C-C-O stretching, O-C-O bending	Fructose
825	824.7	822	824	C-OH bending	Fructose
870	866.5	865	865	C-O-C Cyclic alkyl ethers	Fructose Glucose
918	915.1	904	915	CH, COH bending	Glucose Maltose
983	979.1	979	981	Ring breathing	Fructose
1074	1071.5	1064	1065	C-O-C stretching, C-N vibration of proteins	Fructose Glucose
1127	1124.4	1126	1127	C-OH deformation	Glucose Maltose
1267	1265.6	1266	1264	C-O-C Cyclic alkyl ethers	Fructose
1368	1366.3	1367	1373	CH and OH bending	Glucose
1460	1459.9	1459	1461	CH ₂ bending	Fructose Glucose
2893	-	2904	-	CH ₂ symmetric stretching	Glucose
2940	2941.6	2941	-	CH ₂ asymmetric stretching	
-	-	3234 3319	-	OH stretching	Water

Source: (Anjos et al., 2018; Goodacre et al., 2002; Li et al., 2012; Pierna et al., 2011)

The typical Raman spectrum consists mainly of peaks with their intensities expressed as a function of wavenumber (cm⁻¹), otherwise known as Raman shifts (cm⁻¹). The Raman shift of a peak is equal to the vibrational energy of the corresponding mode. Therefore, the total intensity scattered by a given vibrational mode is the integrated intensity of the corresponding Raman peak (Le Ru & Etchegoin, 2009). The Raman intensity depends on the scattering cross-section, σ_R given as

$$\sigma_R = \frac{8\pi^3(n^2-1)^2}{3\lambda^4N^2} \quad (12)$$

Thus, the intensity of the Raman Scattering is related to the wavelength by an inverse fourth power making the choice of excitation for Raman spectroscopy critical (Kerr et al., 2015; Senior, 2009; Smith & Dent, 2004; Svanberg, 2004).

The majority of the studies on honey involving Raman spectroscopy use long-wavelength excitation sources, mainly 785 nm and 1064 nm lasers (Anjos et al., 2018; Batsoulis et al., 2005; Chekalyuk & Hafez, 2013; Ciaccheri et al., 2015; Corvucci et al., 2015; De Oliveira et al., 2002; Frausto-Reyes et al., 2017; Grazia Mignani et al., 2016b; Kerr et al., 2015; Molnar et al., 2020; Paradkar & Irudayaraj, 2002; Pierna et al., 2011; Salvador et al., 2019). Raman signals produced by long-wavelength excitation sources exhibit lower intensity, which is a result of the inverse fourth power relationship between wavelength and scattering intensity (Kerr et al., 2015; Smith & Dent, 2004). Utilizing such sources necessitates the use of high-powered excitation sources, cooled detectors, and, in certain cases, Fourier Transform (FT) configuration schemes to efficiently detect the low-intensity signals they produce (Bowie et al., 2000).

Furthermore, the instrumentation must consider the incorporation of "special" optical components, such as mirrors and lenses, that are specifically designed to operate efficiently in extended wavelength regions (Kalashnikov et al., 2016; Stuart, 2004). These interventions result in the enlargement of the instrument's physical dimensions, considerations for user safety, and a proportional rise in the overall cost of Raman instrumentation. Ultraviolet (UV) excitation sources are suitable for providing enhanced scattering because they have short wavelengths. Nevertheless, their practical use is limited due to the relatively high cost of UV excitation sources and their capability to cause sample degradation.

Promising advancements are underway in the implementation of shorter wavelength sources, particularly a 532 nm laser, to facilitate Raman spectroscopic analysis of honey with enhanced precision and sensitivity. (Corvucci et al., 2015; Šugar & Bouř, 2016; Tahir et al., 2017). The 532 nm laser excitation source proves highly advantageous due to its ability to generate higher spectral intensity while operating at minimal power, thereby minimizing energy consumption. Furthermore, this excitation wavelength enables the utilization of standard optical components and facilitates the effective performance of dispersive detection schemes in the visible region (Grazia Mignani et al., 2016a).

A challenge identified with Raman spectroscopy is that; biological samples such as honey present high susceptibility to fluorescence interference (Lakowicz, 2006; Lieber & Mahadevan-Jansen, 2003; Zhao et al., 2007). The presence of this interference effect is sufficient to overshadow relatively narrow

and weak Raman peaks. When fluorescence occurs, it is seen as a broad background that overshadows the Raman peaks. The effect of the background is quantitatively seen in its Signal-to-Fluorescence Ratio (SFR). SFR is the intensity ratio of the tallest Raman peak to its baseline height. The mathematical expression for SFR is

$$SFR = \frac{\text{Maximum Raman Peak} - \text{minimum Raman peak}}{\text{baseline maximum} - \text{baseline minimum}} \quad (13)$$

SFR of very high values are desired; otherwise, the fluorescence backgrounds must be removed for lower value SFR to enable good spectra.

Reports by several researchers have provided ways for obtaining Raman spectra with lower SFR by exploiting the differences between the fluorescence and Raman mechanisms. These differences have led to the development of several techniques, including the energy domain, time domain, frequency domain, wavelength domain, and computational methods for Raman spectra recovery (Wei et al., 2015). The Time-domain techniques take advantage of the fact that fluorescence photons have a much longer lifetime (~ ns) than the Raman photons (~ ps to fs). Therefore, the quickly arriving Raman scattered light could be separated temporally from late arriving fluorescence emission of a sample excited by ultrafast pulses and detected by some ultrafast detection mechanism like Kerr gate, streak camera, Intensified Charge-Coupled Device (ICCD) camera, etc. (Kostamovaara et al., 2013; Matousek et al., 1999; Nissinen et al., 2011). Regarding the frequency-domain methods, the Raman and fluorescence signals can be discriminated by extracting the high-frequency (mostly Raman) or low-frequency (mostly fluorescence) components from the output of the detector, which has a lock-in mechanism.

The wavelength domain methods take advantage of the fact that the wavelength of a Raman peak closely follows the excitation source. In contrast, the fluorescence peak does not vary significantly with the excitation wavelength. Hence, the fluorescence spectra can be removed with different excitation wavelengths while enhancing weak Raman signals. Some standard wavelength domain methods include Shifted Excitation Raman Difference Spectroscopy (SERDS) (Martins et al., 2010; Sowoidnich & Kronfeldt, 2012), Wavelength Modulated Raman Spectroscopy (WMRS) (Mazilu et al., 2010) and Subtracted Shifted Raman Spectroscopy (SSRS) (Bell et al., 2000; Bell et al., 1998).

Polarisation domain methods also take advantage of the different responses in Raman scattering and fluorescence emission to polarisation modulation. The polarisation dependence of the excitation light with polarised Raman bands and fluorophore with low fluorescence anisotropy enables the discrimination between Raman molecules from that of Fluorescence (Le Ru & Etchegoin, 2009; McCreery, 2005).

In addition to experimental methods for fluorescence suppression, several computational methods have been widely adopted for preprocessing measured Raman spectra directly to remove any fluorescence background (Schulze et al., 2005). Several studies have reported using derivatives for identifying peaks and rejecting baselines (Brown et al., 2000; Griffiths et al., 1982; Mosier-Boss et al., 1995). the derivative methods can enhance noise in a spectrum. Also, these methods can distort the Raman line shape and require a complex mathematical fitting algorithm to reconstruct the Raman spectra

(Brorsson et al., 2021; Osticioli et al., 2006). The Fourier transform of a spectrum enables signal and noise components within the spectrum to be observed and separated by the application of a digital filter to the Fourier domain spectral data. The filter ensures that only those frequency components contributing to the signal are retained while discarding all others (Mosier-Boss et al., 1995). When the frequency components of the Raman spectra and noise features are not well separated, the Fourier transform method can produce severe artefacts.

Among the computational methods, the polynomial fitting method is popular and most widely used (Hu et al., 2018; Vickers et al., 2001). A setback to this procedure is the subjectivity in choosing the polynomial degree. This choice is based mainly on practical experience. However, Lieber and Mahadevan-Jansen (2003) proposed a modified multi-polynomial fit (ModPoly)-based iterative algorithm (Lieber & Mahadevan-Jansen, 2003). The algorithm is further improved by Zhao et al. (2007) to take care of spectra with high noise or less intense Raman peaks (Zhao et al., 2007). Also, Krishna et al. (2012) recently reported the range-independent background subtraction algorithm (RIA), which estimates the fluorescence background by a modified iterative fitting procedure (Krishna et al., 2012). RIA is reported to efficiently suppress the fluorescence background without any peak distortions or inclusions of spurious peaks in the data. Chen et al. (2014) developed the Savitsky Golay-Successive Relaxation (RIA-SG-SR) method based their iteration instead on a modified Savitsky-Golay method to achieve faster convergence and overcome longer computation time (Chen et al., 2014). Further, Chen et al. (2015) developed the RIA-SG-RPR algorithm, which

intrinsically chooses the convergence criterion to minimise subjective human intervention. Huzortey et al. 2021, further developed a fully automated method for recovering Raman spectra (Huzortey et al., 2021).

Other Methods

Besides all the methods mentioned earlier, numerous other computational methods have been reported for fluorescence suppression. Principal component analysis methods (Hasegawa, 2001), Artificial Neural Networks (ANN) methods (Schulze et al., 2005), Maximum Entropy Methods (MEM) (Fischer et al., 2000), Signal Removal Methods (SRM) (Vekemans et al., 1995), Noise Median Method (NMM) (Friedrichs, 1995). Threshold-Based Classification (TBC) (Dietrich et al., 1991) and Spectral Shift Methods (SSM). These are but a few of the techniques reported in the literature. The use of Surface Enhanced Raman Spectroscopy substrates like gold (Au) and Silver (Ag) nanoparticles is also gaining prominence as an experimental approach for fluorescence suppression in Raman spectroscopy (Le Ru & Etchegoin, 2009; Raduan et al., 2014a, 2014b).

Other Spectroscopic Methods for the Study of Honey

Besides the standard spectroscopic methods used in the analysis of honey, newer optical spectroscopy techniques are also emerging. Laser-induced breakdown spectroscopy is promising for the elemental analysis of Honey (Bilge et al., 2016; Lastra-Mejías et al., 2020; Peng et al., 2020; Stefas et al., 2020, 2021, 2022). Raman Optical Activity and Polarization techniques have also been used for honey studies (García-Alvarez et al., 2002; Šugar & Bouř, 2016).

Optical Spectra Data Analysis

Spectroscopic devices generate different types of data from samples. These data can be in single data points, spectra or images. The data obtained for Transmission, Fluorescence and Raman spectroscopy in this study were in the form of spectra. These spectral data can be analysed using univariate or multivariate methods for classification, regression, clustering, and data compression, depending on the volume of the data and analysis objective.

Spectral Preprocessing

Spectral preprocessing is needed as a first step before analysing spectroscopic data (Rinnan et al., 2009). The preprocessing objective varies depending on the challenge, but mainly they are used to reduce noise, correct baseline and make spectra comparable or easy to evaluate. Some preprocessing steps applied to spectral data include smoothening, derivatives, baseline correction, scaling, and normalisation. More than one preprocessing procedure can be used at a time.

SNV Normalisation

Standard normal variate (SNV) is a common method for normalising spectral data. SNV normalisation method aims to make spectra comparable in intensities (Walach et al., 2018). SNV offers an effective approach for eliminating constant baseline effects and scaling discrepancies from spectra, allowing for reliable comparison. This normalisation method involves subtracting the mean (\bar{S}_j) of each spectrum (S_{ij}) and dividing it by its standard deviation (sd_j), thereby normalising the spectral data as shown in Equation (13).

$$\tilde{S}_{ij} = \frac{S_{ij} - \bar{S}_j}{sd_j} \quad (13)$$

Spectral Deconvolution

Spectral deconvolution resolves the broad spectrum into separate peaks using various algorithms (Schulze et al., 2005). The resolved peaks identify the molecular species (peak position) and concentration (Intensity).

Univariate Spectral Data Analysis

Univariate analysis of the spectra data involves selecting and exploring each variable separately. Univariate data can be described through bar graphs, histograms, pie charts and frequency tables. Univariate analysis helps to summarize data and analyse the pattern present in it. The patterns of interest in univariate analysis are the measures of central tendency (mean, mode and median) and the measures of dispersion (range, variance, Quartiles, Standard deviation and coefficient of Variation). The univariate analysis further explores the cause and the relationship between the groups of variables determined by the coefficient of linear correlation. Linear correlation is used to represent the strength of a linear relationship between the groups of variables if the association between variables is substantial using a t-test for two groups or ANOVA for multiple groups

Multivariate Data Analysis

When the variables of interest are many, Multivariate Analysis (MVA) methods can be used to extract information from spectroscopy data. The MVA methods lead to clustering, classification, modelling, or prediction. Some examples of MVA methods are component analysis (e.g. PCA, ICA): used to

reduce the dimensionality of data, regression analysis (e.g. MLR, PLSR, PCR): used for determining the relationship between variables; discriminant analysis (PLS-DA, FDA, LDA, etc.): used to classify data into predefined classes and cluster analysis (K-means, HCA, Fuzzy C-means, etc.): used to group data based on feature similarity (Ares, 2014; Isaksson & Aastveit, 2006; Jolliffe, 2002; Li Vigni et al., 2013; Sarle et al., 1990). Multivariate analysis also tests for the performance of the clustering methods using various metrics, including root mean squared error (rmse), root mean squared error of prediction (rmsep), coefficient of determination, sensitivity, selectivity, etc.

Principal Component Analysis

The Principal Component Analysis (PCA) is generally a first step towards data transformation. The application of PCA transformation in LIF spectra significantly diminishes the number of potential dimensions by extracting and prioritizing the most influential components (Li Vigni et al., 2013). Initially, PCA determines the relationships between each input data \tilde{F}_{ij} by calculating the Covariance matrix G_{jj}^T , as represented by Equation (14). Subsequently, it identifies the directions along which \tilde{F}_{ij} exhibit dispersion, as outlined in Equation (15).

$$G_{jj}^T = \tilde{F}_{ij} \tilde{F}_{ij}^T \quad (14)$$

$$E_{jj}^T = \tilde{F}_{ij} G_{jj}^T \quad (15)$$

From Equation (14), G_{jj}^T is the eigenvector matrix, and the columns of the matrix, E_{jj}^T denote The eigenvalues, referred to as principal components, play a crucial role in determining the significance of different directions in the

data. These eigenvalues are utilized to generate the score plot, while the eigenvectors are utilized to construct the loadings plot. The PCA scores are derived from the variance across the dataset, enabling the detection of underlying patterns or groupings of samples within a comprehensive dataset. Simultaneously, the associated loadings provide insights into the spectral wavelengths that contribute to these patterns. The PC scores and Loadings can be observed together with PCA-Biplot. The biplot plots together wavelengths with their respective spectral scores showing their influence depending on how further they occur from the origin. As presented by the biplot, the samples' distribution of the molecules is described qualitatively based on which quadrant a sample appears and semi-quantitatively based on the direction of the axis where a sample occurs.

PCA provides a means for classification, Regression and clustering. Classification and Regression are supervised forms of analysis. While clustering is used for unsupervised analysis.

K-Means Clustering Analysis

K-means Clustering Analysis (KCA) is used to find hidden patterns in data based on feature similarity (Kaufman & Rousseeuw, 1990; Na et al., 2010; Sinaga & Yang, 2020). The procedure for KCA involves the following;

1. Defining the number of clusters (K) in which all the spectral data, represented by PCA scores, are grouped.
2. Randomly choose one of the scores to act as the initial cluster centre for the number of clusters defined.

3. Comparing the data set scores with K number of clusters centres and assigning them to the most resembling centre.
4. After all the scores are assigned, new cluster centres are calculated by averaging all scores assigned to that cluster. The procedure is repeated until a stable solution is reached.

Clusters are obtained based on different cluster metrics. The commonest is the Euclidean distance metric. It measures the Euclidean distance between the scores. With the squared Euclidean as a distance metric, In deciding the number of groups (K), different cluster evaluation criteria for the KCA are employed. The cluster evaluation methods used include; silhouette and Davies-Bouldin (Davies & Bouldin, 1979; Rousseeuw, 1987).

The silhouette method measures the similarity (distance) between a score and other scores of the same cluster compared to score positions in different groups using Equation (16).

$$S_i = \frac{b_i - a_i}{\max(a_i, b_i)} \quad (16)$$

Where S_i is the silhouette value for the i th score position, a_i is the average distance from the i th score to the other score position in the same cluster as i , and b_i is the minimum average distance from the i th score position to score positions in a different cluster, minimised over clusters. The possible silhouette values range from -1 to $+1$, where a high silhouette value of $+1$ indicates well to match. The Davies-Bouldin method measures the ratio of within-cluster and between-cluster distances. The optimal clustering solution has the smallest

Davies-Bouldin index value. The Davies-Bouldin (DB) index is defined in Equation (17) as

$$DB = \frac{1}{k} \sum_{i=1}^k \max_{j \neq i} \{D_{i,j}\} \quad (17)$$

Here $D_{i,j}$ in Equation (17) is the within-to-between cluster distance ratio for the i^{th} and j^{th} clusters.

While methods exist (e.g., HPLC, Raman spectroscopy), they are not practical for widespread, low-cost use. Optical spectroscopy is identified as a promising alternative, but it has not been adequately tested on tropical honey varieties, such as those found in Ghana. Thus, the research gap is that while there are advanced methods for honey profiling, there's a need for an affordable, rapid method like optical spectroscopy, especially for tropical honey in Ghana. This gap drives the need for the current research

Chapter Summary

This chapter highlighted the usefulness of optical radiation, a portion of EM radiation, for assessing honey. Practical applications with selected optical spectroscopic techniques including Absorption, FTIR, Raman, Fluorescence, Laser induced break down spectroscopy, etc. from the literature were discussed. Furthermore, the chapter addressed the current state of assessment of honey in Ghana, associated challenges such as adulteration, quality, etc. and how the implementation of multivariate data analysis and optical spectroscopy techniques can together contribute to improving current situation were addressed in this chapter.

CHAPTER THREE

METHODOLOGY

Introduction

This study used three optical spectroscopy techniques to quantitatively and qualitatively explore the optical spectroscopic properties of honey produced in Ghana's AEZ. This chapter, therefore, describes the honey samples, spectroscopic techniques and the analytic methods employed. Samples are described according to how they were obtained and labelled. Each optical spectroscopic technique utilised for studying the honey samples is described in detail about the components of the optical spectroscopic systems and the experimental procedure. Other non-spectroscopic methods used in the study are equally described. The chapter also describes how the data obtained from the various experiments were analysed.

Honey Samples

Thirty-two (32) honey samples were used in this study. Seven (7) of the honey samples were harvested from apiaries in southern Ghana. Twenty-five (25) of the samples, collected from six AEZ of the country, were provided by the Conservation Biology and Entomology Department of the University of Cape Coast (Figure 9).

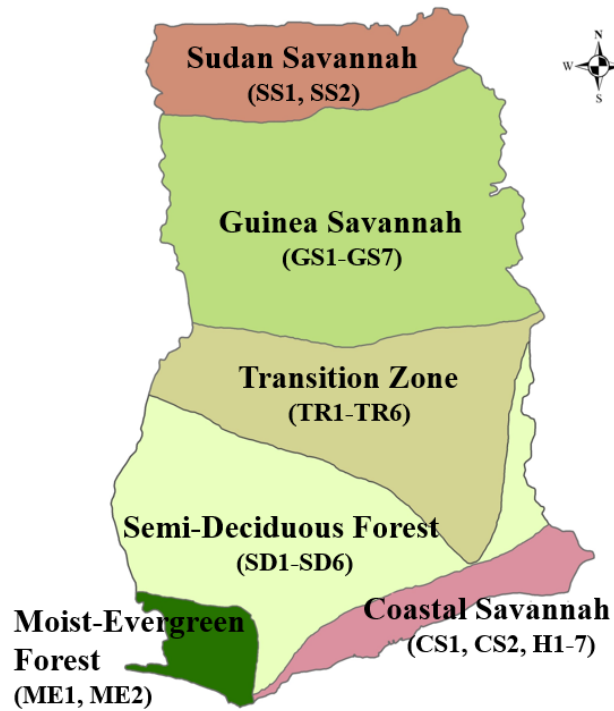


Figure 9: The map of the study area shows the agro-ecological zones of Ghana, where the honey samples were obtained. Samples are coded, as shown in parenthesis for each agro-ecological zone, for identification (FAO, 2005)

The seven (7) harvested honey samples are shown in Figure 10. It shows how the honey samples from the combs were emptied into a sieve to be drained and removed debris before bottling and storage for various measurements. The samples were stored at room temperature in the laboratory. The names of the honey samples with the locations from which they were obtained are also shown in Table 5.



Figure 10: Harvested honey samples (a) in the honeycomb, (b) being drained and (c) bottled for the study

Table 5: Names and locations of honey samples collected from apiaries in some parts of the Central Region and Accra

Samples	Place of Harvest	Region	Host Plant
H1	Jukwa,	Central	Forest, Wild Flowers
H2	3rd Ridge	Central	Forest, Wild Flowers
H3	UCC Forest	Central	Forest, Wild Flowers
H4	Somanya	Greater Accra	Teak Plantation 1
H5	Somanya	Greater Accra	Teak Plantation 2
H6	Somanya	Greater Accra	Mango Plantation
H7	UCC Forest	Central	Forest, Wild Flowers

Source: Field Data (2022)

Honey samples obtained from the Department of Conservation Biology and Entomology of the University of Cape Coast are shown in Figure 11 and described in Table 6. These samples were collected across the different AEZ of Ghana. Twenty-five (25) honey samples in all were provided specifically from these AEZ; Sudan Savanah (SS), Guinea Savanah (GS), Moist Evergreen (ME), Transition Zone (TR), Semi-Deciduous (SD) and Coastal Savanah (CS).



Figure 11: Honey samples from different agro-ecological zones collected into Eppendorf tubes provided by the Conservation Biology and Entomology Department of the University of Cape Coast

Table 6: The honey samples collected from the different agro-ecological zones of Ghana, indicating their host plant, obtained from the Department of Conservation Biology and Entomology, UCC

Samples	Agro-ecological zone	Host plant
A	Sudan Savana (SS1)	Cashew
C	Sudan Savana (SS2)	Wildflowers
D	Sudan Savana (SS3)	Wildflowers
B	Semi Deciduous (SD1)	Forest
L	Semi Deciduous (SD2)	Unknown
Q	Semi Deciduous (SD3)	Unknown
R	Semi Deciduous (SD4)	Unknown
S	Semi Deciduous (SD5)	Unknown
T	Semi Deciduous (SD6)	Unknown
E	Transition (TR1)	Cashew
H	Transition (TR2)	Cashew
I	Transition (TR3)	Cashew
J	Transition (TR4)	Cashew
K	Transition (TR5)	Cashew
N	Transition (TR6)	Unknown
F	Moist Evergreen (ME1)	Forest
G	Moist Evergreen (ME2)	Forest
O	Coastal Savana (CS1)	Unknown
P	Coastal Savana (CS2)	Unknown
M	Guinea Savana (GS1)	Unknown
U	Guinea Savana (GS2)	Unknown
V	Guinea Savana (GS3)	Unknown
W	Guinea Savana (GS4)	Unknown
X	Guinea Savana (GS5)	Unknown
Y	Guinea Savana (GS6)	Unknown
Z	Guinea Savana (GS7)	Unknown

Source: Field Data (2022)

Other Samples

An adulterant, sugar caramel, prepared with sugar, was used in various aspects of the study. Also, an HMF standard (CAS 67-47-0, lot FCB014361, Fluorochem, United Kingdom) was obtained and used for honey quality determination in some aspects of the study.

Sample Preparation Procedure for Raman Spectroscopy Measurements

For Raman spectroscopy measurements using 532 nm excitation, in order to enhance the Raman signal, certain pre-treatments were applied to the highly fluorescent honey samples prior to spectral data acquisition. Three pre-treatment methods were considered: dilution of honey with distilled water in equal proportions, heating of the diluted mixture, and treatment with activated charcoal. These methods were aimed at minimizing the fluorescence interference and improving the quality of the Raman signal in the honey samples (Frausto-Reyes et al., 2017; Molnar et al., 2020; Šugar & Bouř, 2016). Figure 12 visually depicts the activated charcoal treatment process utilized in the experimental procedure (Molnar et al., 2020; Smart & Simpson, 2002; Smyth et al., 2001; Šugar & Bouř, 2016). 10 ml of each honey sample was mixed with 10 ml of Distilled water. 1g of oral activated charcoal tablet was added to the mixture to dissolve and stirred to homogeneity. Following the preparation of the homogeneous mixture, it was subjected to heat treatment at 50°C for a duration of 20 minutes. Subsequently, the heated mixture underwent centrifugation at 14,000 rpm for 10 minutes and was filtered using a 0.45 µm pore size PFTE filter. The filtrate was used for the Raman spectroscopy measurement.

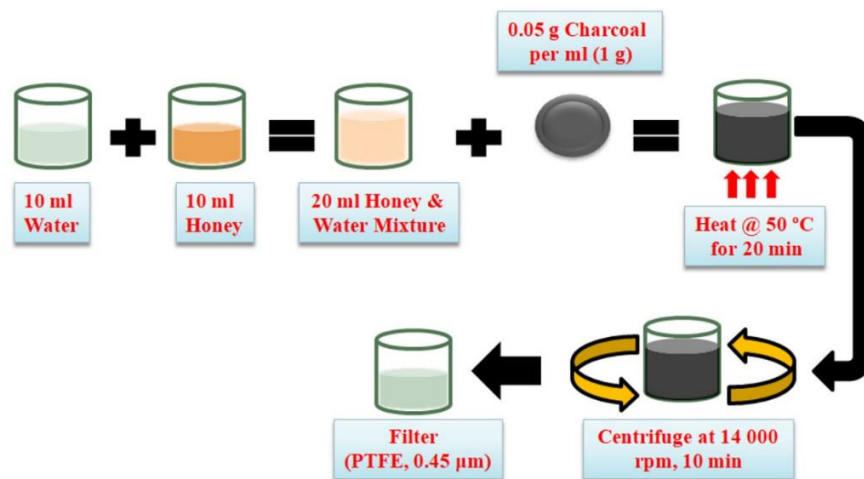


Figure 12: Sample preparation procedure of honey with charcoal to avoid fluorescence contamination for Raman spectral analysis when using 532 nm laser excitation

Instrumentation, Setups and Spectral Measurements

Three main optical spectroscopy measurements were employed in the study. These included Ultraviolet–Visible (UV-Vis) Transmission, Fluorescence, and Raman spectroscopy measurements. Each optical measurement system's instrumentation and set-ups comprised an optical source, an optical detector and other auxiliary optical components for manipulating the source to obtain the desired result.

Raman Spectral Measurements

Raman spectral measurements were carried out at the Laser Research and Plasma Institute of Shahid Beheshti University, Tehran, Iran. The measurements were carried out with a Raman system fitted with two excitation sources. The Raman system is a commercial Benchtop Raman Microscope (Teksan IR) with dual excitations of a 532 nm and 785 nm laser detector (Figure 13). The system's spectrometer is optimised for detection in both the visible and NIR region. The system uses the backscattering (0°) configuration with a notch

filter placed on the path of the collection beam before the detector, i.e., 532 and 785 nm. It runs on Tunsu software capable of performing visualisation and post-processing tasks. The Raman spectra obtained from the honey samples using the 532 and 785 nm excitations were recorded with a dispersive spectrometer. The spectrometer was set to an integration time of 30 ms and had a resolution of 12 cm^{-1} .

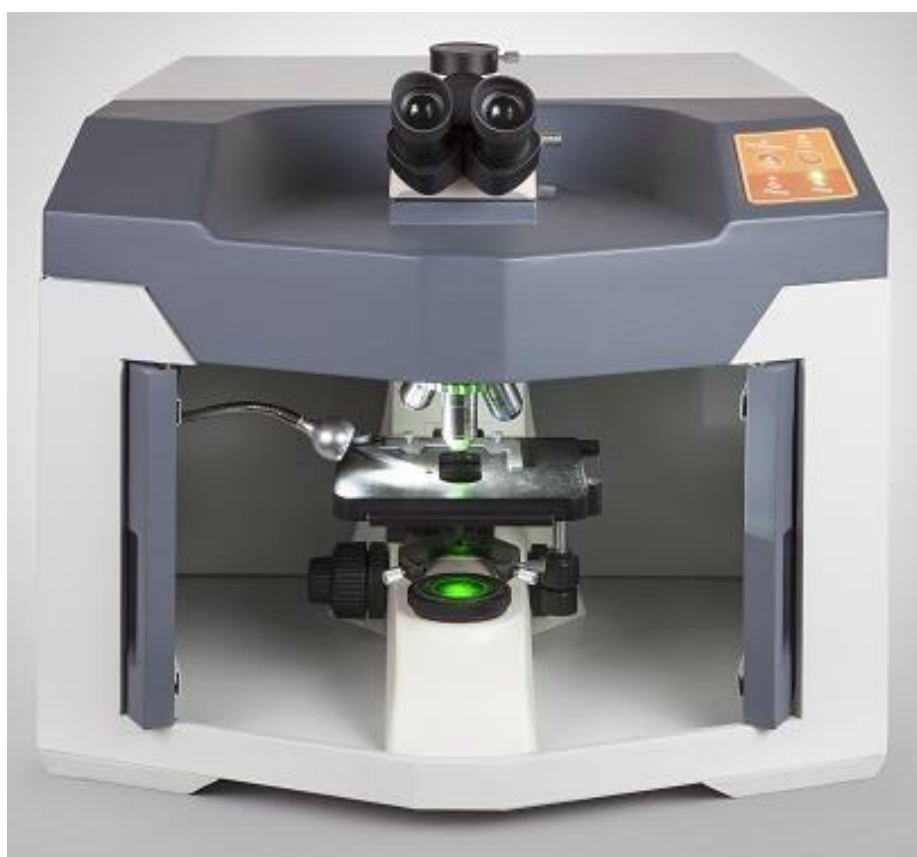


Figure 13: Benchtop Raman Microscope used for the Raman spectra measurement of honey samples in this study

The Raman spectra of honey samples were acquired directly using 785 nm excitation; however, for the 532 nm excitation, the differently prepared samples (Figure 12) were measured. For the 785 nm excitation, Raman spectral measurement was also obtained for honey on different substrates; silicone, glass and back-coated mirror surface. The Raman spectra of the honey samples

through a plastic vial were also recorded. The honey samples' Raman spectra were recorded and saved in triplicates on a computer for further processing.

UV-Vis Transmission Measurements

The UV-Vis transmission measurements were conducted at the Laser and Fibre Optics Centre, Department of Physics, University of Cape Coast. The transmission spectra of the honey samples were measured using the setup shown in Figure 14. Major components of the set-up include an ultraviolet-visible-infrared (UV-VIS-NIR) light source (DT-2-MINI-GS, Mikropack, Ocean Optics, Germany) and a spectrometer (USB 4000, Ocean Optics, USA). Other optical components include; a transparent glass disk as a sample holder, connecting optical fibres and a computer with installed spectra suite software accompanying the spectrometer. This software enables the visualisation and recording of spectral data. The optical source has a wavelength range of 200-2000 nm, but the spectrometer has a detection range of 200-1100 nm. The sample holder was transparent within the wavelength range of the source.

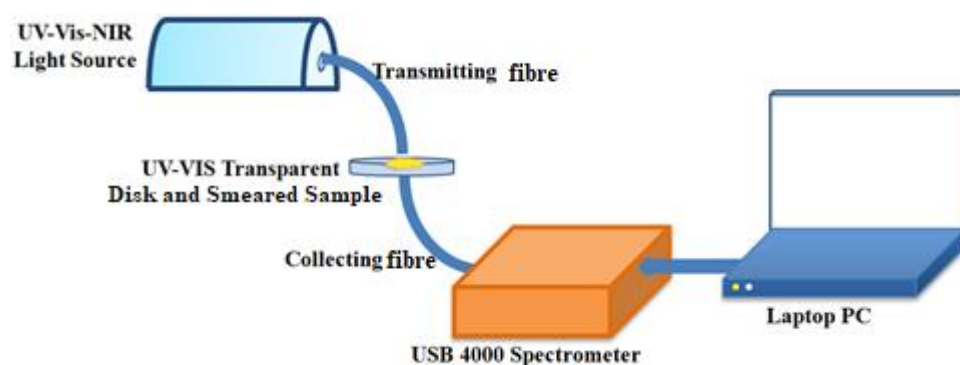


Figure 14: Experimental set-up for optical transmission measurement of honey samples

Each honey sample was uniformly smeared as a thin layer on a UV-Vis Transparent glass disk for transmission measurements. For each measure, light

from the optical source via one of the optical fibre cables is incident on the smeared honey sample. A second optical fibre, positioned beneath a glass slide with the smeared honey sample on top, collects light that comes through the honey sample to the spectrometer. The spectrometer was set to record spectral data of the sample for 120 seconds at 300 ms integration time. Measurements were repeated thrice at different positions of each sample to check for reproducibility. All the spectral data were collected and saved for further processing. Background (when the light source is off) and reference spectra (when there is no sample on the UV – Vis Transparent glass disk) were initially taken and used for calculating the percentage transmission (Equation 5).

Laser-Induced Fluorescence Measurements

The experimental set-up used for the various laser-induced fluorescence measurements in this study is shown in Figure 15. The set-up comprised a 445 nm laser for the excitation (O’like, China), a 450 (+/- 20) nm high pass edge filter (Edmund Optics, US), a USB 2000 spectrometer (Ocean Optics, Germany) and two optical fibre cables.

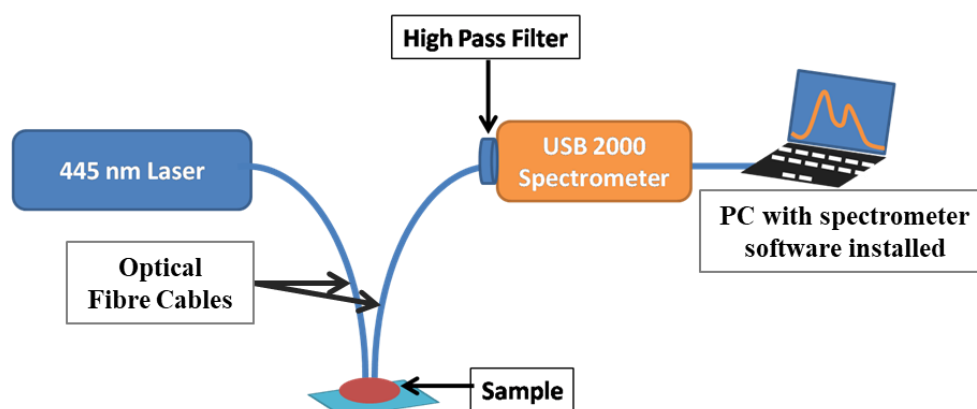


Figure 15: Experimental set-up for Laser Induced Fluorescence measurement of honey samples

The fluorescence spectra of the honey and other samples were obtained using the front-face fluorescence technique. Light from the laser is delivered to the sample through one of the optical fibre cables, and the other collects the backscattered light from the sample through the high pass filter into the spectrometer. The spectrometer, therefore, only recorded photons with longer wavelengths than the excitation wavelength. The spectrometer was set to record spectra data of the sample for 120 seconds at 300 ms integration time, providing ~293 spectra. All 293 spectra from each measurement were averaged to become a representative spectrum of that sample. The measurements were repeated thrice to check for reproducibility. The spectra data were collected and saved for post-processing and further analysis.

The LIF set-up was used in measuring the spectra of honey samples under different conditions, including heating, ageing, water dilution, and sugar caramel adulteration. For the heating effect, two honey samples (H1 and H2) were selected and heated at the same temperature (40 °C) in a water bath. By direct heating, their fluorescence spectra were compared with the non-heated honey samples. Also, for sugar caramel adulteration, sugar caramel was prepared by heating table sugar until it darkened like honey. the caramel was mixed in 50%, 30%, 20% and 10% ratio with honey sample H1 and sample H6. The ageing study was done with honey sample H1 and sample H6. The LIF spectra of the two honey samples were initially measured upon harvest and when stored in room conditions for four months (2019), one year (2020) and three years (2022). Sample V was also studied to compare the effect of adding water to honey. Water was added in different ratios (25% and 50%) to the honey and compared.

Other Measurements and Related Experimental Instruments Used

Other measures conducted on the honey samples during the study include the determination of the Brix, moisture contents, colour and 5-Hydroxymethylfurfural.

Brix and Moisture Content Measurements

The Brix and Moisture contents of the honey samples were determined using the hand-held digital refractometer device shown in Figure 16. The device features a sample compartment with a cover, display screen, and three buttons; READ, CAL, and SCALE. A few drops were placed in the sample compartment and covered with a dark lid to measure the Brix and moisture of the honey sample. The display screen then shows the values obtained from the measurement by pressing the READ button. Pressing the SCAN button alternates the readout on the screen between Brix, Moisture and refractive index. Before each measurement, the device had to be calibrated by putting a drop of distilled water on the glass in the sample compartment and covering it with the lid while holding on to the CAL button. The device is well calibrated and ready for measurement if the refractive index reads 1.444, 0.000 for Brix and OL (overload) for Moisture. To ensure accuracy, the measurements were repeated three times for each sample.



Figure 16: The Digital Refractometer used in measuring the Brix and Moisture levels in the Honey samples

Colour Measurement

The colour of each honey sample was measured by the spectrophotometric approach using a software-controlled JENWAY 7315, S/N – 59681 UV-Visible Spectrophotometer (Cole-Palmer, USA). The measurement was done by carefully dispensing into two different 10-mm quartz cuvettes the pure honey sample and distilled water as blank, respectively. The absorbance of each sample was measured at 560 nm and multiplied by a factor of 3.15 to compare to the sample result range in the literature (Frasco, 2018).

HMF Content Measurements with HPLC

High-Performance Liquid Chromatography (HPLC) was employed to determine the content of Hydroxymethylfurfural (HMF) in the honey samples at the Central Laboratory of the Kwame Nkrumah University of Science and Technology (KNUST). Fifteen samples were randomly selected out of the total number of samples for the study. The selected samples were put into zip lock bags and stored in the fridge at 4 °C before measurement using the QuEChERS

method. Firstly, the samples were homogenised, and 5g of each sample (test sample) was weighed and spiked with (13 C) internal standard solutions into falcon tubes. Afterwards, 10 mL deionised H₂O, 10 mL acetonitrile and acetic acid (ratio 9+1) were added, centrifuged in tubes for 10 min at 300 rpm, and 5 g QuEChERS salts (MgSO₄/ NaCl (4+1; w/w)) added. The centrifuged solution was mixed by tapping to prevent lump formation and placed on a mechanical shaker for 10 min. The mixture was subjected to centrifugation at a speed of 4000 × g for 1 minute, followed by the collection of a 5 mL aliquot acetonitrile supernatant and defat with 5 mL hexane. The defat supernatant was again placed on a mechanical shaker for 10 min, centrifuged at 4000 rpm for 1 min, and the upper n-hexane phase discarded. 1 mL of the acetonitrile phase was pipetted and evaporated to dryness under a stream of nitrogen at about 40 °C. The eluents were reconstituted with 75 µL methanol 425 µL H₂O and Vortexed to mix the extract for about 5 s. A 200 uL of the supernatant is taken and injected into the HPLC system after centrifuging at 8500 rpm at room temperature for 10 min. Chromatograms from the HPLC measurement were used to determine the HMF of the honey samples.

Data Analysis

The spectral data were saved as an Excel file for each experimental method. Matlab software was mainly used for all the analysis and to create figures for various visualisations. Data obtained were preprocessed and analysed using multiple multivariate and other statistical methods.

Spectral Preprocessing

Three main preprocessing methods were employed in the study. These include spectral normalisation, deconvolution and baseline correction.

Spectral Normalisation

The spectral data from the Fluorescence, Transmission and Raman spectroscopy measurements were each normalised according to Equation (13) by the SNV method. The SNV normalised spectra were used as input for all the further analyses.

Spectral Deconvolution

To address the issue of overlapping bands in the fluorescence spectral data, spectral deconvolution was employed. This technique enabled the separation and fitting of the overlapping bands, thereby facilitating a more accurate analysis of the individual spectral components. Spectral deconvolution was performed using PeakFit software (version 4.12, SYSTAT Software Inc.). This software employs a least square minimization iteration process to ensure that the coefficient of determination (R^2) value of the fitted spectra consistently exceeds 0.995 before the fitting routine is terminated. After separating the overlapping bands, each peak was fitted to a Gaussian function to obtain peak parameters, including peak intensity, Full Width at Half Maximum (FWHM), and centre wavelength.

Spectral Baseline Correction

The SDT-RIA algorithm was applied to remove background features in all the measured Raman spectra. The SDT-RIA initially determines the magnitude of the most intense Raman peak in the input spectral data using the

second derivative approach before continuing with a smoothing iteration process to estimate and remove the fluorescence background. Figures 17-19 show the steps involved in background correction of the Raman spectra (simulated) and honey obtained using the 532 nm and 785 nm excitation, respectively.

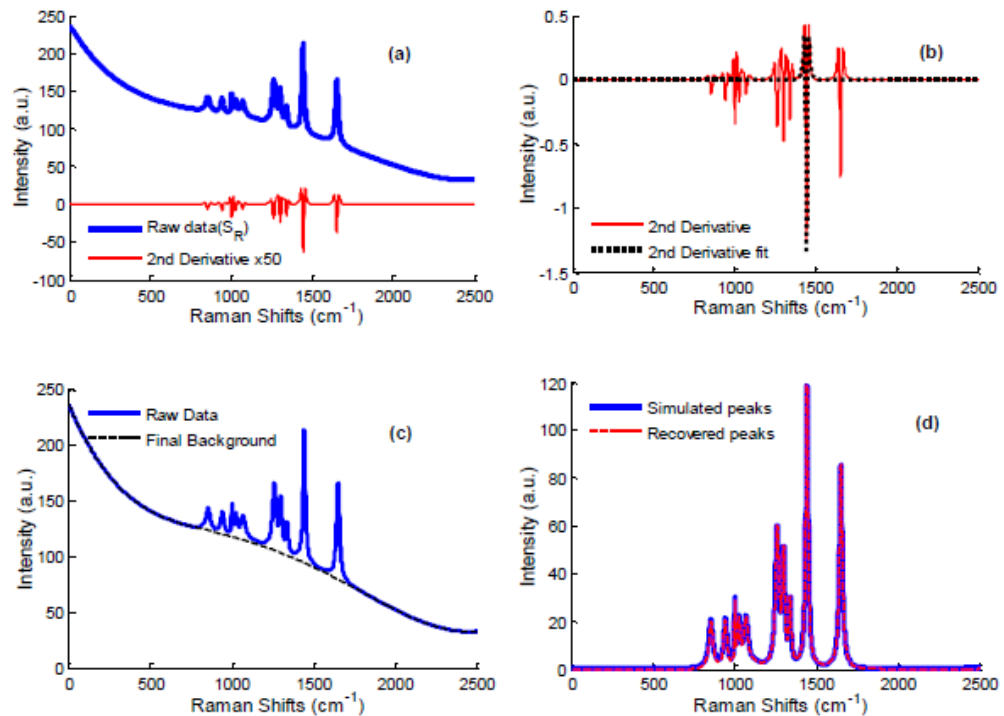


Figure 17: Raman signal recovery processes using SDT-RIA, (a) the simulated Raman spectra and its second derivative, (b) the most intense peak fitted in the second derivative spectrum, (c) how SDT-RIA estimates the background, and (d) how accurately the recovered signal compares with the original spectrum having no baseline.

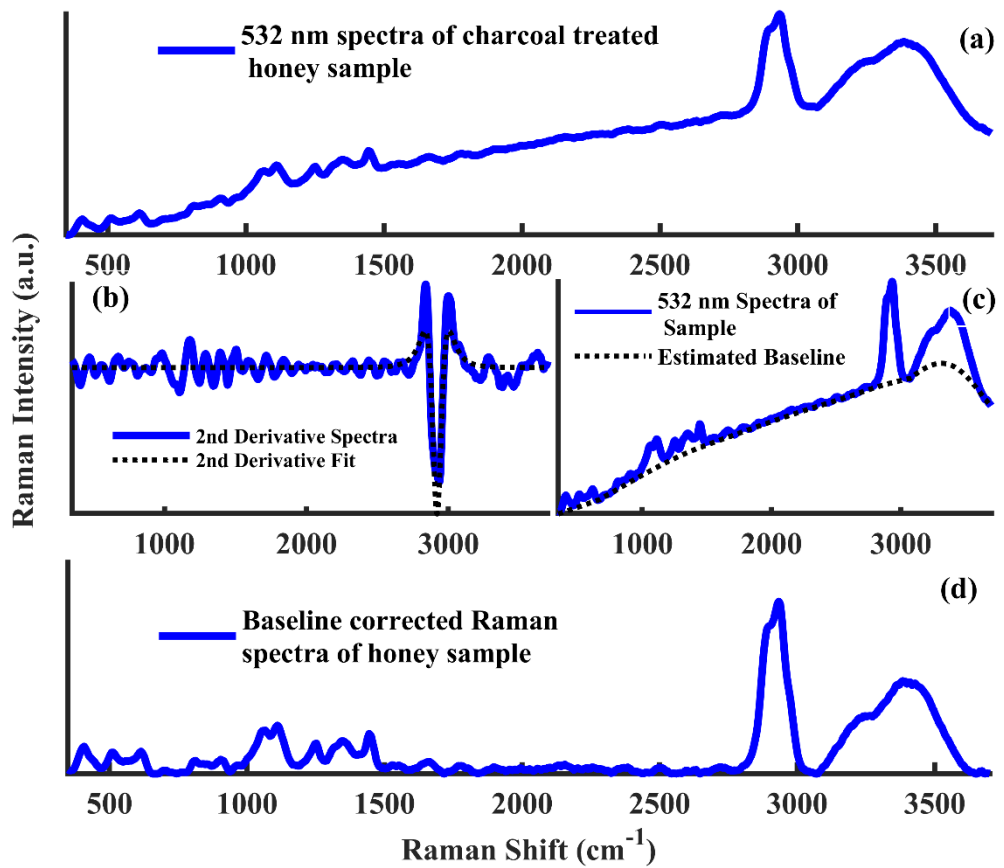


Figure 18: Baseline correction for 532 nm excited Raman spectra of charcoal treated honey. (a) Experimentally measured Raman spectra of the honey contaminated by fluorescence baseline. (b) Second derivative and fitting of the contaminated spectra to obtain peak parameters for baseline correction. (c) Estimated baseline for the contaminated spectra based on parameters of the fitting. (d) Recovered spectra after the baseline is subtracted from the experimentally measured spectra

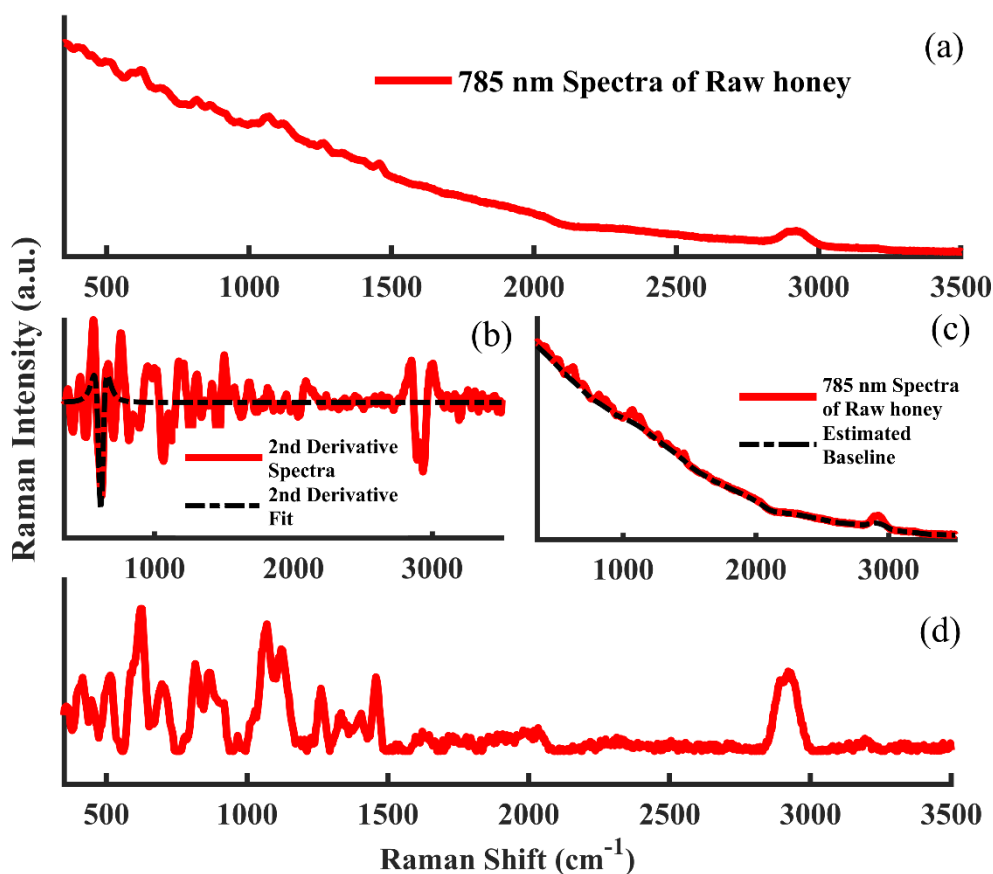


Figure 19: Baseline correction for 785 nm excited Raman spectra of charcoal treated honey. (a) experimentally measured Raman spectra of the honey contaminated by fluorescence baseline. (b) Second derivative and fitting of the of the contaminated spectra to obtain peak parameters for baseline correction. (c) Estimated baseline for the contaminated spectra based on parameters of the fitting. (d) Recovered spectra after the baseline is subtracted from the experimentally measured spectra

Multivariate Methods

The study incorporated various multivariate methods, with a main focus on principal component analysis (PCA) and K-Means clustering analysis. PCA was employed to identify significant patterns and reduce the dimensionality of the data, while K-Means clustering facilitated the grouping and classification of samples based on their similarities in the dataset.

Principal Component Analysis

PCA was applied in the case of all three optical spectroscopy measurements. PCA was performed on the input data, which had been subjected to SNV normalisation. This analysis enabled the transformation of each sample's spectrum into a singular point within the principal component (PC) space. PCA provided each spectroscopic technique's variance, scores, and loading plots. The elbow method was employed to analyse the variance plot and determine the appropriate number of PCs required to capture the most prominent variations in the data. (Cangelosi & Goriely, 2007). The scores plot enabled the visualisation of the general distribution pattern of all the samples in PC space. Furthermore, the loading plot helped to give information on the contribution of each spectral wavelength in the observed distribution from the score plot patterns. For Raman and Fluorescence measurement specifically, a PCA biplot was employed to graphically explore the distribution of the spectral scores and the loadings to identify the influence of specific molecules on the various samples.

K-means Clustering Analysis

K-means Clustering Analysis (KCA) was used to find hidden patterns in data based on feature similarity in the PCA scores for the Raman and Transmission measurement. The cluster silhouette (Equation 16) and Davies-Bouldin (Equation 17) evaluation methods were used to determine the optimal number of clusters (K).

Additional Statistical Analysis

Apart from the implementation of PCA and KCA, various other statistical analyses were conducted in the study. These encompassed calculations such as mean, Coefficient of Variation (CV), Pearson correlation coefficient, R^2 value, and Analysis of Variance (ANOVA). These statistical measures facilitated the examination of central tendencies, variabilities, relationships, and significant differences within the dataset. ANOVA was used to determine the significance of the relation between fluorescence peak spectral parameters (intensity, FHM, centre, wavelength) and the measured physicochemical parameters (Color, Brix and Moisture, HMF). Also, ANOVA was used to determine significant groups in honey clusters found after applying the K-Means Clustering on PCA analysed data from the transmission measurement.

Chapter Summary

This chapter detailed the study's samples, experimental setups, measurements, and how measured data were analysed. The samples comprised 32 types of honey, an HMF standard, and caramelised sugar, clearly explaining how they were obtained. The experimental measurements for Raman, fluorescence, and UV-visible transmission, were described in detail, along with the setups and components used for each technique. The study's data analysis methods were explained in detail, including preprocessing methods for normalisation, baseline correction, and spectral deconvolution. The multivariate methods of PCA and K-means clustering, in addition to other statistical analyses

employed in the study, Overall, this chapter provided a comprehensive overview of the study's techniques and methods.

CHAPTER FOUR

RESULTS AND DISCUSSION

Introduction

This chapter describes and discusses the results obtained using spectroscopic techniques and multivariate analysis methods. Specifically, the outcome of the Laser-Induced Fluorescence (LIF) measurement for different conditions of honey and the LIF spectra's relation with some physicochemical properties are discussed. Also, Raman spectroscopic technique has been used to observe and analyse honey's molecular composition. Additionally, the transmission method was used to examine the constituents of the honey for classification. With each spectroscopic technique, data obtained were processed and analysed with Multivariate methods, making it possible to divulge needed information for discussion and comparison to the literature.

Laser-Induced Fluorescence Spectra

The LIF spectra of the honey samples with 445 nm excitation are shown in Figure 20. Generally, the samples' emission range was all within 450 to 720 nm, representing broad spectra.

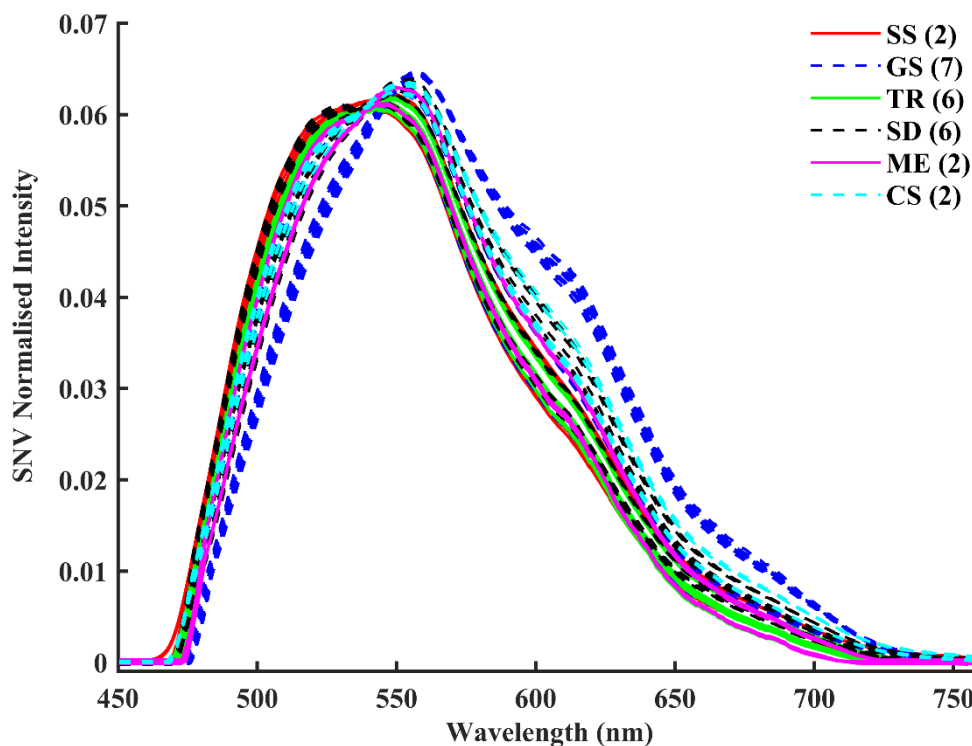


Figure 20: SNV normalised and averaged Fluorescence spectra of honey samples collected from the various agro-ecological zones of Ghana (Sudan Savana (SS), Guinea Savana (GS), Transition, zone (TS), Semi-Deciduous forest (SD), Moist Evergreen (ME) and Coastal Savana (CS)) used in the study. The number of honey samples from each Agro-ecological zone is stated in the legend

The broad fluorescence emission observed between 450–750 nm indicates the presence of polyphenols in honey samples (Parri et al., 2020). The various polyphenols responsible for fluorescence emission within the 450 to 750 nm range of the honey samples used in this study are similar to that in the literature, as summarised in Table 3. Variations in the shape of these fluorescence spectra can be attributed to different quantities of the polyphenols in each honey sample. From the LIF spectra, it can be observed that each sample had a slightly different spectral line shape from others, even though some had closer semblance by visual inspection. As observed from Figure 20, there are variations in the intensity of the LIF spectra of the honey samples, especially

the regions between 450 nm to 550 nm and 550 nm to 750 nm. The intensity variations in these regions imply that quantities of honey's underlying constituents or fluorophores varied from one sample to another.

Principal Component Analysis of the 445 nm Fluorescence Spectra

The results of the principal component analysis (PCA) on the fluorescence data set of all the honey samples are shown in Figure 21. The PCA results are described by the variance (Figure 21a), scores (Figure 21b), and loadings plot (Figure 21c-e).

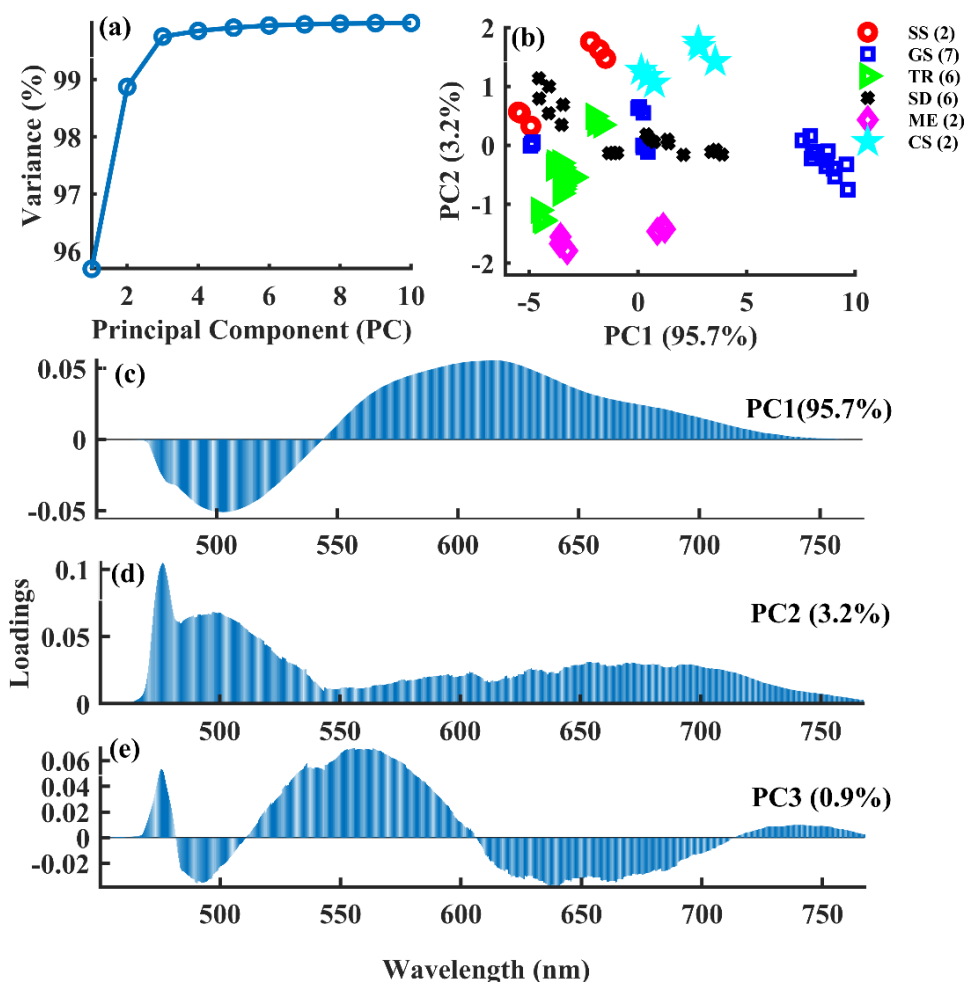


Figure 21: Principal component analysis of fluorescence spectra of honey samples showing the variance plot (a), score plot for PC2 against PC1 of samples from different Agro-ecological zones with the respective number of samples from each agro-ecological zone described in the legend (b), and the loadings plot for PC1-PC3 (c-e)

Using the elbow method, the total variance in the data was found mainly with the first three principal components (99.4%), as shown in Figure 21a. The first principal component (PC1) alone accounted for almost 92.0 % of the variance in the data, followed by 5.8% in PC2 and 1.9 % in PC3. The remaining PCs accounted for no more than 0.5% variation in the data. Thus, the entire data set of the honey samples' fluorescence spectra can be summarised with the first two or three PCs for further analysis.

The scores are randomly scattered in the score plot (Figure 21b) comprising the first two PCs, with no apparent clusters observed. The random distribution of the data emphasises heterogeneity in the composition of all the samples. The loading plot, as shown for PC1, PC2 and PC3 in Figure 21(c-e), identified the main wavelengths responsible for the observed distributions in the score plot. Wavelengths with the highest coefficients in absolute terms (negative and positive direction) were the most critical variables. The loading results are therefore summarised in Table 7 by listing all significant ranges with their respective peak centre wavelengths at which the highest loading coefficient value is observed.

Table 7: PCA Loading Ranges and Peak Centres

Principal Components (PCs)	Ranges (nm)	Peak Centre (nm)
PC1	460 – 540	500
	525 – 730	600
PC2	460 – 530	475, 488
	530 – 570	544
	570 – 760	650
PC3	465 – 480	475
	480 – 500	488
	500 – 600	535, 550
	600 – 690	620, 640
	690 – 760	730

Source: This study

The loadings highlighted by the various ranges of PC1, PC2, and PC3 can be attributed to the different molecules bringing about variations in the honey samples. According to the table, the honey samples could be distinguished based on two main ranges with reference to 500 nm and 600 nm as central peak wavelengths bringing about variations for PC1. In contrast, PC2 and PC3 show four and seven major peak centres, respectively, as the basis for

the differences in the honey samples. The major peak wavelengths for PC1, PC2 and PC3 are shown in Table 7.

Based on Table 7, a PCA biplot was employed to graphically explore the distribution of the spectral scores with the wavelengths (specific fluorophores) of the fluorescence spectra in the honey samples in Figure 22. In the biplot, the various wavelengths are plotted together with their respective spectral scores showing their influence depending on how further they occur from the origin. As presented by the biplot, the samples' distribution of the molecules is described qualitatively based on which quadrant a sample appears and semi-quantitatively based on the direction of the axis where a sample occurs. The specific wavelengths with known related molecular constituents are shown in green.

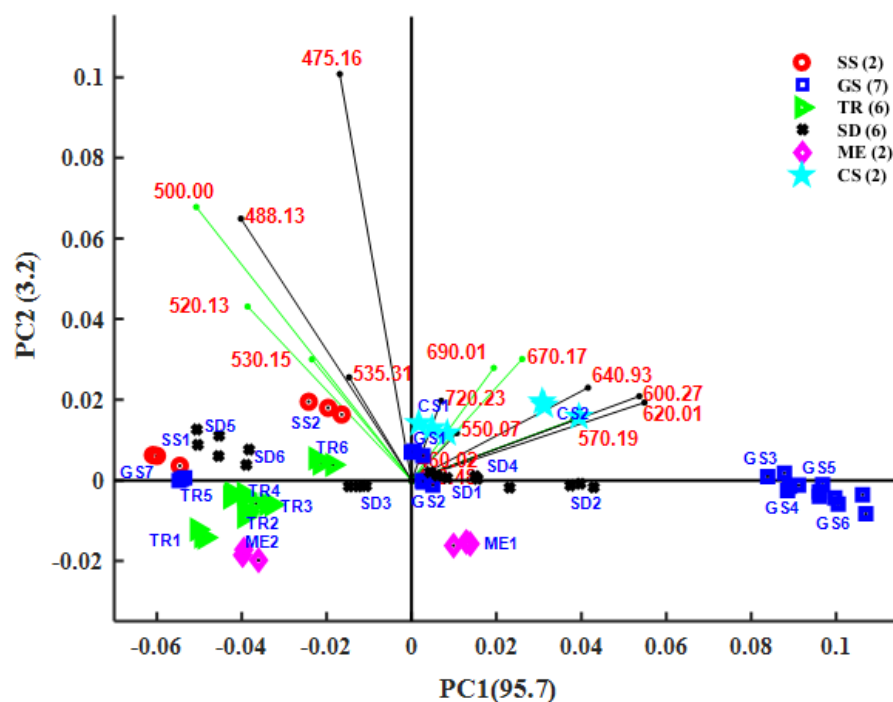


Figure 22: PCA Biplot showing PC1 and PC2 score distribution with loading coefficients of identified fluorophores in honey

In the first quadrant, for example, along the PC1 axis, Chlorophyll derivatives (670 – 720 nm) are the dominating constituents, followed by Beta carotene (570 nm) to the extreme right (positive). Samples with higher spectral scores in PC1, such as GS3, GS4, GS5 and GS6, show the dominance of these molecular constituents. On the other hand, samples such as GS7, TR1, SS1, and SD5, which occur in the longer wavelength towards negative PC1, are highly dominated mainly by O-coumaric (500 nm), a flavonoid, Quercetin (520 nm), Riboflavin (530 nm).

The levels of the phenolics (like Sina pinic acid at 450 nm) obtained were lower because of the excitation light source (445 nm) used. Flavonoids and vitamins other than proteins (including Phenols) are best probed at 445 nm excitation (Mehretie et al., 2018; Parri et al., 2020; Ruoff et al., 2005).

Deconvoluted Laser Induced Fluorescence Spectra

Spectral deconvolution was used similarly to obtain semi-quantitative information on the various constituents in the honey samples. A deconvoluted SNV-normalised fluorescence spectrum of a honey sample is shown in Figure 23a. The deconvoluted spectra revealed the presence of five prominent peaks. Peaks were selected based on the shoulders observed from the spectra and prior knowledge of possible molecular species in the literature (Parri et al., 2020). Significant regions were defined by the loadings in the PCA, as well as prior knowledge about the constituents of honey within the 450 to 750 nm fluorescence range. The spectral parameters, i.e., Intensity, centre wavelength, Full Width at Half Maximum (FWHM) and area, derived from each peak, are

compared among the samples and correlated with different physicochemical properties of the honey.

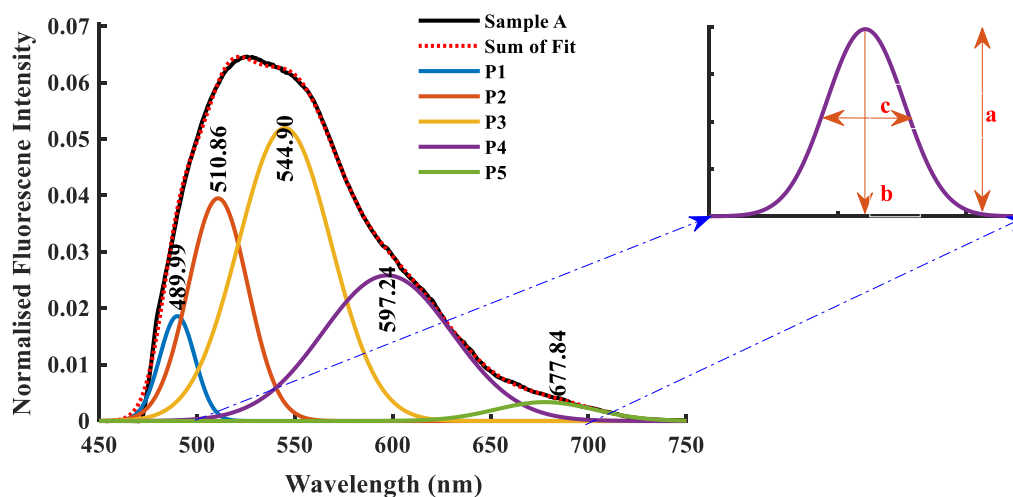


Figure 23: Deconvoluted SNV normalised LIF spectra of one of the honey samples showing peaks of possible emissions from fluorophores, with an inset demarcating the peak parameters (a = Intensity, b = Full Width at Half Maximum, c = Centre wavelength)

The five prominent peaks derived from the deconvolution given the label P1 (489.9 nm), P2 (510.8 nm), P3 (544.9 nm), P4 (597.2 nm), and P5 (677.8 nm) are summarized for the entire samples in Table 8. Also, they are labelled with the respective biochemical compounds present as indicated.

Table 8: Spectral Parameters from the five bands of the Deconvoluted LIF spectra of the samples

Peak	Spectral Parameters	Range (Min-Max)		Mean	Standard Deviation	Coefficient of Variation
P1	Intensity	0.39	0.88	0.60	0.13	0.21
	Wavelength (nm)	485.03	492.94	489.96	1.49	0.00
	Width (nm)	11.28	16.22	13.90	1.19	0.09
P2	Intensity	1.09	1.89	1.52	0.18	0.12
	Wavelength (nm)	506.98	514.54	511.30	1.77	0.00
	Width (nm)	20.46	24.67	22.42	0.84	0.04
P3	Intensity	2.13	2.62	2.43	0.13	0.05
	Wavelength (nm)	541.84	552.23	547.65	2.92	0.01
	Width (nm)	31.33	36.69	34.22	1.07	0.03
P4	Intensity	0.86	1.79	1.26	0.22	0.18
	Wavelength (nm)	592.77	608.72	601.42	3.74	0.01
	Width (nm)	35.78	48.66	42.27	3.05	0.07
P5	Intensity	0.03	0.43	0.22	0.10	0.43
	Wavelength (nm)	655.67	680.21	671.07	4.90	0.01
	Width (nm)	24.14	52.28	38.28	6.76	0.18

Source: This study

Like the PCA results described in Table 7, the deconvoluted fluorescence spectra of the honey samples also help to observe better the presence of the significant biochemicals in the honey samples. A comparison of the CV shows that samples did not vary much except for the intensity of the 5th Peak. The less variation in all the peak positions (0.00 – 0.01) shows that honey samples had almost the same significant constituents. The peak width (0.03 – 0.18) remained relatively broad for all the samples, possibly due to numerous closely related fluorophores in the honey samples. The width of the 5th Peak, which recorded the most variance (0.18) compared to all the other peaks, is the fluorescence emission from chlorophyll. This peak thus reveals

differences in the chlorophyll concentrations in the honey samples, which can be attributed to floral differences (Parri et al., 2020; Ruoff et al., 2005).

Correlation of Deconvolved LIF Spectra with Brix, Moisture and Colour of Honey

Physicochemical parameters are essential for evaluating honey (Mehryar et al., 2013). The correlation between the measured physicochemical parameters, Brix, Moisture colour and the deconvolved spectral peak intensity (a), width (b), position (c) and area (d) are shown in Figure 24.

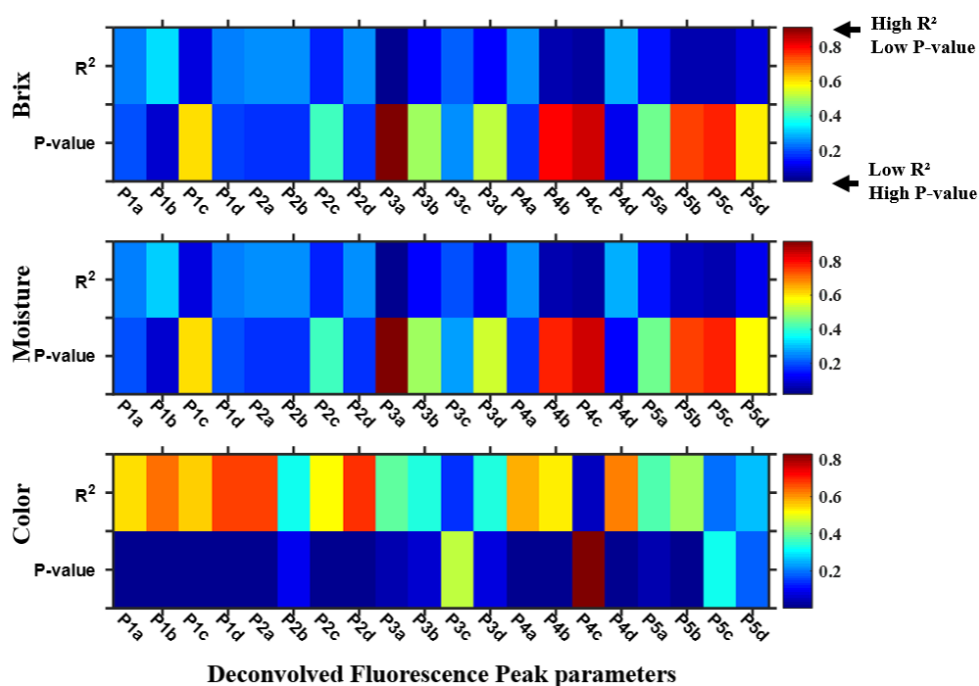


Figure 24: Correlation coefficient (R^2) and Significance (P-value) for the correlation between physicochemical parameters; Brix, Moisture, Color, and deconvolved LIF spectral parameters shown by a colour map. P1, P2, P3, P4, and P5 represent each deconvolved peak, while the alphabets a, b, c and d represent each peak's intensity, wavelength, width and area, respectively.

From Figure 24, Brix and moisture had a very low correlation with all the peak parameters, which indicates that the LIF method will be less informative about honey's Brix (sweetness) or moisture content. The colour

parameter, however, showed a significantly high correlation with most of the peak parameters, notably Peak 1, Peak 2 and Peak 4. These peak parameters could further be used in modelling to predict honey colour.

LIF Monitoring of Honey Quality via 5-Hydroxymethylfufural (HMF)

Honey quality determination with the LIF method is demonstrated. The LIF spectra of honey samples (14, i.e. A-N) selected from different years, including one non-honey sample (O), are shown in Figure 25. The concentration of the HMF, as determined by HPLC, is shown in the legend of the LIF spectra. The figure is colour-mapped so that samples having lower HMF show cool colours (blue to cyan), while those with higher HMF offer hot colours (yellow to red). The HPLC spectra of the honey samples from which the actual HMF was obtained are reported in Appendices A and B.

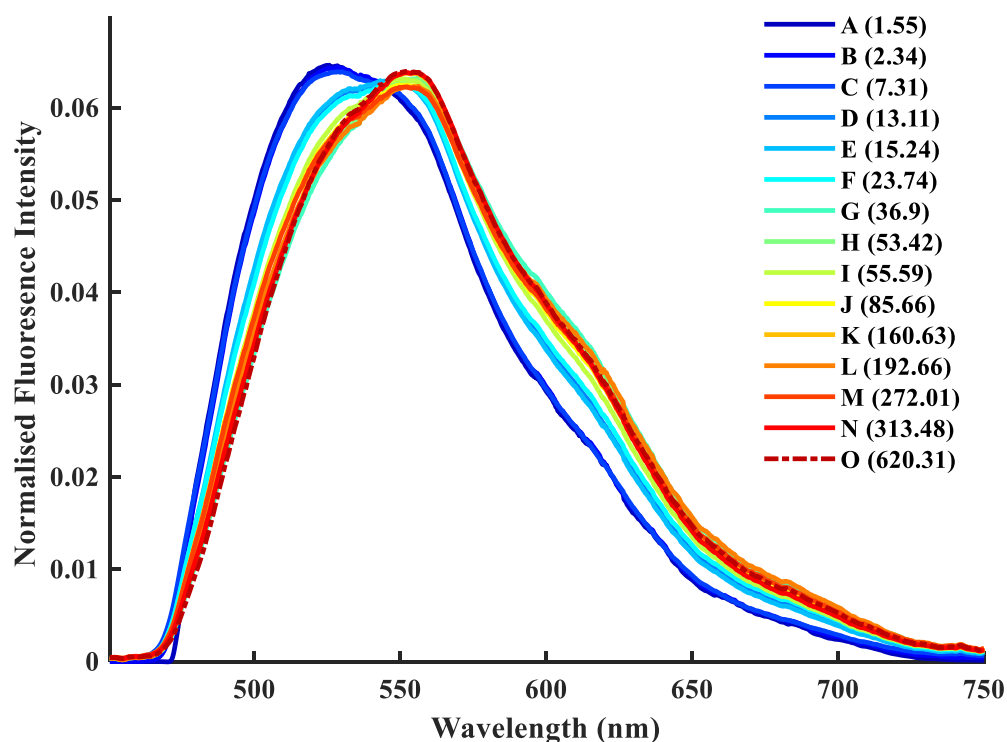


Figure 25: Normalised LIF spectra of honey samples selected from different years to study their HMF. Each spectrum is colour mapped in order of the HMF value, as indicated in the legend

Visual inspection of Figure 25 reveals contrasting differences between honey samples. Samples having HMF with low (A - F), moderate (G - I) and high (J - O) concentrations can easily be distinguished at some wavelength ranges of the LIF spectra. These differences were further analysed by correlating actual HMF concentration with the spectra parameters by deconvoluting their LIF spectra and finding parameters with a significant correlation (p-value < 0.005), as shown in Table 9.

Table 9: The p-values obtained by correlating deconvoluted LIF spectral parameters with measured HMF of samples

Sample	HMF	P-value														
Set	(mg/100g)	P1a	P1b	P1c	P2a	P2b	P2c	P3a	P3b	P3c	P4a	P4b	P4c	P5a	P5b	P5c
A - N	1.5 - 313.4	0.04	0.03	0.15	0.02	0.02	0.37	0.75	0.03	0.83	0.90	0.04	0.14	0.04	0.15	0.15
A - J	1.5 - 85.6	0.01	0.06	0.15	0.00	0.02	0.24	0.57	0.01	0.24	0.48	0.00	0.07	0.01	0.08	0.06
A - G	1.5 - 36.9	0.00	0.07	0.11	0.00	0.00	0.16	0.59	0.01	0.67	0.54	0.01	0.09	0.00	0.08	0.06

Source: This study

For the different range of samples considered, samples from A-G with HMF of less than 40 mg/100g showed a better correlation with high significance. Also, among these samples (A-G) sets, the first band's intensity, P1a, showed very high significance (p=0.001). A graph of the P1a values obtained with the LIF data correlated with actual HMF concentration shown in Figure 26a produced a 0.92 correlation coefficient with a linear equation given as $HMF = -4435.700 (\text{Normalised Fluorescence Intensity}) + 89.015$. As a validation step, a leave-one-out cross-validation (LOOCV) test applied on the dataset predicted each HMF value, which, when correlated against the HPLC-measured HMF of the samples, yielded a 0.87 correlation coefficient.

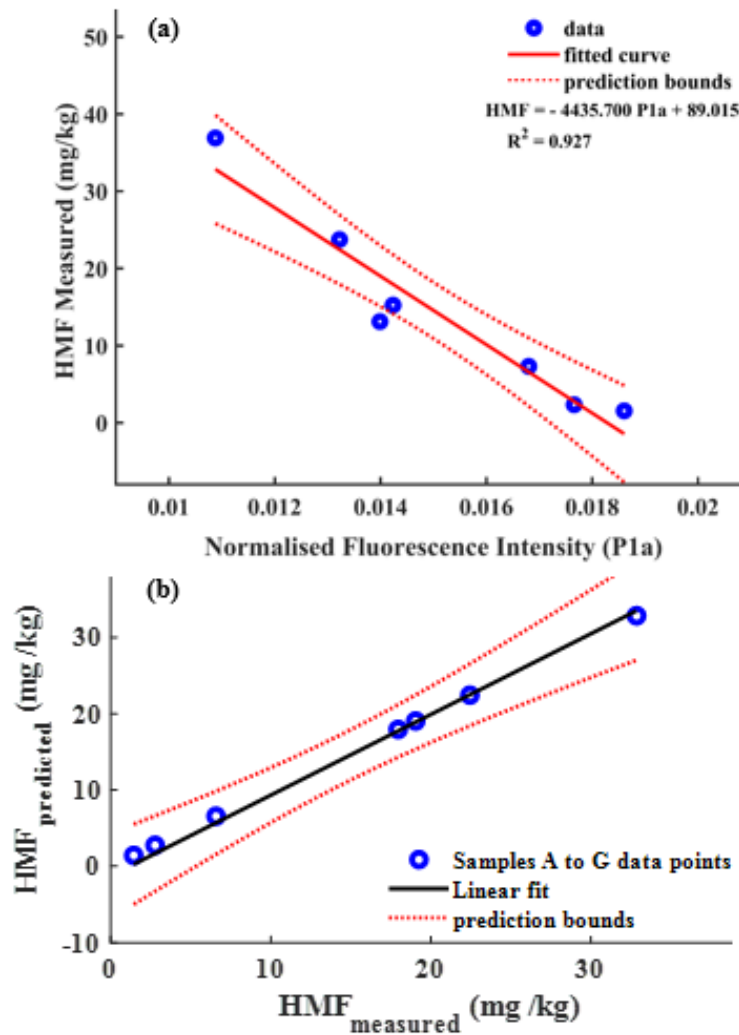


Figure 26: Correlation between (a) deconvolved LIF Peak 1a intensity with HPLC measured HMF for samples with HMF concentration below 40 mg/kg and (b) HPLC Measured HMF with Predicted HMF by the Peak 1a

The results from the correlation show that the HMF of the honey can be determined for honey with HMF up to 40 mg/ 100g, which qualifies this process for determining the quality of honey for temperate regions where the allowed limits are set to 40 mg/ 100g.

LIF Spectra of Harvested Honey under Different Conditions (Heating, Ageing, Water and Sugar Adulteration)

LIF spectra of two freshly harvested Honey samples are shown in Figure 27. The slight difference between the two spectra is expected because of the variabilities associated with honey due to geographical, entomological, seasonal and hive practices. Changes in the spectra of each sample after four months, one year and three years are shown in Figure 28.

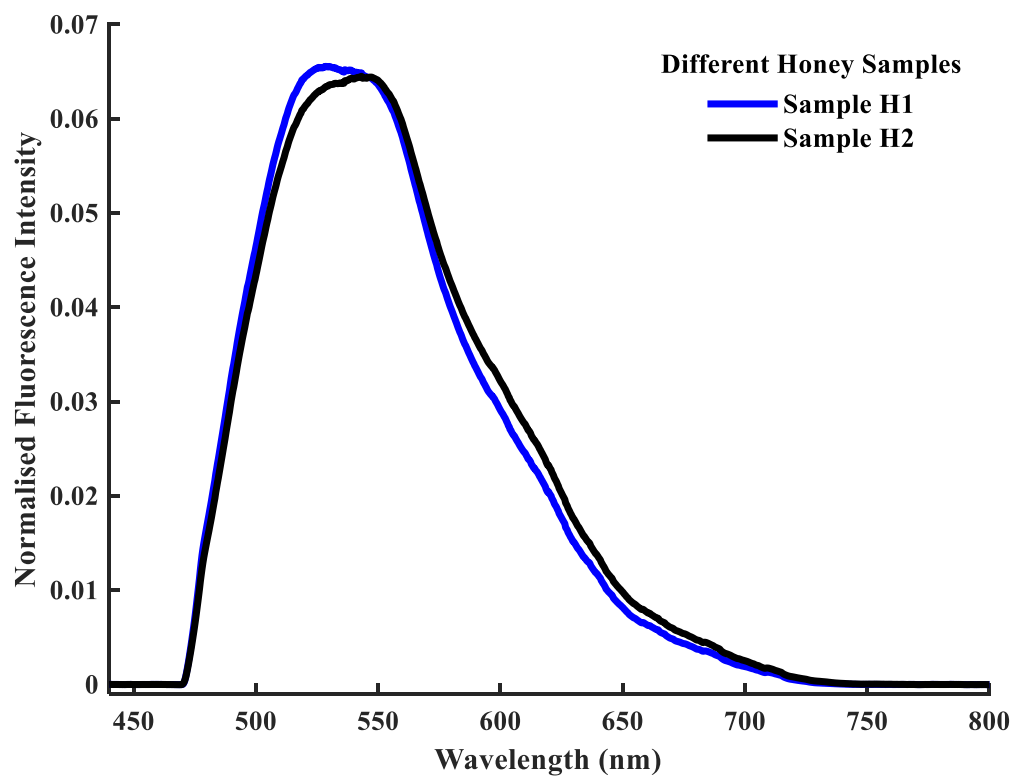


Figure 27: LIF spectra of two freshly harvested Honey samples used for ageing studies

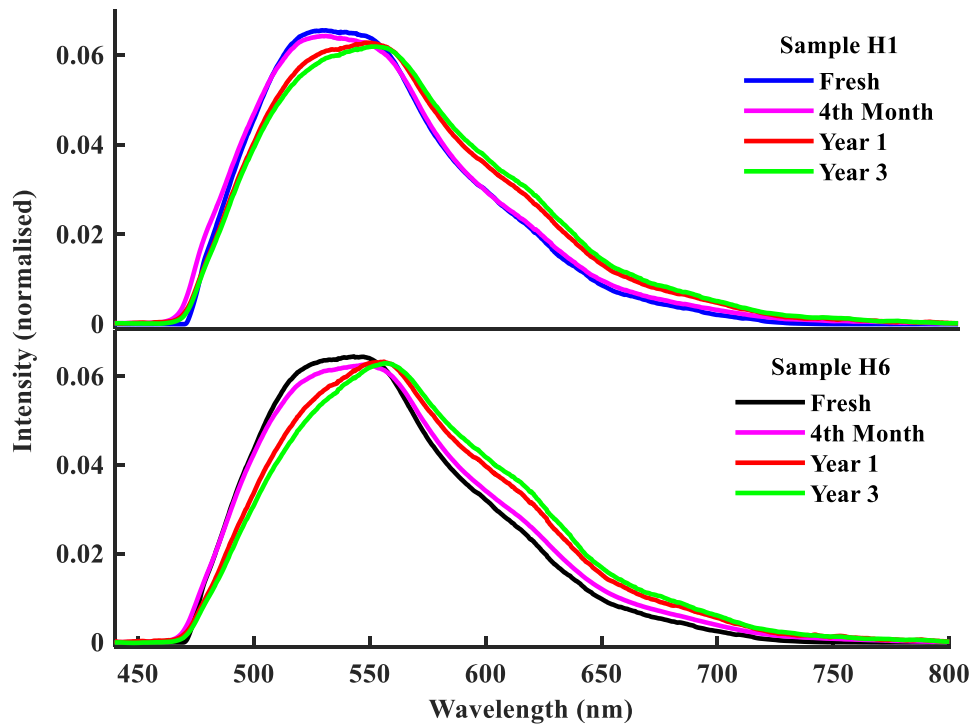


Figure 28: LIF spectra of honey samples measured at different times from the harvesting period to 3 years

From Figure 28, significant changes in both samples can be observed after the first year onwards compared to the first four months. These changes are red-shifted for both samples, associated with increasing molecular weights of the honey samples (Cuss & Guéguen, 2015; Ye et al., 2011). Bong et al. (2016) study identified the changing constituent as Millard reaction agents, which could be used as spectral markers for age determination.

The effect of heating honey demonstrated with samples H1 and H6 is shown in Figure 29. For the two samples, the impact of the heating is observed to be quite similar for the two honey samples. Nevertheless, changes in the spectral line shape with heating were identical to those due to ageing, as shown in Figure 28.

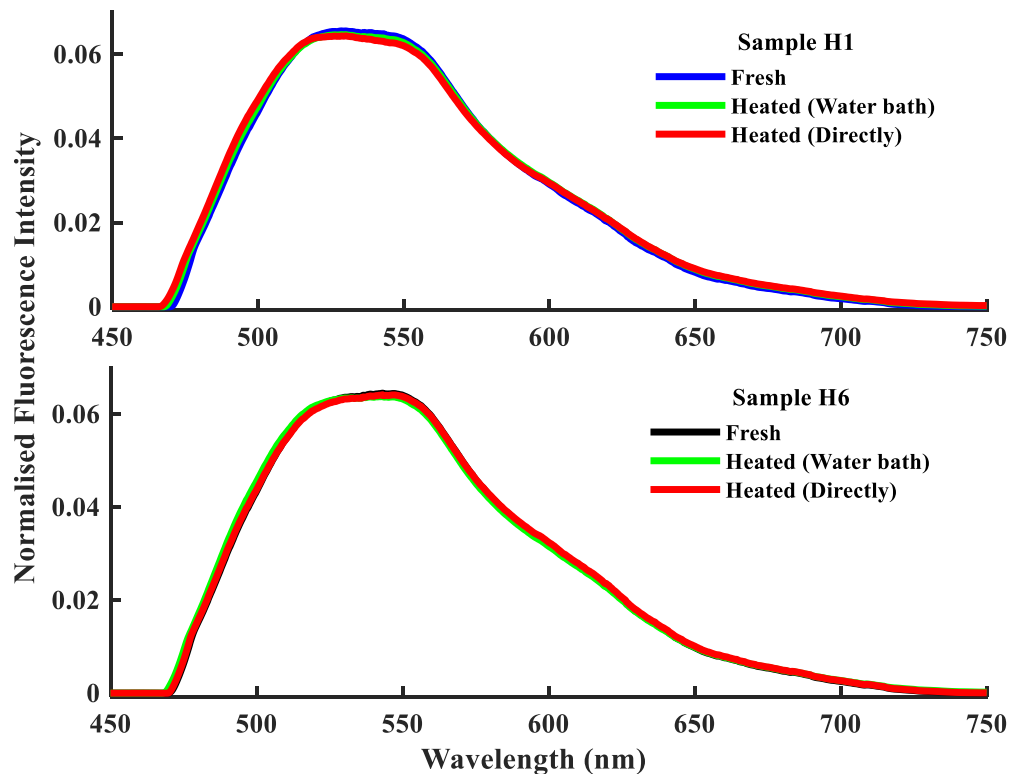


Figure 29: LIF spectra of honey heated in different methods

The changes in the LIF spectra of honey due to water addition are observed in Figure 30. The LIF spectrum obtained by measuring distilled water is included for comparison.

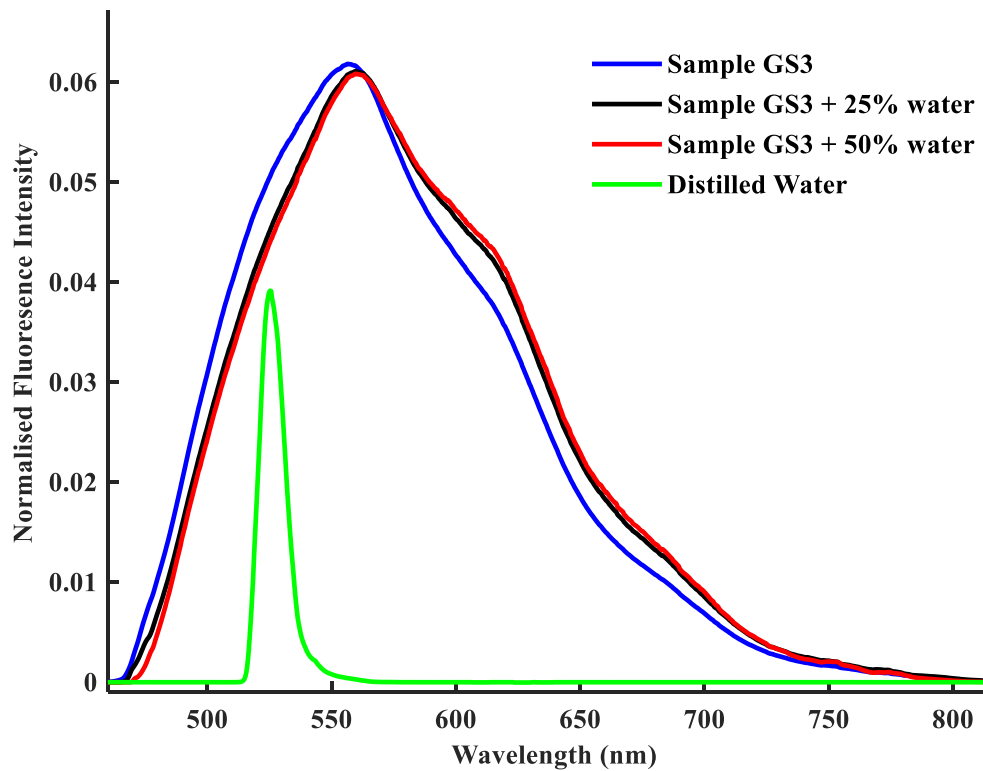


Figure 30: LIF spectra of fresh honey, water-diluted honey samples and distilled water for comparison

Interestingly, these changes did not occur in the same wavelength region as the LIF spectra of the distilled water. Instead, the observed changes are red-shifted, similar to that observed in the ageing honey samples (Figure 28). Again, sharp differences can be observed in the raw spectra of the honey irrespective of how much water (25% or 50%) was added. However, there is not much difference in the spectra for different quantities of water added. Thus, adding water to honey causes significant changes detectable by the fluorescence spectroscopic technique. Nonetheless, as observed in Figure 24, there was very little correlation between moisture content and the fluorescence spectra of honey.

Sugar Adulteration

The fluorescence spectra of honey samples (H1 and H4) with the sugar caramel adulterant are shown in Figure 31. As observed from Figure 31, the honey sample H4 has a nearly identical spectrum to the adulteration (sugar caramel).

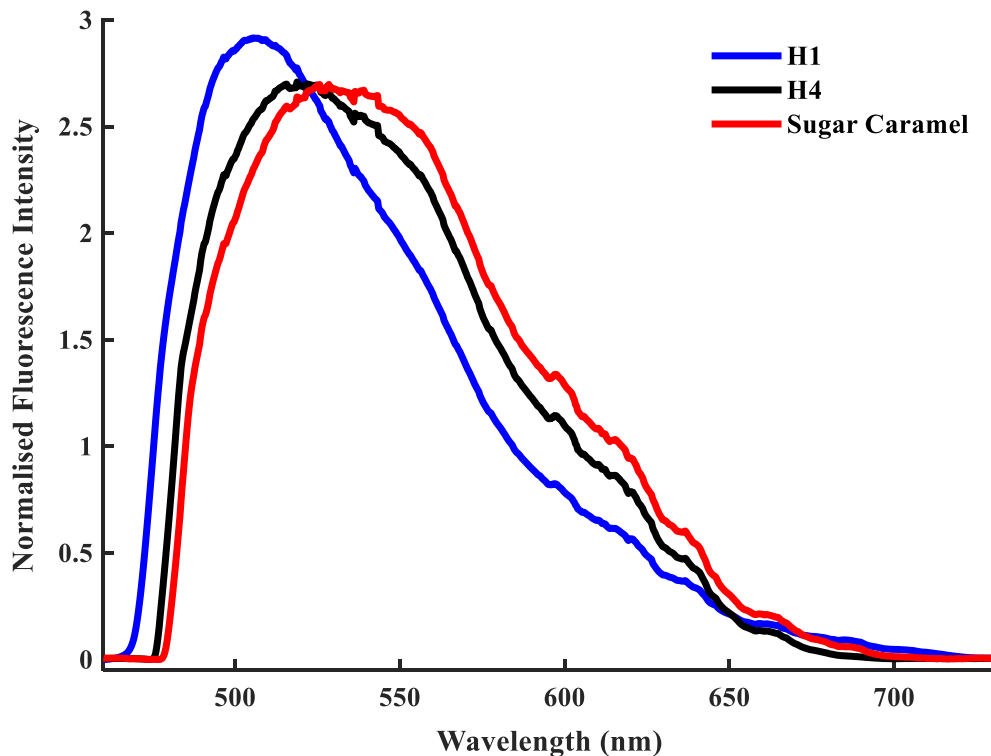


Figure 31: Spectra of selected honey samples (H1 and H4) compared with sugar caramel as a suspected adulterant

The results of the sugar caramel added to the honey samples in different concentrations (10%, 20%, and 50%) are shown in Figure 32. Generally, changes to the LIF spectra of the adulterated honey occurred both intensity-wise and wavelength-wise. This effect can be well observed better for sample H1 as compared to H4.

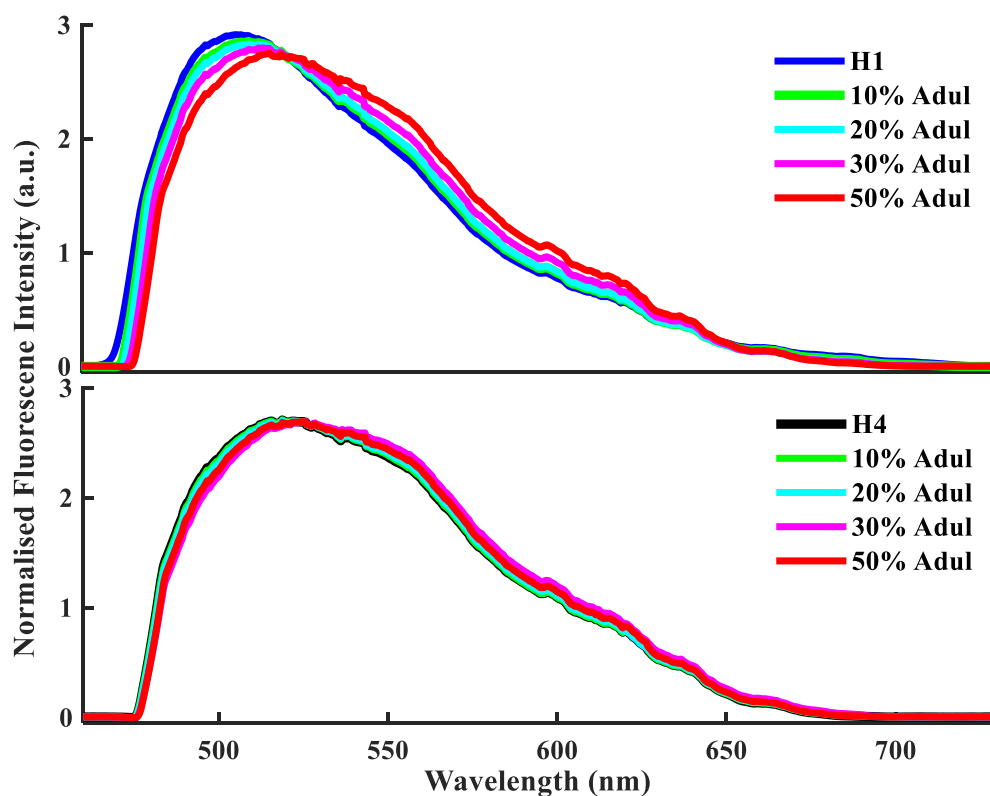


Figure 32: LIF spectra of two harvested Honey samples (H1 and H4) adulterated with 10, 20, 30 and 50% sugar caramel

Interestingly the LIF spectra of the sugar-adulterated honey (Figure 32) show similar features to that of the ageing honey (Figure 28). The main observation is that as the adulteration level increases, the LIF spectra are red-shifted, and the intensity decreases simultaneously relative to the fresh sample. These changes could be explained by changing molecular structure, polarity and other molecular characteristics that bring about spectral shifts in fluorescence spectra. In Figure 32, it can be observed that though the changes due to the adulteration occurred in the same direction for all the samples, the rate of change shown by the slope (Figure 33) was different for H1 and H4. This difference in the slope values indicates that the honey samples are different; therefore, all honey samples' fluorescence spectra related to adulteration changes cannot be generalised.

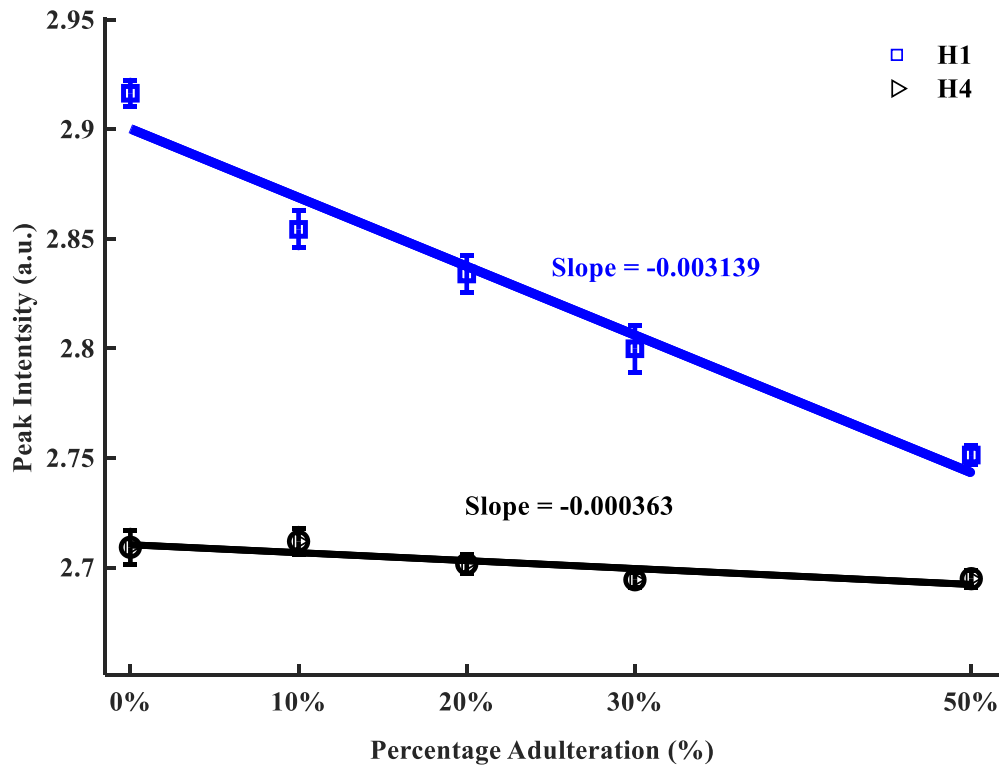


Figure 33: The plot of peak intensities against the honey level of adulteration showing the Rate of change in spectra of honey adulterated with sugar caramel

532 nm and 785 nm Excited Raman Spectra

The typical Raman spectrum of a honey sample measured with 532 and 785 nm excitation is shown in Figure 34. Both excitation sources led to Raman spectra with fluorescent background, a characteristic of Raman spectra measured with excitation sources within the visible region of the EM spectrum. The high fluorescence is because of the high energy of the excitation sources, causing electronic transitions in the honey molecules, leading to the fluorescence mechanism being observed more easily. Hence, 532 nm excitation has a high fluorescent emission such that the Raman peaks in the spectrum are almost entirely obscured (Figure 34a).

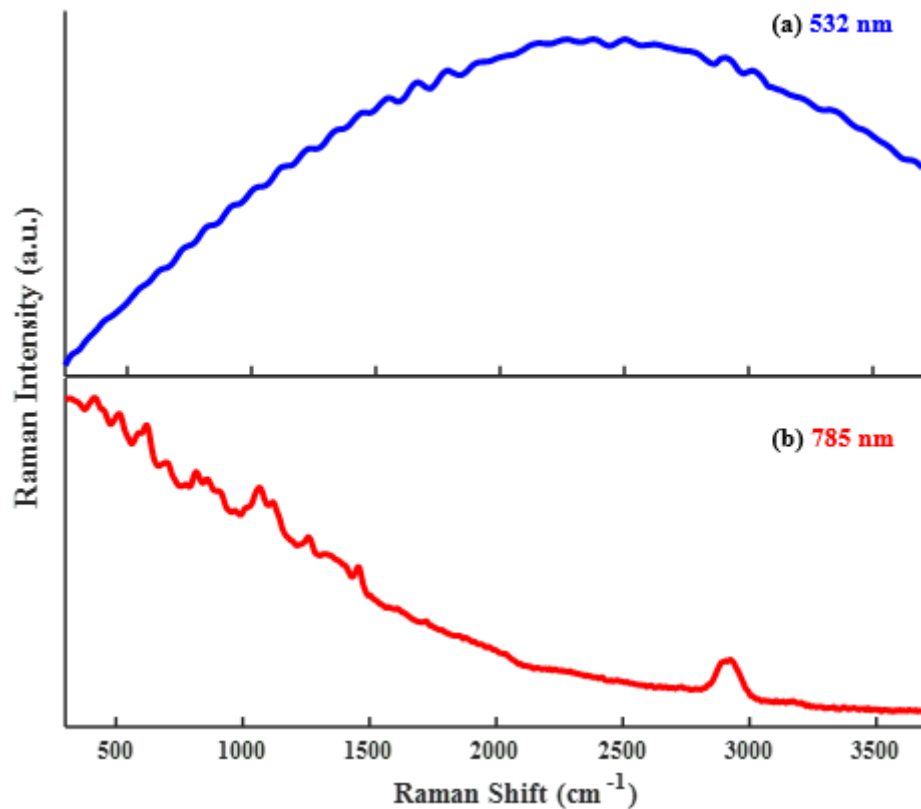


Figure 34: Raman spectra of raw honey samples acquired using different laser excitation sources of wavelengths (a) 532 nm and (b) 785 nm

A comparison between Figure 34a (532 nm excitation) and Figure 34b (785 nm excitation) reveals distinct differences in the spectral characteristics of raw honey. Figure 34a depicts an extensive and intense fluorescence background without noticeable Raman peaks. In contrast, Figure 34b illustrates the presence of Raman peaks in the honey's spectrum alongside some trailing fluorescence background. The fluorescence observed during 785 nm excitation is minimal due to the limited capability of energy within the near-infrared (NIR) region to induce electronic transitions that typically result in fluorescence.

532 nm Excited Raman Spectra of Different Pretreatments applied to Honey Samples

As described in the methodology, different pretreatment methods were applied to the samples to reduce the fluorescence background in the Raman

spectra of the honey to make the spectra data more useful for further analysis. Figure 35 clearly shows that the raw honey spectra (a) exhibits a significant and intense fluorescence background, rendering the Raman peaks indiscernible. In contrast, the pretreated samples show a reduction in the fluorescence background, thereby revealing the distinct Raman peaks of the honey.

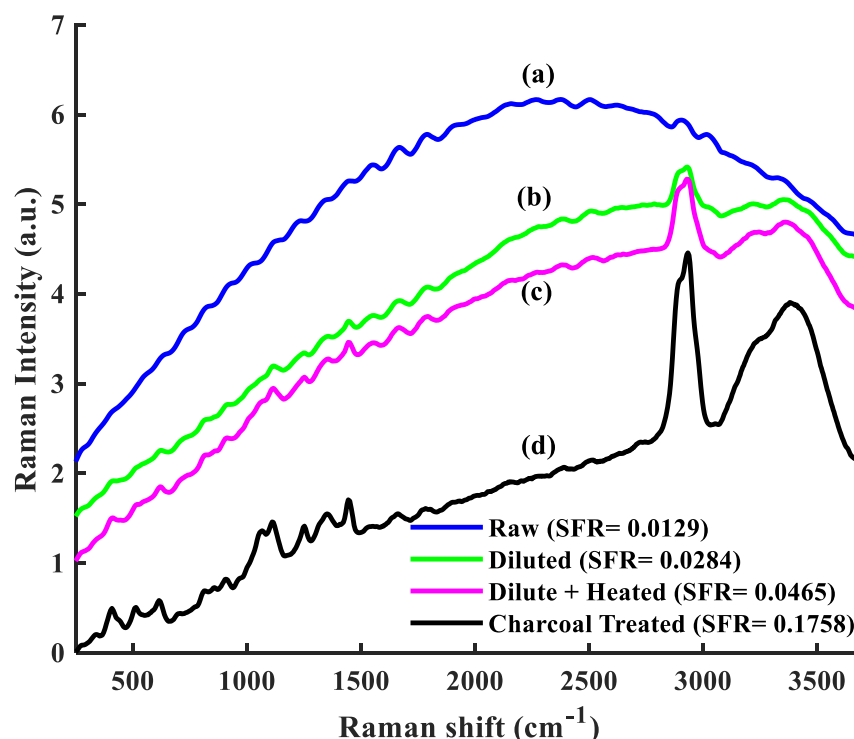


Figure 35: 532 nm excited Raman spectra obtained from (a) raw honey, (b) water diluted honey, (c) heated honey and (d) activated charcoal-treated honey with computed SFR values shown in the legend

The legend of Figure 35 provides insights into the effectiveness of reducing the fluorescence background in the Raman spectra of each pretreated honey, as evaluated by the SFR. The charcoal treatment exhibited a higher SFR value of 0.1758 compared to the other two treatments: dilution with water (0.0284) and heating after dilution with water (0.0465). Previous studies (Smart & Simpson, 2002; Smyth et al., 2001; Tatarkovič et al., 2015) have reported that activated charcoal acts as an adsorptive quencher for organic molecules

responsible for fluorescence in honey. Consequently, pretreatment involving activated charcoal enables the adsorption and removal of these fluorescent organic molecules through filtering, thereby enhancing the intensity of the honey's Raman spectra.

Figure 36 displays the corrected baseline of the Raman spectra obtained from raw and various pretreated honey samples excited using the 532 nm excitation. The figure clearly demonstrates that the baseline-corrected spectra simplifies the identification of peak positions in both the raw and pretreated honey samples. This enables an easy and straightforward comparison of the respective peak intensities between the different samples.

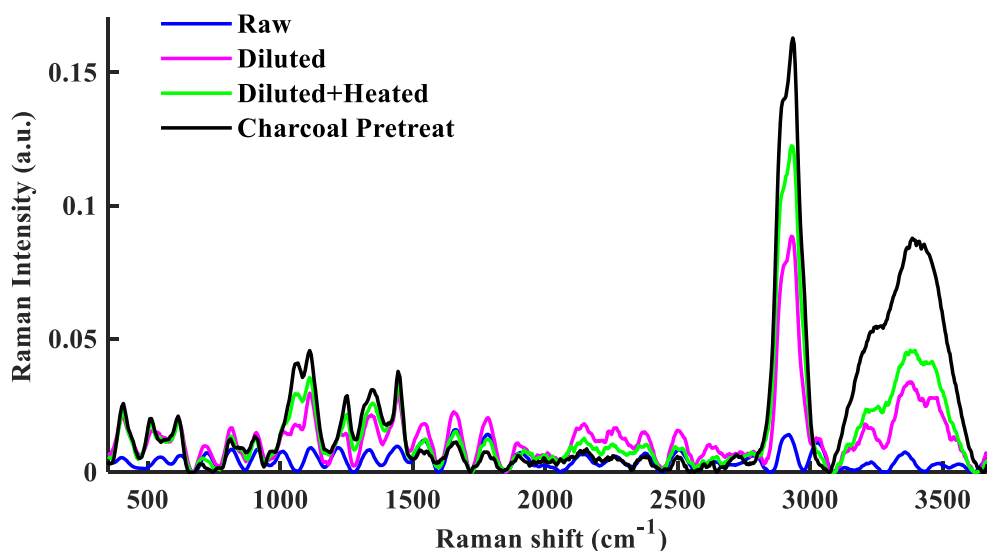


Figure 36: Comparison of baseline preprocessed 532 nm excited Raman spectra of raw and pretreated honey samples

The charcoal method was better at producing Raman spectra with fewer false peaks, as seen within the 1500 cm to 2500 cm region. The dilution method, even though it had some false peaks, can be improved for honey pretreatment as a less stressful, cost-effective and time-saving approach. Molnar et al. (2020)

have demonstrated that 50:50 v/v dilution of honey with water is also effective for fluorescence reduction (Molnar et al., 2020).

Comparison of the Preprocessed 532 nm and 785 nm Excited Raman Spectra of Honey and Molecular Assignment

Figure 37 illustrates the preprocessed Raman spectra of honey samples acquired using the 532 nm and 785 nm excitation sources, covering the range from 300 cm^{-1} to 3600 cm^{-1} . The observed spectra are consistent with the broad Raman spectra of honey reported in the literature (Anjos et al., 2018; De Oliveira et al., 2002; Tahir et al., 2017).

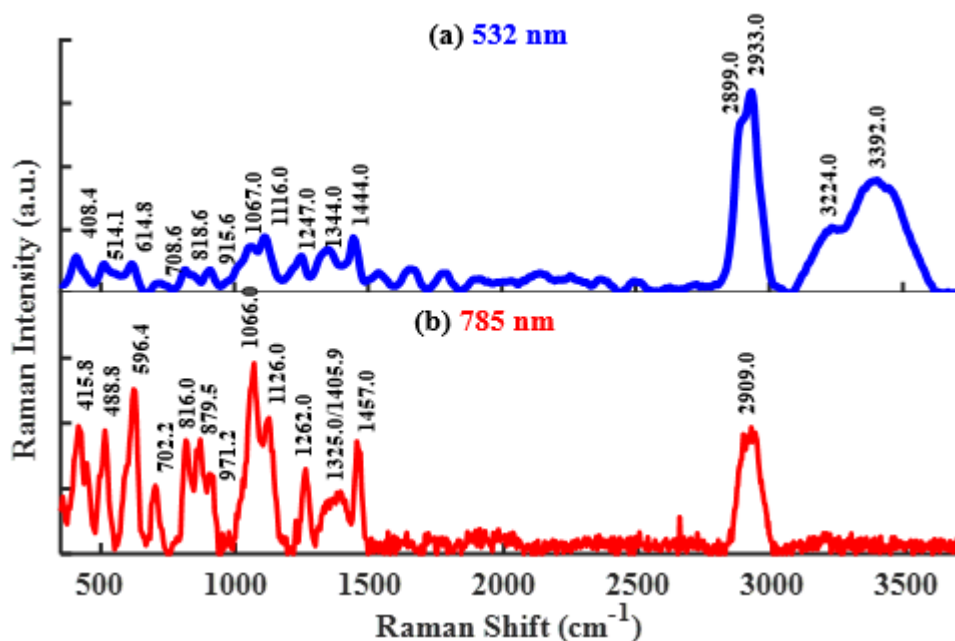


Figure 37: Raman spectra of honey samples measured under different conditions: (a) Honey subjected to activated charcoal pretreatment, measured with a 532 nm laser excitation, and (b) Honey without pretreatment, measured with a 785 nm laser excitation

The range of 300 cm^{-1} to 1500 cm^{-1} is recognised as the fingerprint region, while the range of 2600 cm^{-1} to 3600 cm^{-1} is referred to as the high wavenumber region. The 3500 cm^{-1} spectral band, in the high wavenumber

region, confirms the presence of OH molecule in the sample, which includes water (Artlett & Pask, 2015; Casella et al., 2013; Mabrouk et al., 2013; Pierna et al., 2011), because honey consists mainly of water (10 - 20 % w/w), carbohydrates (70 - 80% w/w) and other components (Ouchemoukh et al., 2007). Moisture is, therefore, inherently present in honey. Still, it is supposed to be negligible, accounting for the extremely low intensity of the 3500 cm^{-1} spectral bands in the Raman spectra obtained with the 785 nm excitation source. This spectral band had far more moderate intensity in the 785 nm excitation than the 532 nm excitation. However, this more moderate intensity is justifiable because the sample preparation method with the 532 nm excitation required that some amount of water be mixed with the honey (Šugar & Bouř, 2016), leading to some moisture level in the sample.

The Raman spectral profile of the honey exhibited distinct characteristics depending on the laser excitation used. The Raman spectra obtained with 532 nm excitation displayed a higher signal-to-noise ratio, resulting in smoother spectra with well-defined peaks. The sample preparation, including the pretreatment, contributed to the reduced noise in the 532 nm excited Raman spectra, potentially due to the homogeneous state achieved by the honey during pretreatment. In contrast, the 785 nm excited Raman spectra showed greater resolution, revealing a higher number of spectral bands compared to the 532 nm excitation. Table 10 provides an overview of the characteristic Raman bands observed in honey for both 532 nm and 785 nm laser excitations, along with distinctive Raman bands reported in the literature. These unique Raman bands serve as molecular fingerprints based on the biochemical composition of the honey samples. (Goodacre et al., 2002). The

table shows that kinds of honey generally have the same Raman spectral profile from different excitation sources and studies. Slight variations observed in the band positions can be attributed to factors such as variations in the botanical origins of the different AEZ.

Table 10: Raman spectra bands of honey obtained using a 532 nm laser compared with a 785 nm laser, and that in literature (a= (Goodacre et al., 2002), b= (Anjos et al., 2018), c= (Pierna et al., 2011) and d= (Li et al., 2012))

Excitation Wave-length (cm ⁻¹)		Reported Raman band of honey in literature (cm ⁻¹)				Possible vibration	Related sugars
532 nm	785 nm	A	B	C	D		
408.4	415.8	430	421.5	424	425	C-C-O and C-C bending	Fructose Glucose
-	488.8	460	-	449	-	Skeletal Vibration	Maltose Sucrose
514.1	-	523	520.8	519	517	C-C-O and C-C deformation	Glucose Fructose
614.8	596.4	631	625.7	630	629	Ring deformation	Fructose Sucrose
708.6	702.24	709	705.4	708	705	C-O and C-C-O stretching, O-C-O bending	Fructose
818.6	816.0	825	824.7	822	824	C-OH bending	Fructose
-	879.5	870	866.5	865	865	C-O-C Cyclic alkyl ethers	Fructose Glucose
915.6	-	918	915.1	904	915	CH, COH bending	Glucose Maltose
-	971.2	983	979.1	979	981	Ring breathing	Fructose
1067.0	1066.0	1074	1071.5	1064	1065	C-O-C stretching, C-N vibration of proteins	Fructose Glucose
1116.0	1126.0	1127	1124.4	1126	1127	C-OH deformation	Glucose Maltose
1247.0	1262.0	1267	1265.6	1266	1264	C-O-C Cyclic alkyl ethers	Fructose
1344.0	1405.9	1368	1366.3	1367	1373	CH and OH bending	Glucose
1444.0	1457.0	1460	1459.9	1459	1461	CH ₂ bending	Fructose Glucose
2899.0	-	2893	-	2904	-	CH ₂ symmetric stretching	Glucose
2933.0	2909.0	2940	2941.6	2941	-	CH ₂ asymmetric stretching	
3224.0	-	-	-	3234	-	OH stretching	Water
3392.0				3319			

Source: This study

As previously stated, honey predominantly consists of carbohydrates, particularly glucose and fructose, which account for 70-80% of its composition and are discernible in the fingerprint region. These carbohydrates play a crucial

role in determining the physical, chemical, and nutritional properties of honey. Consequently, the analysis of sugar composition holds great significance in evaluating honey. conventional methods for evaluating the sugar content of local honey have involved laborious chemical analyses. (Adjaloo et al., 2017; Ankrah, 1998; Combey et al., 2021; Klutse et al., 2021). However, the Raman spectroscopic technique can be cost-effective, non-destructive and rapid.

532 nm Excited Raman Spectra Compared for Honey Samples on Different Types of Substrate

Figure 38 shows the 785 nm excited Raman spectra of honey from different substrates: glass, silicone and back-coated glass mirror used in the measurement. Comparatively, all the substrates produced similar results. The Silica substrate, however, introduced an unwanted peak around 520 cm^{-1} (Borowicz et al., 2012). Thus, a standard glass or mirror can still be used for the Raman spectroscopic study of honey samples. The silica substrate can also be used if the 520 cm^{-1} regions are non-essential in the measurement.

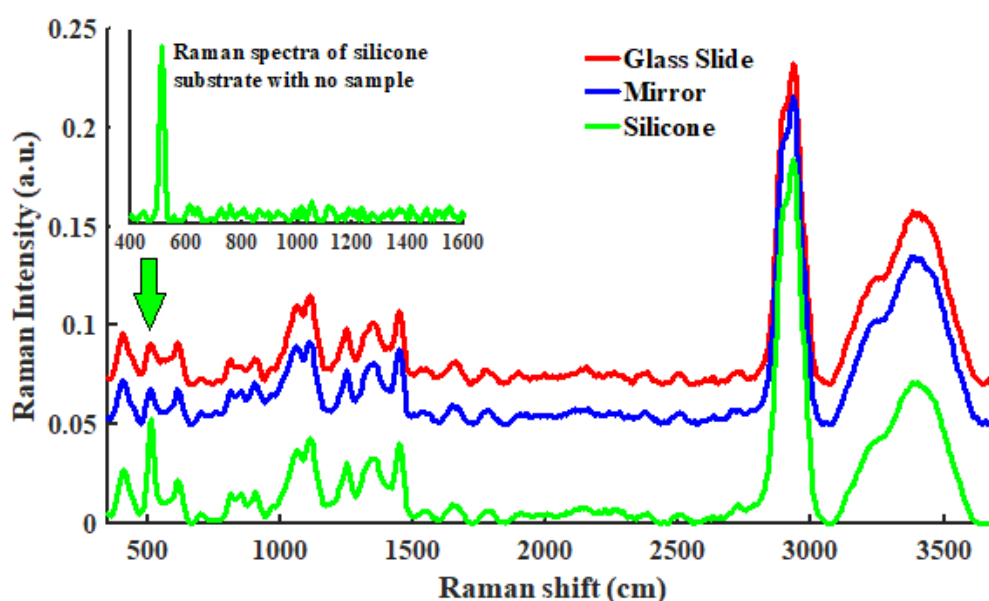


Figure 38: Comparison of Raman spectra of honey on glass, silicone, and back-coated mirror surface substrate

785 nm Excited Raman Spectra Compared for Honey on a Glass Slide and Honey in Vial

Figure 39 shows the Raman spectra of honey measured through a plastic vial compared with the raw honey measured directly as a drop on a glass slide. Variations in the Raman spectra are apparent for both the vial and glass slide.

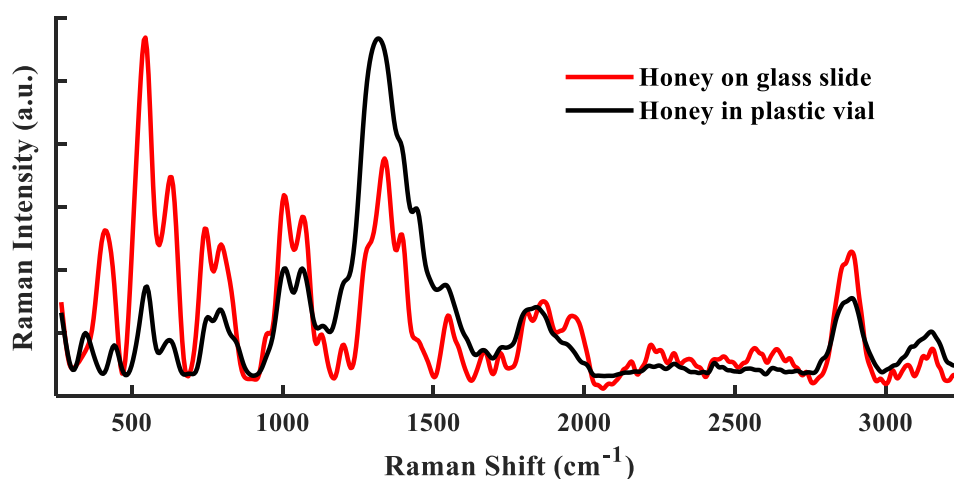


Figure 39: Raman spectra of the honey sample measured on a glass slide compared with a plastic vial

There is interest in non-destructive monitoring through sample packaging (Adar et al., 2014; Eliasson & Matousek, 2007, Zhao et al., 2018). However, in this study, as seen in Figure 39, the Raman spectral measurements of honey conducted through their respective containers resulted in alterations of certain peaks in the Raman spectra, particularly in terms of their intensity. The discrepancy in intensity can affect the spectral analysis quantitatively since intensities of the peaks play a significant role in the quantification of individual sugar molecules present. However, the peak positions in terms of wavelength remained intact; hence, qualitative studies, i.e., studies that identify molecular species based on peak position, are possible. The study on measuring Raman

spectra of honey via packaging could be further explored for different container types and optimized in future studies.

Principal Components and K-means Clusters of the 785 nm Excited Raman Spectra

The fingerprint region of the 785 nm excited Raman spectra of all samples used is shown in Figure 40. To ensure comparability, the spectra were processed by subtracting the background and subsequently normalised using the SNV method (Huzortey et al., 2021; Rinnan et al., 2009).

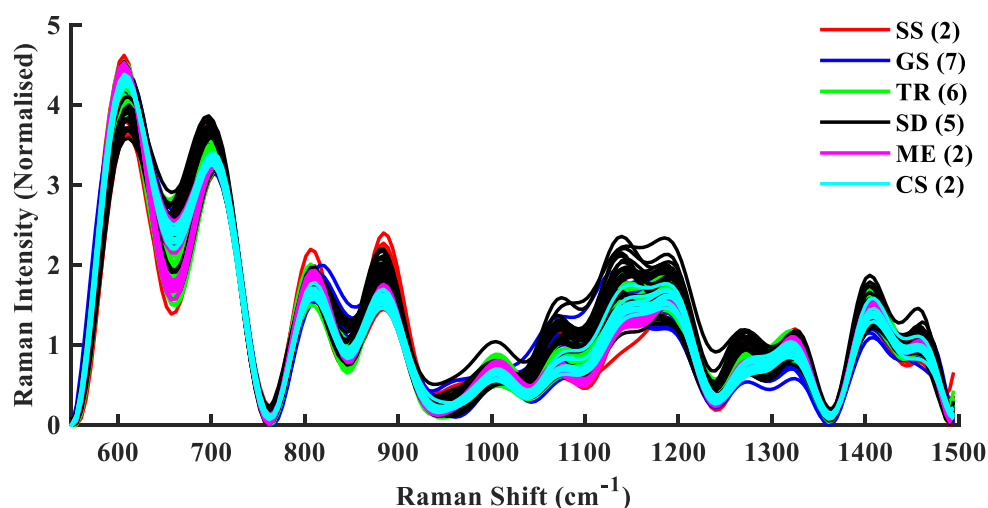


Figure 40: The 785 nm excited normalised Raman spectra of all the honey samples from the different Agro-ecological zones of Ghana. (Sudan Savana (SS), Guinea Savana (GS), Transition, zone (TS), Semi-Deciduous forest (SD), Moist Evergreen (ME) and Coastal Savana (CS)) used in the study. The number of honey samples from each Agro-ecological zone is stated in the legend

PCA biplot of scores and loadings after applying PCA to the honey samples' 785 nm excited Raman spectra are shown in Figure 41. The scores show that the samples are vastly distributed, indicating heterogeneity. However, the scores of the first two PCs, PC1 (54%) and PC2 (24%), are relatively low,

inferring that the samples slightly varied between each other over a broad continuum.

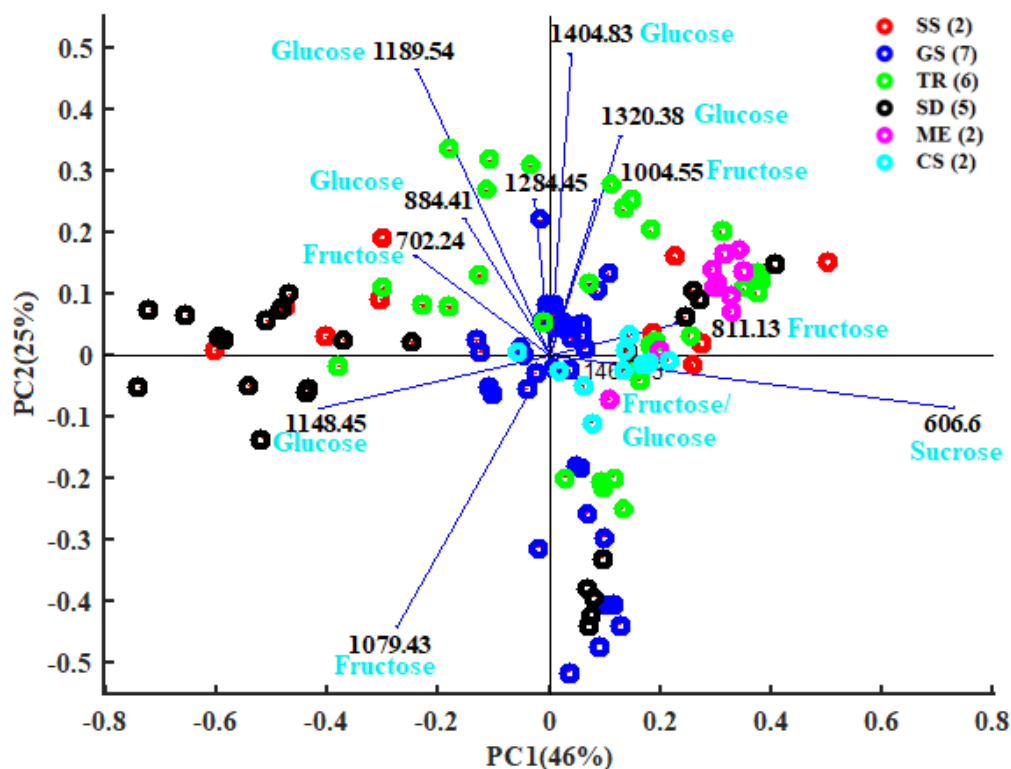


Figure 41: PCA- Biplot showing scores distribution of samples in PC1 and PC2 axis with respective loadings influencing the sample distribution indicated by the wavelength and associated constituent from literature

Again, from Figure 41, the loadings have been used to show the influence of the honey's peak wavelengths designated for specific sugars over the distribution of the samples in PC space. For instance, from Figure 41, along the PC1 axes, the sucrose band at 606.6 cm^{-1} has the most decisive influence on the positive PC1 axes, while the glucose/maltose band at 1148.45 cm^{-1} also had the highest impact on the negative PC1 axes. Therefore, samples in the positive PC1 axes have an amount of sucrose and vice versa for samples in the negative PC1 axes. Samples with more glucose were on the positive of the PC2 axes,

whereas those high in fructose were closer to the origin of the negative PC2 axes.

K-means clustering analysis applied to the PC scores identified subgroups of honey samples with similar sugar constituents (Figure 42). Cluster evaluation to determine the best number of subgroups identified optimal clusters of two and three using the Silhouette (Equation 16) and Davies Bouldin (Equation 17) methods, respectively, as shown in Figure 42.

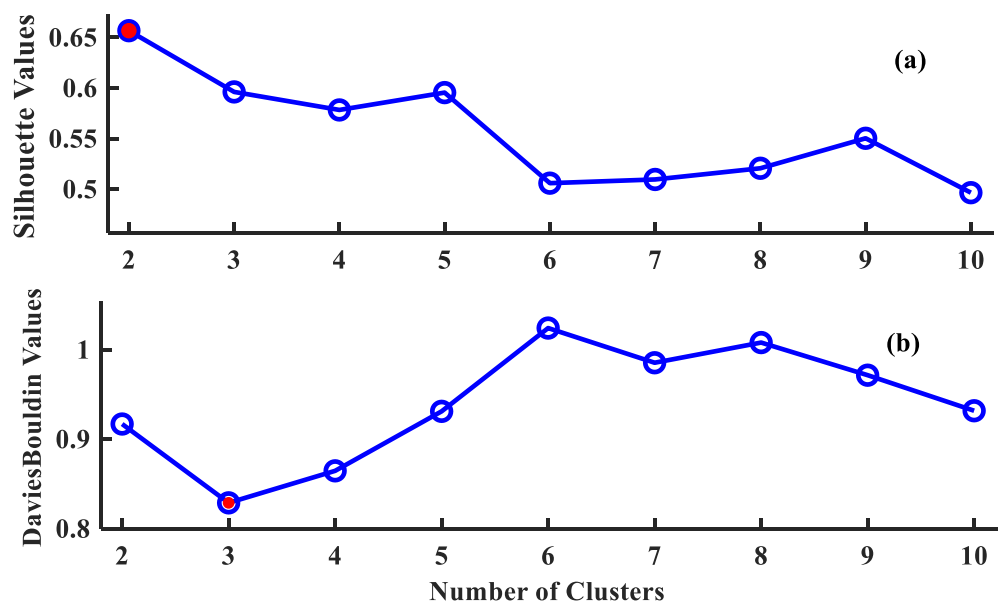


Figure 42: The evaluated K-means clustering using (a) the Silhouette and (b) the Davies-Bouldin method of scores from the principal component analysis of the Raman spectra from the honey sample to select the optimal number of classes existing among the samples from different agro-ecological zones

The analysed K-means clustering of the PCA scores and respective spectra are shown in Figure 43. The identified clusters projected onto Raman spectra of the honey samples show each cluster's scores and separate spectral profile.

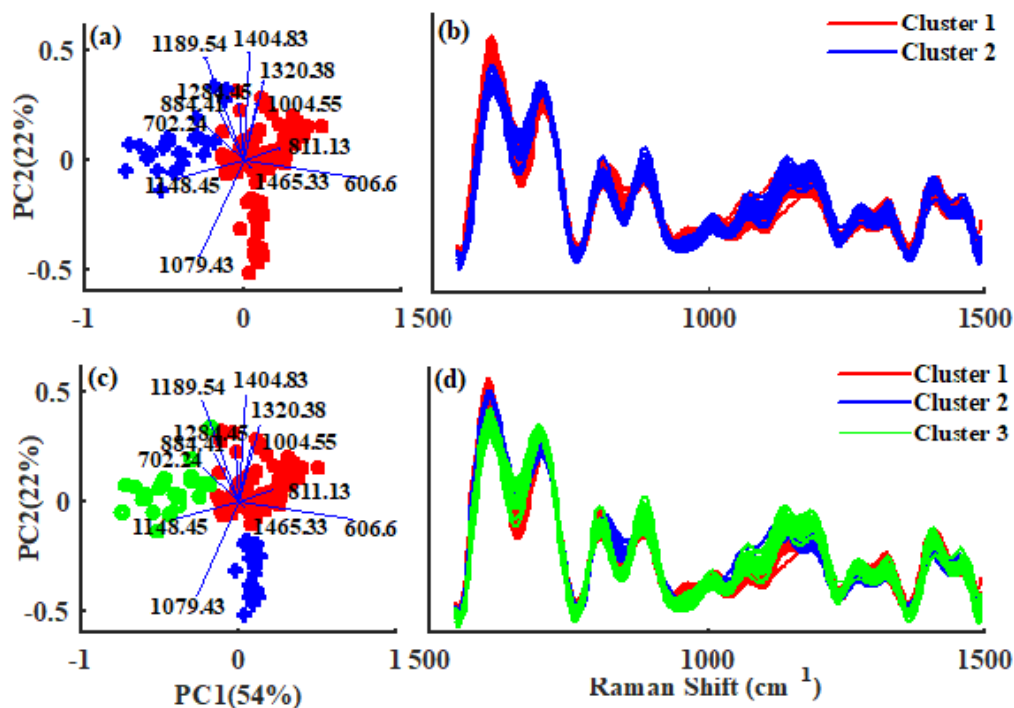


Figure 43: Groups of honey identified using K-Means Clustering analysis on the PC scores and their related Raman spectra for K=2 (a-b) and K=3 (c-d)

Figure 43a shows that honey samples from the different agroecological zones dominated by sucrose (606.60 nm) for one group and glucose (1148.45 nm) for the other group in the case of two clusters. However, in the case of three clusters, as seen in Figure 43c, a third group introduced by the Davies Bouldin method identified honey samples dominated by fructose (1079.43 nm). The spectral profile of each cluster, as shown in Figures 43b and 43d, are distinct and can therefore be averaged to represent each group.

Knowledge of the dominance or proportions of these sugars in honey samples has significant implications for nutrition, marketing, and quality assessment. For instance, honey with high sucrose concentration will likely have been degraded or adulterated (Damto, 2019). Also, much more fructose content honey is encouraged for diabetic patients (Bobiş et al., 2018; Erejuwa

et al., 2012). Hence the importance of combining PCA and K Means for easy and rapid screening to group honey samples from different AEZ having similar properties.

UV-Vis Transmission Spectra

The SNV normalised optical transmission spectra from the honey samples are shown in Figure 44. The nature of the transmitted spectra is similar to that reported by other authors (Almaleeh et al., 2017; Bergamo et al., 2020; Ferreiro-González et al., 2018; Frausto-Reyes et al., 2017; Huang et al., 2019; Vlaeva et al., 2017; Zhao et al., 2011).

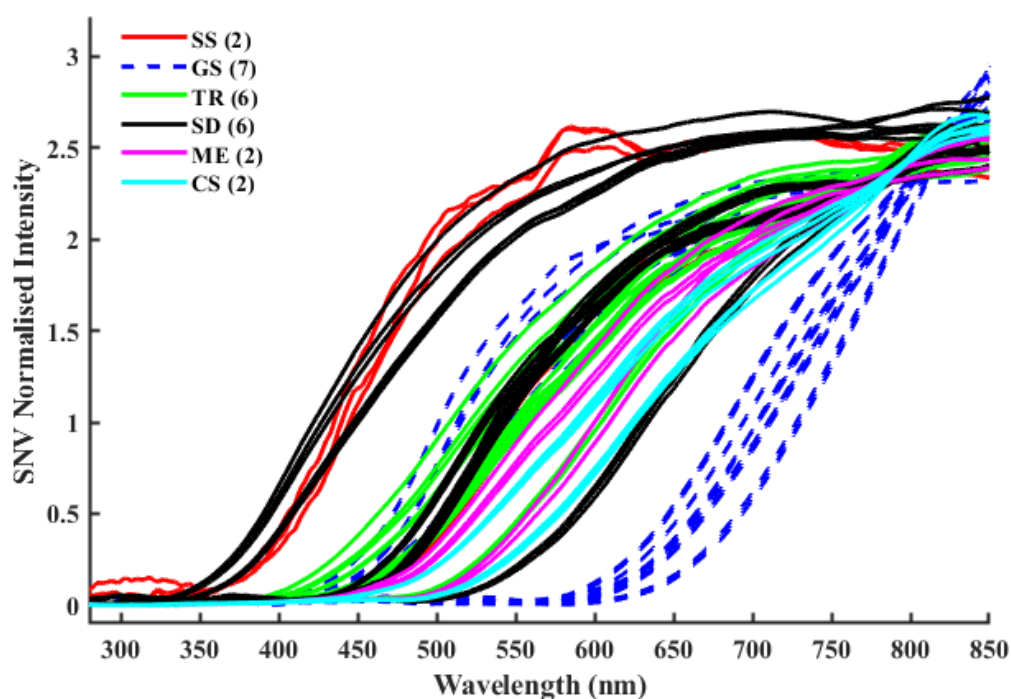


Figure 44: SNV Normalised optical transmission spectra of all honey samples from the six agro-ecological zones of Ghana: Sudan Savannah (SS = 2), Guinea Savannah (GS =7), Transition Zone (TR = 6), Semi-Deciduous Forest (SD = 6), Moist evergreen Forest (ME = 2) and Coastal Savannah (CS = 2)

All the samples showed differences in transmission patterns. Each sample blocks the deep UV portion (< 350 nm) of the light source entirely and

allows higher transmission in the near-infrared region (> 750 nm). Some further blocked varying transmission portions of the visible parts of the light source. The blockades in the various regions of the transmission spectra can be attributed to phenomena such as absorption, reflection or scattering, depending on the nature of the samples worth investigating further. However, the variations in the transmission properties for different honey samples inadvertently indicate the presence of other underlying molecular species. These differences may be due to the reported absorbing molecules within the optical window between 200 – 650 nm, suggesting the presence of phenols, flavonoids, proteins, vitamins, carotenoids, and in some cases, chlorophyll derivatives (Parri et al., 2020; Ulloa et al., 2013).

Principal Components and K-means Clusters of the Transmission Spectra

Figure 45 shows the PCA results for the transmission spectra of the honey samples. Using the elbow method, the variance plot (Figure 45a) reveals that the first three Principal Components (PC): PC1, PC2, and PC3 represent above 99% of the variance in the data. The important wavelengths responsible for the spectral variations observed from the loading plot (Figure 45b) are 580 nm for PC1, 480 nm, 650 nm for PC2, 450 nm, 565 nm, and 740 nm for PC3.

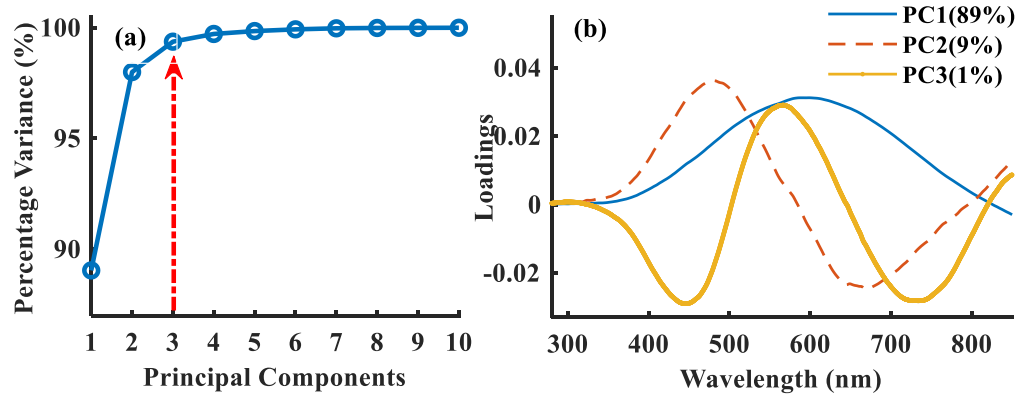


Figure 45: The variance and (b) the loadings plots from the principal component analysis of the normalised transmission spectra of the honey samples. The arrow in the variance plot indicates the selected number of components by the elbow method

Figure 46 shows the optimal number of clusters applied to the selected PCs using K-Means Clustering Analysis (KCA). From the figure, a maximum Silhouette value of 0.86 (Figure 46a) and a minimum Davies-Bouldin value of 0.38 (Figure 46b) were both obtained for four (4) clusters.

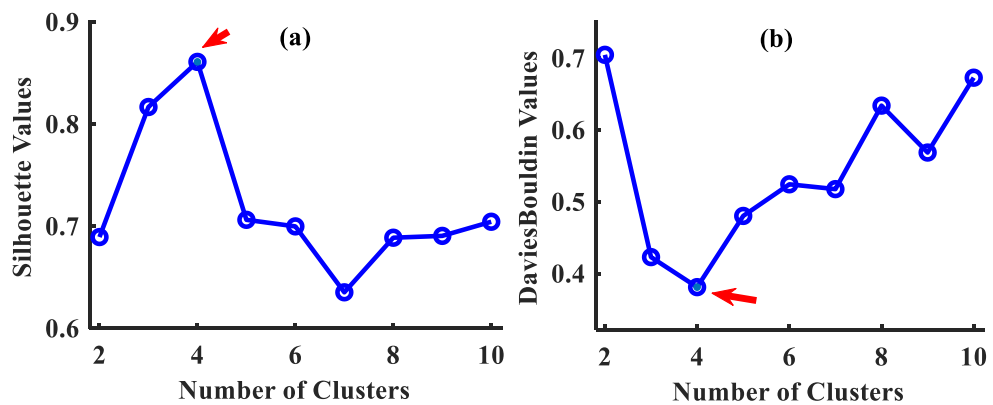


Figure 46: The evaluated K-means clustering using (a) the Silhouette and (b) the Davies-Bouldin method of scores from the principal component analysis of the transmission spectra from the honey sample to select the optimal number of classes existing among the samples from different agro-ecological zones. The arrows indicate the optimal number of clusters, where the Silhouette value is maximized and the Davies-Bouldin value is minimized.

Figure 47 shows the re-plotted normalised spectra after using the KCA. Similarities and differences in the transmission spectra of the samples are more apparent with the re-plotting. Compared with the AEZ, each cluster included a representative from different AEZ except cluster 4. All the honey in cluster 4 was from Guinea Savanna. However, other samples from Guinea Savanna were also found in the other clusters. That implies that the honey samples' optical transmission properties are not generally dependent on their AEZ. The observed clusters can be categorized as *C-350* (Cluster 1), *C-430* (Cluster 2), *C-500* (Cluster 3), and *C-600* (Cluster 4) to reflect the average wavelength position where transmission for the majority of samples in each cluster begins.

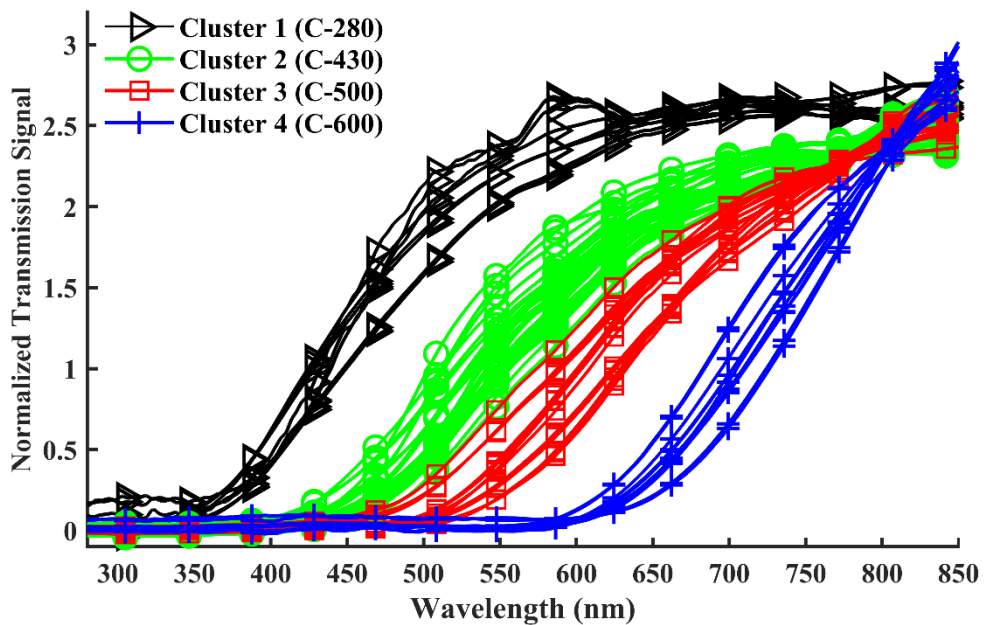


Figure 47: Optical transmission signals depicting the four classes of honey, based on the K-Means Clustering analysis. Cluster 1: 350 nm, Cluster 2: 430 nm, Cluster 3: 500 nm, and Cluster 4: 600 nm can be identified by the wavelength at which transmission begins to occur for most of the samples in each group

The various samples in each category and the possible molecular absorption species responsible for the spectra observed for honey varieties, as reported by Parri et al., (2020) are shown in Table 11.

Table 11: Honey classification based on transmission spectra showing the potential absorption species in the four clusters: Each cluster is composed of the honey samples established by their sample code

Cluster	Sample Code	No of samples	Potential absorbing species
<i>C-350</i>	SS1, SD5, SD6	3	Tryptophan,4-hydroxybenzoic, caffeic, vanillic, ferulic/ chlorogenic acid, syringic, and p-coumaric acids (280 – 290 nm); vitamin B6, vitamin B9, and quercetin (330 – 340 nm);
<i>C-430</i>	SS1, TR1, ME2, TR3, TR4, TR5, SD2, GS1, TR6, SD3, SD4, GS2, GS7	13	Tryptophan,4-hydroxybenzoic, caffeic, vanillic, ferulic/ chlorogenic acid, syringic, and p-coumaric acids (280 – 290 nm); vitamin B6, vitamin B9, and quercetin (330 – 340 nm); vitamin B2 (430 nm); carotenoids (400 – 500 nm)
<i>C-500</i>	SD1, ME1, TR2, CS1, CS2	5	Tryptophan,4-hydroxybenzoic, caffeic, vanillic, ferulic/ chlorogenic acid, syringic, and p-coumaric acids (280 – 290 nm); vitamin B6, vitamin B9, and quercetin (330 – 340 nm); vitamin B2 (430 nm); carotenoids (400 – 500 nm)
<i>C-600</i>	GS3, GS4, GS5, GS6	4	Tryptophan,4-hydroxybenzoic, caffeic, vanillic, ferulic/ chlorogenic acid, syringic, and p-coumaric acids (280 – 290 nm); vitamin B6, vitamin B9, and quercetin (330 – 340 nm); vitamin B2 (430 nm); carotenoids (400 – 500 nm); Chlorophyll pigments (600 – 700 nm)

Source: This study

From Table 11, *C-430* contains most samples, implying that most honey samples from Ghana allow light transmission in wavelengths beyond 430 nm. Even though *C-430* and *C-500* had almost the same molecular species, slight differences can be seen in their spectral profile from Figure 48. The difference between the two categories of honey could be due to their carotenoid content

since *C-430* honey samples had comparatively higher transmission within the 400 nm - 500 nm region than *C-500* samples. The *C-350* generally comprises only amino acids, proteins, and phenolic acids. Meanwhile, the *C-600* included every absorbing species found in all three different categories of honey, including chlorophyll.

The matrix plot of different PC1, PC2, and PC3 combinations, as shown in Figure 48, reveals that the observed four groups occurred along the PC1 axes. The plots of PC1 vs PC2 and PC1 vs PC3 and the diagonals of the histogram plot confirm these groupings.

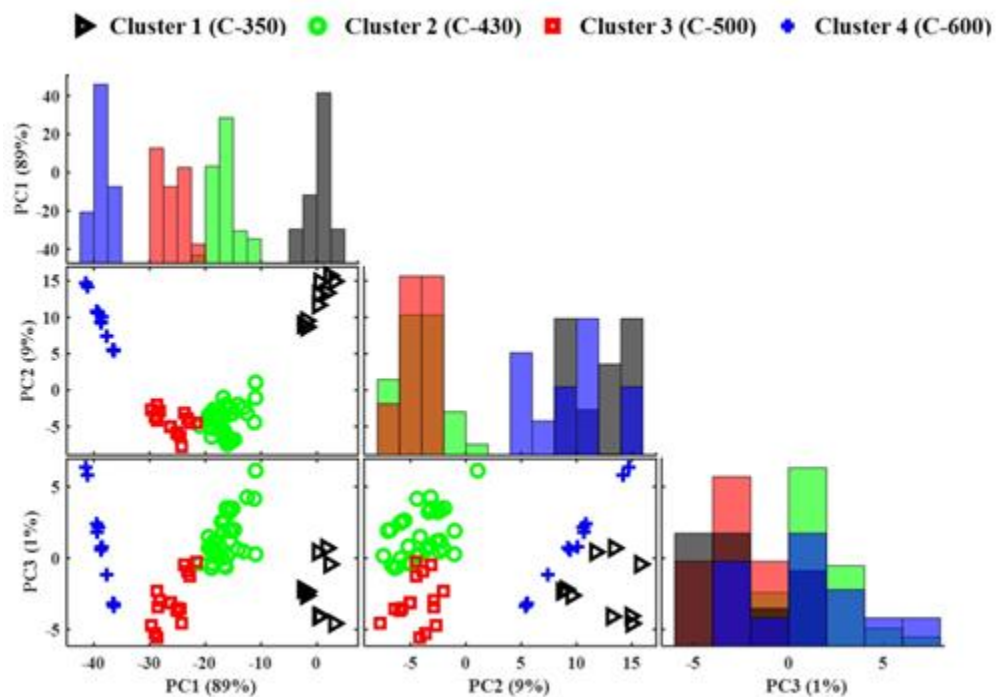


Figure 48: Matrix plot comparing cluster pattern for different Principal Component (PC) score plot combinations. The matrix plot's diagonal shows each cluster's score distribution as a histogram. The four groups are better separated along the first Principal Component (PC1)

From Figure 48, the four main clusters in honey can be identified along the PC1 axis. Hence, the wavelength with the highest loading value in the PC1

loading plot found to be 580 nm previously in Figure 45b is a critical wavelength for identifying honey in the different clusters. ANOVA and Tukey post-hoc test of the transmission intensities at 580 nm for each of the classes as 0.000 reveals significant differences ($p < 0.005$) among each pair of classes. As such, the class a new honey sample may belong to can be suitably determined by the transmission intensity around 580 nm. Therefore, 580 nm can be an optical marker to identify the various honey classes from the agroecological zones.

Chapter Summary

In this chapter, the results and analysis of data obtained from diverse optical spectroscopic techniques employed to investigate honey samples from distinct AEZ in Ghana were presented and discussed. The findings shed light on the comprehensive characterisation of honey, highlighting the variations and unique features observed across different regions, providing valuable insights into the composition and quality of the honey samples. Thus, this section shows the study's findings on honey using Transmission, Fluorescence, and Raman spectroscopic techniques. The results obtained from other measurements, including HPLC (for HMF), Refractometry (for Brix and Moisture) and UV Vis Absorbance (for colour), were presented. The data analysis outcomes obtained from the spectroscopic and other measurements were discussed after preprocessing, multivariate, and other statistical analyses. The study used preprocessing methods, including normalisation, on all the spectra data from each spectroscopic measurement. Spectral deconvolution and baseline correction, were specifically applied to the fluorescence and Raman spectral data, respectively. The results of the multivariate analysis, including PCA, KCA, and statistical metrics such as coefficient of variation, correlation

coefficient, and ANOVA, are also reported and discussed. The study shows how the spectroscopic techniques and other measurements combined with the different methods of analysis were used to identify the molecular constituents of raw honey from AEZ, observe the effects of conditions such as ageing, water dilution, heating, and adulteration, examine the relationship with physicochemical parameters such as colour, moisture Brix, and HMF. Also, it investigated how different excitation sources, sample preparation methods, substrate types, and sample containers affect the Raman spectral measurement of honey samples.

CHAPTER FIVE

SUMMARY, CONCLUSIONS, AND RECOMMENDATIONS

Overview

Honey obtained from AEZ of Ghana have not been studied, thus the need for research to examine honey types from these zones to gain valuable insights into their composition and potential applications. The optical spectra of honey samples from the AEZ were measured using Laser-Induced Fluorescence (LIF), Ultra Violet–Visible (UV-Vis) Transmission, and Raman spectroscopy. The measured spectra of the honey samples were analysed using Multivariate analysis techniques, including PCA and KCA. The physicochemical properties of the honey samples such as colour, moisture, Brix, and HMF, correlated with the deconvoluted LIF spectra. Again, the LIF technique was used to study some conditions affecting honey, such as ageing, heating, adulteration by water dilution, and sugar caramel. The study further examined the effects on the Raman spectra of honey obtained with different excitation sources, sample preparation methods, substrate types, and container samples. The results of the entire study are summarised with drawn conclusions, recommendations, and suggestions for further studies have been provided.

Summary

This research explored the optical spectroscopic properties of honey produced in Ghana's AEZ using three optical spectroscopic techniques. Thirty-two samples were obtained from the six AEZ of Ghana and used for the studies. The optical spectroscopic techniques, i.e. Raman, Fluorescence and UV-Vis Transmission spectroscopy, mainly identified the molecular constituents of the

honey samples. Specifically, the UV-Vis Transmission and LIF spectroscopy identified the honey samples' phytochemical constituents, especially flavonoids, polyphenols, vitamins, carotenoids, and chlorophyll derivatives. The Raman spectral analysis described the sugar composition of the honey samples, primarily glucose, fructose and sucrose. These molecules identified were confirmed with literature.

The spectra data acquired through the three spectroscopic techniques were subjected to multivariate statistical methods for analysis. PCA and KCA were employed to extract meaningful patterns and groupings within the data, enabling comprehensive exploration and interpretation of the spectral information. The PCA score plot showed a scattered distribution of the spectral data from all three techniques, thus, establishing the heterogeneity of honey samples' diverse flora and overlapping of the different AEZ. Despite the scattered distribution of the scores, KCA applied to the PC scores for Raman and UV-Vis transmission spectroscopic techniques found clusters of honey samples with similar characteristics. KCA combined with PCA biplot revealed important wavelengths (or molecular constituents) responsible for each cluster.

Three clusters were identified for the Raman spectra analysis, which was dominated by sucrose at 606.60 nm for one group, glucose at 1148.45 nm for the second group, and fructose at 1079.43 nm for the last group. Four clusters were identified for the UV-Vis Transmission spectra analysis; each cluster was identified by the wavelength at which transmission begins to occur for most of the samples in each group. Thus, the four clusters are identified by an onset of transmission around 350 nm, 430 nm, 500 nm, and 600 nm. Using ANOVA, the

intensity of the group spectra at 580 nm was significantly different for each cluster; therefore, 580 nm serves as a critical wavelength for identifying the cluster in which any honey will belong.

The study again analysed the LIF spectra of the honey samples under different conditions and correlated the deconvolved spectral parameters with physicochemical parameters. Observations made by comparing the LIF spectra of honey under different conditions showed that with ageing (four months, one, two, three years), water dilution (25%, 50%), heating (direct, in a water bath), and sugar caramel adulteration (10%, 20%, 30%, 50%), the LIF spectra were red-shifted in all the conditions tested. However, the LIF spectra were redshifted and intensity reduced simultaneously for sugar caramel adulteration. The changes in the LIF spectra of the honey samples concerning the various conditions occurred at different rates depending on the sample, thus reemphasising the heterogeneous nature of the samples.

For the correlation study, the deconvolved LIF spectra parameters of the honey samples were highly correlated to colour much more than Brix and Moisture. LIF spectra correlation with 5-hydroxymethylfurfural (HMF) showed general differences between honey samples having low (< 40 mg/kg), mild (40 – 80 mg/kg), and high (>80 mg/kg) HMF based on the maximum peak position. However, a good linear correlation was only obtained for honey with low HMF ($R^2 = 0.927$) for the deconvolved peak at 490 nm (P1a) of the LIF spectra. Thus, using the linear model $HMF = -44435.7 (P1a) + 89.015$ relation between HMF and P1a, i.e. the freshness of honey produced in Ghana can be predicted with up to 92% accuracy for honey with low HMF (40 – 80 mg/kg).

Also, further analysis of the Raman spectra of the honey samples obtained with different excitation sources, sample preparation methods, substrate types, and container samples revealed that high Fluorescence, which interferes with the Raman spectral measurement of honey samples, can be controlled using either the 785 nm excitation source or by pretreating the honey samples through dilution, heating, and charcoal treatment for 532 nm laser excitation. The charcoal pretreatment was most effective compared to the other methods. Additionally, usage of the recently proposed Second derivative preprocessing technique made it easier to completely recover and observe the Raman spectra of the honey samples from their noisy backgrounds for all the analysis. The study further showed that Raman spectral measurement was not affected by glass and mirror substrate but by minimal interference around 520 cm^{-1} for Silicone substrate. Measurement of the Raman spectra of the honey sample through a container showed reduced intensity only, not the wavelengths; thus, Raman spectroscopy of analysis of honey is possible, but on a qualitative basis.

Conclusions

Based on the quantitative and qualitative analysis of the various optical spectra, this study has revealed that the Raman, Laser-Induced Fluorescence (LIF), and UV-Vis Transmission optical spectroscopic techniques in combination with Principal component and K-means clustering multivariate statistical methods are instrumental in analysing honey from different AEZ in Ghana. Generally, the results showed that the honey samples from each AEZ were highly heterogeneous in composition. However, the spectral characteristics of the honey samples were not unique to their respective AEZ.

Specifically, the UV-Vis Transmission spectroscopic technique showed that honey from all the AEZ transmitted UV and visible light in four ways. Thus, four groups of honey were identified. Among the four groups, all the honey samples blocked the deep UV portion of the transmitted light. Some further blocked part of the visible portion of the electromagnetic spectrum (EM), while others blocked the almost entirely visible portion of the EM spectrum. The 580 nm has been identified as a wavelength marker for discriminating the groups. The honey samples can therefore act as radiation filters in the UV-visible region of the EM spectrum which can be used in products and devices that control radiation, like sunscreens in cosmetics and filters in optical devices.

With the Raman spectroscopic technique, this study has shown that honey samples from all the agroecological zones can be categorised into three groups based on the dominance of either glucose, sucrose or fructose in the honey. The Raman spectroscopic technique, therefore, offers an invaluable approach that can be used to study honey from the various AEZ to prescribe for their appropriate dietary needs. The study further has shown that visible excitation sources can avoid fluorescence interference when the honey samples are pretreated, of which charcoal pretreatment is the best. Again, the study has shown a variety of sample substrates and samples in containers from which honey can be studied. Honey from Ghana can therefore be studied cost-effectively since visible sources are more available and affordable in this jurisdiction and other emerging economies.

The results from Laser-Induced Fluorescence (LIF) showed that honey samples from the various AEZ can be monitored for ageing, water dilution,

heating, and sugar caramel adulteration. It was also helpful in accurately predicting colour and, more particularly, the 5-Hydroxymethylfural (HMF) content of honey to determine its quality.

Overall, this study has for the first time highlighted the capability of utilizing optical spectroscopic techniques for valorizing local honey from Ghana. These techniques are non-destructive, rapid, and cost-effective, making them a suitable alternative for helping producers label their honey properly to project their values and promote appropriate usage. This study has provided baseline data on local honey and highlighted its optical properties for future studies.

Recommendations

According to the study's outcome,

1. Optical spectroscopy techniques are highly recommended to help producers distinguish honey for their different properties such as for cosmetic and dietary applications.
2. Regulatory and monitoring bodies in the country, like the Food and Drugs Authority (FDA), Ghana Standards Authority, Centre for Scientific and Industrial Research (CSIR), etc., can incorporate in their regulatory and monitoring activities to ensure quality control of fraudulent practices in the honey industry.

These organisations can adopt optical spectroscopic techniques as simple, cost-effective, and rapid alternatives for analysing honey.

This study can also be further expanded to

1. Explore additional optical spectroscopic techniques to further investigate honey samples, such as Fourier Transform Infrared spectroscopy (FTIR), Laser Induced Breakdown Spectroscopy (LIBS), and polarisation spectroscopy. These techniques offer valuable insights into different aspects of honey composition, such as molecular vibrations, elemental analysis, etc. enabling a comprehensive characterization of honey samples.
2. Consider honey from other agro-ecological zones of the Sub-Saharan African region.
3. Study other common adulterants.
4. Measure more physicochemical parameters and correlate with the optical spectra parameters of honey produced in Ghana.

REFERENCES

- Adadi, P., & Obeng, A. K. (2017). Assessment of bacterial quality of honey produced in Tamale metropolis (Ghana). *Journal of Food and Drug Analysis*, 25(2), 369–373.
- Adar, F., Kubic, T., & Leary, P. (2014). Raman Microscopy for Detecting Counterfeit Drugs—A Study of the Tablets Versus the Packaging. *Spectroscopy*, 29(6), 142-145.
- Adjalloo, M. K., Asare, C. Y., Appaw, W., & Boahene, O. (2017). Assessment of Honey Quality in Ghana : A Pilot Study of Honeys Produced in Drobo and Berekum. *Journal of Food : Microbiology , Safety & Hygiene*. 2(3), 2–6.
- Agashe, S. N., & Caulton, E. (2019). Pollen and spores: applications with special emphasis on aerobiology and allergy. In *Pollen and spores* (pp. 1-20). Boca Raton, FL, USA: CRC Press.
- Aghamirlou, H. M., Khadem, M., Rahmani, A., Sadeghian, M., Mahvi, A. H., Akbarzadeh, A., & Nazmara, S. (2015). Heavy metals determination in honey samples using inductively coupled plasma-optical emission spectrometry. *Journal of Environmental Health Science and Engineering*, 13(1), 1-8.
- Akpabli-Tsigbe, N. D. (2015). *Quality evaluation of artisanally produced honey sold in the Ghanaian markets*. (MPhil thesis, University of Ghana, Accra, Ghana). Retrieved April 10, 2021 from <https://ugspace.ug.edu.gh/handle/123456789/8731>.
- Almaleeh, A. A., Adom, A. H., & Fathinul-Syahir, A. S. (2017). Classification of the botanical origin for Malaysian honey using UV-Vis

spectroscopy. *AIP Conference Proceedings*, 1808, 1-5.

- Alvarez-Suarez, J. M., Tulipani, S., Romandini, S., Bertoli, E., & Battino, M. (2010). Contribution of honey in nutrition and human health: a review. *Mediterranean Journal of Nutrition and Metabolism*, 3, 15-23.
- Anjos, O., Santos, A. J. A., Paixão, V., & Estevinho, L. M. (2018). Physicochemical characterization of *Lavandula* spp. honey with FT-Raman spectroscopy. *Talanta*, 178, 43–48.
- Ankrah, E. (1998). Chemical composition of some Ghanaian honey samples. *Ghana Journal of Agricultural Science*, 31(1), 119–121.
- Antônio, D. C., de Assis, D. C. S., Botelho, B. G., & Sena, M. M. (2022). Detection of adulterations in a valuable Brazilian honey by using spectrofluorimetry and multiway classification. *Food Chemistry*, 370 (131064), 1-9.
- Ares, G. (2014). Cluster analysis: Application in food science and technology. *Mathematical and statistical methods in food science and technology*, 103-120.
- Arida, H., Hassan, R., & El-Naggar, A. (2012). Quality assessment of honey using modern analytical tools. *Analytical letters*, 45(11), 1526-1536.
- Artlett, C. P., & Pask, H. M. (2015). Optical remote sensing of water temperature using Raman spectroscopy. *Optics Express*, 23(25), 31844-31856.
- Bakar, N. A., Cui, H., Abu-Siada, A., & Li, S. (2016). A review of spectroscopy technology applications in transformer condition monitoring.

CMD 2016 - International Conference on Condition Monitoring and Diagnosis, 372–375.

- Balas, C. (2009). Review of biomedical optical imaging—a powerful, non-invasive, non-ionizing technology for improving in vivo diagnosis. *Measurement Science and Technology*, 20(10), 1-12.
- Banwell, C. N., & McCash, E. M. (2017). *Fundamentals of molecular spectroscopy* (4th ed.). USA: McGraw-Hill.
- Batsoulis, A. N., Siatis, N. G., Kimbaris, A. C., Alissandrakis, E. K., Pappas, C. S., Tarantilis, P. A., Harizanis, P. C., & Polissiou, M. G. (2005). FT-Raman spectroscopic simultaneous determination of fructose and glucose in honey. *Journal of Agricultural and Food Chemistry*, 53(2), 207–210.
- Becker, E. M., Christensen, J., Frederiksen, C. S., & Haugaard, V. K. (2003). Front-Face Fluorescence Spectroscopy and Chemometrics in Analysis of Yogurt: Rapid Analysis of Riboflavin. *Journal of Dairy Science*, 86(8), 2508–2515.
- Bell, S. E. J., Bourguignon, E. S. O., & Dennis, A. (1998). Analysis of luminescent samples using subtracted shifted Raman spectroscopy. *Analyst*, 123(8), 1729-1734.
- Bell, S. E. J., Bourguignon, E. S. O., Dennis, A. C., Fields, J. A., McGarvey, J. J., & Seddon, K. R. (2000). Identification of dyes on ancient Chinese paper samples using the subtracted shifted raman spectroscopy method. *Analytical Chemistry*, 72(1), 234-239.
- Bentum, N. A., Annobil, P., Nkrumah, P., Asare, C., Quansah, I., & Tandoh, M. (2022). Comparing Antioxidant and Antimicrobial Properties of

- Local and Foreign Honey in Kumasi - Ghana. *Current Developments in Nutrition*, 6(1), 92–92.
- Bergamo, G., Seraglio, S. K. T., Gonzaga, L. V., Fett, R., & Costa, A. C. O. (2020). Use of visible spectrophotometric fingerprint and chemometric approaches for the differentiation of *Mimosa scabrella* Benth honeydew honey. *Journal of Food Science and Technology*, 57, 3966-3972.
- Besah-Adanu, C., Bosselmann, A. S., Hansted, L., & Kwapong, P. K. (2019). Food origin labels in Ghana: Finding inspiration in the European geographical indications system on honey. *The Journal of World Intellectual Property*, 22(5-6), 349-363.
- Bilge, G., Sezer, B., Eseller, K. E., Berberoglu, H., Koksel, H., & Boyaci, I. H. (2016). Ash analysis of flour sample by using laser-induced breakdown spectroscopy. *Spectrochimica Acta - Part B Atomic Spectroscopy*, 124, 74–78.
- Bishop, C. M., & Nasrabadi, N. M. (2006). *Pattern recognition and machine learning*. New York, NY: Springer.
- Bobiş, O., Dezmirean, D. S., & Moise, A. R. (2018). Honey and Diabetes: The Importance of Natural Simple Sugars in Diet for Preventing and Treating Different Type of Diabetes. *Oxidative Medicine and Cellular Longevity*, 2018, 4757893-4757893.
- Bogdanov, S. (2009). Harmonised Methods of the International IHC. *Bee Product Science*, 5, 1–62.
- Bogdanov, S. (2015). Honey as Nutrient and Functional Food : A Review. *Bee Product Science*, 4, 1–47.

- Bogdanov, S., Jurendic, T., Sieber, R., & Gallmann, P. (2008). Honey for nutrition and health: a review. *Journal of the American college of Nutrition*, 27(6), 677-689.
- Bogdanov, S., Lüllmann, C., Martin, P., Von Der Ohe, W., Russmann, H., Vorwohl, G., ... & Vit, P. (1999). Honey quality and international regulatory standards: review by the International Honey Commission. *Bee world*, 80(2), 61-69.
- Bong, J., Loomes, K. M., Schlothauer, R. C., & Stephens, J. M. (2016). Fluorescence markers in some New Zealand honeys. *Food chemistry*, 192, 1006-1014.
- Borowicz, P., Latek, M., Rzodkiewicz, W., Łaszcz, A., Czerwinski, A., & Ratajczak, J. (2012). Deep-ultraviolet Raman investigation of silicon oxide: Thin film on silicon substrate versus bulk material. *Advances in Natural Sciences: Nanoscience and Nanotechnology*, 3(4), 45003 - 45010.
- Bowie, B. T., Chase, D. B., & Griffiths, P. R. (2000). Factors affecting the performance of bench-top Raman spectrometers. Part I: instrumental effects. *Applied Spectroscopy*, 54(5), 164-173.
- Brorsson, A., Nordberg, M., & Gustafsson, D. (2021). Reconstruction of CASSI-Raman images with machine-learning. In *Proceedings of the IEEE/CVF Conference on Computer Vision and Pattern Recognition*. 4388-4395.
- Brown, C. D., Vega-Montoto, L., & Wentzell, P. D. (2000). Derivative preprocessing and optimal corrections for baseline drift in multivariate calibration. *Applied Spectroscopy*, 54(7), 1055-1068.

- Butcher, G., Mottar, J., Parkinson, C., & Wollack, E. (2016). *Tour of the electromagnetic spectrum* (3rd ed.). Lanham, USA: Science Systems and Applications, Inc.
- Cangelosi, R., & Goriely, A. (2007). Component retention in principal component analysis with application to cDNA microarray data. *Biology direct*, 2(1), 1-21.
- Carter, D. A., Blair, S. E., Cokcetin, N. N., Bouzo, D., Brooks, P., Schothauer, R., & Harry, E. J. (2016). Therapeutic manuka honey: No longer so alternative. *Frontiers in Microbiology*, 7(569), 1-12.
- Casella, A. J., Levitskaia, T. G., Peterson, J. M., & Bryan, S. A. (2013). Water O–H stretching Raman signature for strong acid monitoring via multivariate analysis. *Analytical chemistry*, 85(8), 4120-4128.
- Chekalyuk, A., & Hafez, M. (2013). Analysis of spectral excitation for measurements of fluorescence constituents in natural waters. *Optics Express*, 21(24), 29255-29268.
- Chen, K., Zhang, H., Wei, H., & Li, Y. (2014). Improved Savitzky–Golay-method-based fluorescence subtraction algorithm for rapid recovery of Raman spectra. *Applied Optics*, 53(24), 5559-5569.
- Chen, Z., & Segev, M. (2021). Highlighting photonics: looking into the next decade. *ELight 2021*, 1(1), 1–12.
- Chen, Z., Dinh, H. N., & Miller, E. (2013). *Photoelectrochemical water splitting*. New York: Springer.
- Ciaccheri, L., Mignani, A. G., Mencaglia, A. A., Di Sanzo, R., Carabetta, S., & Russo, M. T. (2015). Nondestructive and rapid authentication of honey using dispersive raman spectroscopy. *Proceedings of the*

2015 18th AISEM Annual Conference, 1–4.

Codex Alimentarius. (2001). *Revised Codex Standard for Honey, Standards and Standard Methods*. FAO/OMS. Rome, Italy.

Combey, R., Dordunu, P., Badu, I. K., & Quandahor, P. (2021). *Physico-chemical properties and microbiological status of admixture and single-hive honey produced in Ghana*. [Preprint]. Research Square. doi.org/10.21203/rs.3.rs-861909/v1

Corvucci, F., Nobili, L., Melucci, D., & Grillenzoni, F. V. (2015). The discrimination of honey origin using melissopalynology and Raman spectroscopy techniques coupled with multivariate analysis. *Food Chemistry*, 169, 297–304.

Cozzolino, D., Corbella, E., & Smyth, H. E. (2011). Quality control of honey using infrared spectroscopy: a review. *Applied Spectroscopy Reviews*, 46(7), 523-538.

Crittenden, A. N. (2011). The importance of honey consumption in human evolution. *Food and Foodways*, 19(4), 257-273.

Cuss, C. W., & Guéguen, C. (2015). Relationships between molecular weight and fluorescence properties for size-fractionated dissolved organic matter from fresh and aged sources. *Water Research*, 68, 487–497.

Damto, T. (2019). *A review on effect of adulteration on honey properties*. SSRN Electronic Journal. Retrieved June 6, 2022, from <https://ssrn.com/abstract/3359494>.

Davies, D., & Bouldin, D. (1979). A cluster separation measure. *IEEE Transactions on Pattern Analysis and Machine Intelligence*, 2, 224–227.

- De Oliveira, L. F. C., Colombrá, R., & Edwards, H. G. M. (2002). Fourier transform Raman spectroscopy of honey. *Applied Spectroscopy*, *56*(3), 306–311.
- Demtröder, W. (1982). *Laser spectroscopy*. Berlin, Germany: Springer-Verlag.
- Dietrich, W., Rüdél, C. H., & Neumann, M. (1991). Fast and precise automatic baseline correction of one- and two-dimensional nmr spectra. *Journal of Magnetic Resonance (1969)*, *91*(1), 1-11.
- Ding, H., Hu, D. J. J., Yu, X., Liu, X., Zhu, Y., & Wang, G. (2022). Review on all-fiber online Raman sensor with hollow core microstructured optical fiber. *Photonics*, *9*(3), 134. 1-26.
- Efremenko, D., & Kokhanovsky, A. (2021). *Foundations of atmospheric remote sensing* (pp. 124). Cham, Switzerland: Springer.
- El Sohaimy, S. A., Masry, S. H. D., & Shehata, M. G. (2015). Physicochemical characteristics of honey from different origins. *Annals of Agricultural Sciences*, *60*(2), 279–287.
- Eliasson, C., & Matousek, P. (2007). Noninvasive authentication of pharmaceutical products through packaging using spatially offset Raman spectroscopy. *Analytical Chemistry*, *79*(4), 1696-1701.
- Erejuwa, O. O., Sulaiman, S. A., & Ab Wahab, M. S. (2012). Honey - A Novel Antidiabetic Agent. *International Journal of Biological Sciences*, *8*(6), 913-933.
- Escuredo, O., Rodríguez-Flores, M. S., Meno, L., & Seijo, M. C. (2021). Prediction of Physicochemical Properties in Honeys with Portable Near-Infrared (microNIR) Spectroscopy Combined with Multivariate Data Processing. *Foods*, *10*(2), 317-332.

- Ferreiro-González, M., Espada-Bellido, E., Guillén-Cueto, L., Palma, M., Barroso, C. G., & Barbero, G. F. (2018). Rapid quantification of honey adulteration by visible-near infrared spectroscopy combined with chemometrics. *Talanta*, *188*, 288–292.
- Fischer, R., Hanson, K. M., Dose, V., & von der Linden, W. (2000). Background estimation in experimental spectra. *Physical Review E - Statistical Physics, Plasmas, Fluids, and Related Interdisciplinary Topics*, *61*(2), 1152-1160.
- Flanjak, I., Kenjerić, D., Strelec, I., Rajs, B. B., & Primorac, L. (2022). Effect of Processing and Storage on Sage (*Salvia Officinalis* L.) Honey Quality. *Journal of Microbiology, Biotechnology and Food Sciences*, *11*(6), 1-6.
- Food and Agriculture Organisation [FAO]. (2005). Agro-ecological zones of Ghana. Rome, Italy: FAO.
- Forbes, M. D. E. (2015). What we talk about when we talk about light. *ACS Central Science*, *1*(7), 354–363.
- Frasco, D. (2018). Analysis of Honey Color and HMF Content using a GENESYS UV-Visible Spectrophotometer. *Thermoscientific*, *2*, 1–4.
- Frausto-Reyes, C., Casillas-Peñuelas, R., Quintanar-Stephano, J. L., Macías-López, E., Bujdud-Pérez, J. M., & Medina-Ramírez, I. (2017). Spectroscopic study of honey from *Apis mellifera* from different regions in Mexico. *Spectrochimica Acta - Part A: Molecular and Biomolecular Spectroscopy*, *178*, 212–217.
- Friedrichs, M. S. (1995). A model-free algorithm for the removal of baseline

- artifacts. *Journal of Biomolecular NMR*, 5(2).
- García, N. L. (2018). The Current Situation on the International Honey Market. *Bee World*. 95(3), 89–94.
- García-Alvarez, M., Ceresuela, S., Huidobro, J. F., Hermida, M., & Rodríguez-Otero, J. L. (2002). Determination of Polarimetric Parameters of Honey by Near-Infrared Transflectance Spectroscopy. *Journal of Agricultural and Food Chemistry*, 50(3), 419–425.
- Goodacre, R., Radovic, B. S., & Anklam, E. (2002). Progress toward the rapid nondestructive assessment of the floral origin of European honey using dispersive Raman spectroscopy. *Applied Spectroscopy*, 56(4), 521–527.
- Griffiths, T. R., King, K., Hubbard, H. V. S. A., Schwing-Weill, M. J., & Meullemeestre, J. (1982). Some aspects of the scope and limitations of derivative spectroscopy. *Analytica Chimica Acta*, 143(3), 163-176.
- Hasegawa, T. (2001). Detection of minute chemical signals by principal component analysis. *TrAC - Trends in Analytical Chemistry*, 20(2), 53-64.
- Hegazi, N. M., Elghani, G. E. A., & Farag, M. A. (2021). The super-food Manuka honey, a comprehensive review of its analysis and authenticity approaches. *Journal of Food Science and Technology* 2021 59:7, 59(7), 2527–2534.
- Hu, H., Bai, J., Xia, G., Zhang, W., & Ma, Y. (2018). Improved Baseline Correction Method Based on Polynomial Fitting for Raman Spectroscopy. *Photonic Sensors*, 8(4), 332-340.

- Huang, Z., Liu, L., Li, G., Li, H., Ye, D., & Li, X. (2019). Nondestructive determination of diastase activity of honey based on visible and near-infrared spectroscopy. *Molecules*, *24*(7), 1244-1256.
- Huzortey, A. A., Anderson, B., & Owusu, A. (2021). Raman spectra recovery using a second derivative technique and range independent baseline correction algorithm. *OSA Continuum*, *4*(9), 2468-2480.
- Isaksson, T., & Aastveit, A. H. (2006). Classification methods. In J. M. Chalmers & P. R. Griffiths (Eds.), *Handbook of vibrational spectroscopy* (2, pp. 1041-1070). Chichester, United Kingdom: Wiley.
- Jolliffe, I. T. (2002). *Principal component analysis*. New York, USA: Springer.
- Kalashnikov, D. A., Paterova, A. V., Kulik, S. P., & Krivitsky, L. A. (2016). Infrared spectroscopy with visible light. *Nature Photonics*, *10*(2), 98–101.
- Karoui, R., Dufour, E., Bosset, J.-O., & De Baerdemaeker, J. (2007). The use of front face fluorescence spectroscopy to classify the botanical origin of honey samples produced in Switzerland. *Food Chemistry*, *101*(1), 314–323.
- Kaufman, L., & Rousseeuw, P. J. (1990). *Finding groups in data: an introduction to cluster analysis*. Hoboken, New Jersey, USA: John Wiley & Sons.
- Kerr, L. T., Byrne, H. J., & Hennelly, B. M. (2015). Optimal choice of sample substrate and laser wavelength for Raman spectroscopic analysis of biological specimen. *Analytical Methods*, *7*(12), 5041-5052.
- Klutse, C. K., Larbi, D. A., Adotey, D. K., & Serfor-Armah, Y. (2021).

Assessment of effect of post-harvest treatment on microbial quality of honey from parts of Ghana. *Radiation Physics and Chemistry*, 182(109368), 1-6.

Kostamovaara, J., Tenhunen, J., Kögler, M., Nissinen, I., Nissinen, J., & Keränen, P. (2013). Fluorescence suppression in Raman spectroscopy using a time-gated CMOS SPAD. *Optics Express*, 21(25), 31632-31641.

Krishna, H., Majumder, S. K., & Gupta, P. K. (2012). Range-independent background subtraction algorithm for recovery of Raman spectra of biological tissue. *Journal of Raman Spectroscopy*, 43(12), 1884–1894.

Lakowicz, J. R. (2006). *Principles of fluorescence spectroscopy*. New York, NY: Springer

Lastra-Mejías, M., Izquierdo, M., González-Flores, E., Cancilla, J. C., Izquierdo, J. G., & Torrecilla, J. S. (2020). Honey exposed to laser-induced breakdown spectroscopy for chaos-based botanical classification and fraud assessment. *Chemometrics and Intelligent Laboratory Systems*, 199, 103939-103953.

Le Ru, E. C., & Etchegoin, P. G. (2009). Principles of surface-enhanced Raman spectroscopy. In E. C. Le Ru & P. G. Etchegoin (Eds.), *Principles of surface-enhanced Raman spectroscopy* (pp. 1-26). Amsterdam, Netherlands: Elsevier.

Leme, L. M., Rocha Montenegro, H., da Rocha dos Santos, L., Sereia, M. J., Valderrama, P., & Março, P. H. (2018). Relation Between Near-Infrared Spectroscopy and Physicochemical Parameters for

- Discrimination of Honey Samples from Jatai weyrauchi and Jatai angustula Bees. *Food Analytical Methods*, 11(7), 1944–1950.
- Lenhardt, L., Bro, R., Zeković, I., Dramićanin, T., & Dramićanin, M. D. (2015). Fluorescence spectroscopy coupled with PARAFAC and PLS DA for characterization and classification of honey. *Food Chemistry*, 175, 284–291.
- Lenhardt, L., Zeković, I., Dramićanin, T., Dramićanin, M. D., & Bro, R. (2014). Determination of the botanical origin of honey by front-face synchronous fluorescence spectroscopy. *Applied Spectroscopy*, 68(5), 557–563.
- Letsyo, E., & Ameka, G. (2019). Major plants foraged by bees for honey production in Ghana: mapping of bee floral sources for the development of the apicultural industry. *Grana*, 58(6), 472-482.
- Letsyo, E., Jerz, G., Winterhalter, P., Dübecke, A., von der Ohe, W., von der Ohe, K., & Beuerle, T. (2017). Pyrrolizidine alkaloids in floral honeys of tropical Ghana: a health risk assessment. *Food Additives & Contaminants: Part B*, 10(4), 300-310.
- Leyva-Jimenez, F. J., Lozano-Sanchez, J., Borrás-Linares, I., de la Luz Cadiz-Gurrea, M., & Mahmoodi-Khaledi, E. (2019). Potential antimicrobial activity of honey phenolic compounds against Gram positive and Gram negative bacteria. *LWT*, 101, 236-245.
- Li Vigni, M., Durante, C., & Cocchi, M. (2013). Exploratory Data Analysis. *Data Handling in Science and Technology*, 28, 55–126.
- Li, S., Shan, Y., Zhu, X., Zhang, X., & Ling, G. (2012). Detection of honey adulteration by high fructose corn syrup and maltose syrup using

- Raman spectroscopy. *Journal of Food Composition and Analysis*, 28(1), 69–74.
- Li, Y., & Yang, H. (2012). Honey Discrimination Using Visible and Near-Infrared Spectroscopy. *International Scholarly Research Notices*, 2012(1), 487040.
- Lieber, C. A., & Mahadevan-Jansen, A. (2003). Automated Method for Subtraction of Fluorescence from Biological Raman Spectra. *Applied Spectroscopy*, 57(11), 1363–1367.
- Lu, J., Yuan, Y., Duan, Z., Zhao, G., & Svanberg, S. (2020). Short-range remote sensing of water quality by a handheld fluorosensor system. *Applied Optics*, 59(10), 1-7.
- Mabrouk, K. B., Kauffmann, T. H., & Fontana, M. D. (2013). Abilities of Raman sensor to probe pollutants in water. In *Journal of Physics: Conference Series*, 450(1), 012014-12021.
- Mahmoodi-Khaledi, E., Lozano-Sánchez, J., Bakhouch, A., Habibi-Rezaei, M., Sadeghian, I., & Segura-Carretero, A. (2017). Physicochemical properties and biological activities of honeys from different geographical and botanical origins in Iran. *European Food Research and Technology*, 243, 1019-1030.
- Masilamani, V., Ghaithan, H. M., Aljaafreh, M. J., Ahmed, A., al Thagafi, R., Prasad, S., & Alsalhi, M. S. (2017). Using a spectrofluorometer for resonance raman spectra of organic molecules. *Journal of Spectroscopy*, 2017(1), 4289830-4289839.
- Manefjord, H., Muller, L., Li, M., Salvador, J., Blomqvist, S., Runemark, A., Kirkeby, C., Ignell, R., Bood, J., & Brydegaard, M. (2022). 3D-

- Printed Fluorescence Hyperspectral Lidar for Monitoring Tagged Insects. *IEEE Journal of Selected Topics in Quantum Electronics*, 28(5), 1-9.
- Martins, M. A. da S., Ribeiro, D. G., Pereira dos Santos, E. A., Martin, A. A., Fontes, A., & Martinho, H. da S. (2010). Shifted-excitation Raman difference spectroscopy for in vitro and in vivo biological samples analysis. *Biomedical Optics Express*, 1(2), 617-626.
- Mashhadi, A., Bavali, A., & Mokhtari, F. (2022). Assay of honey freshness by a novel optical technique. *Scientific Reports*, 12(1), 1–14.
- Mashhadi, A., Bavali, A., Hashemi, M., & Mokhtari Kheyraadi, F. (2020). Measurement of hydroxymethyl furfural (HMF) by quantitative analysis of laser induced fluorescence spectra to detect freshness of honey. *Optics and Photonics Society of Iran*, 26(0), 521–524.
- Matousek, P., Towrie, M., Stanley, A., & Parker, A. W. (1999). Efficient Rejection of Fluorescence from Raman Spectra Using Picosecond Kerr Gating. *Applied Spectroscopy*, 53(12), 1485–1489.
- Mazilu, M., De Luca, A. C., Riches, A., Herrington, C. S., & Dholakia, K. (2010). Optimal algorithm for fluorescence suppression of modulated Raman spectroscopy. *Optics Express*, 18(11), 11382-11395.
- McCreery, R. L. (2005). Sampling modes in Raman spectroscopy. In R. L. McCreery (Ed.), *Raman spectroscopy for chemical analysis* (pp. 95-126). Hoboken, New Jersey, USA: John Wiley & Sons.
- Mehretie, S., Al Riza, D. F., Yoshito, S., & Kondo, N. (2018). Classification of raw Ethiopian honeys using front face fluorescence spectra with

multivariate analysis. *Food Control*, 84, 83–88.

- Mehryar, L., Esmaili, M., & Hassanzadeh, A. (2013). *Evaluation of Some Physicochemical and Rheological Properties of Iranian Honeys and the Effect of Temperature on its Viscosity*. 13(6), 807–819.
- Mignani, A. G., Ciaccheri, L., Mencaglia, A. A., Di Sanzo, R., Carabetta, S., & Russo, M. (2016). Dispersive raman spectroscopy for the nondestructive and rapid assessment of the quality of southern Italian honey types. *Journal of Lightwave Technology*, 34(19), 4479-4485.
- Mordor Intelligence. (2022). *BioPhotonics market - Growth rate by region* [Map]. Mordor Intelligence. Retrieved February 8, 2022, from <https://www.mordorintelligence.com/industry-reports/global-biophotonics-market>
- Mosier-Boss, P. A., Lieberman, S. H., & Newbery, R. (1995). Fluorescence Rejection in Raman Spectroscopy by Shifted-Spectra, Edge Detection, and FFT Filtering Techniques. *Applied Spectroscopy*, 49(5), 630–638.
- Molnar, C. M., Berghian-Grosan, C., & Magdas, D. A. (2020). An optimized green preparation method for the successful application of Raman spectroscopy in honey studies. *Talanta*, 208(9), 120432-120447.
- Na, S., Xumin, L., & Yong, G. (2010). Research on k-means clustering algorithm: An improved k-means clustering algorithm. In *2010 Third International Symposium on intelligent information technology and security informatics*, 63-67.
- Naila, A., Flint, S. H., Sulaiman, A. Z., Ajit, A., & Weeds, Z. (2018). Classical

and novel approaches to the analysis of honey and detection of adulterants. *Food Control*, 90, 152–165.

- Narang, S. B., & Pubby, K. (2017). Electromagnetic characterization of Co-Ti-Doped Ba-M ferrite-based frequency-tunable microwave absorber in 12.4–40 GHz. *Journal of Superconductivity and Novel Magnetism*, 30, 511-520.
- Nissinen, I., Nissinen, J., Lämsman, A. K., Hallman, L., Kilpelä, A., Kostamovaara, J., ... & Tenhunen, J. (2011). A sub-ns time-gated CMOS single photon avalanche diode detector for Raman spectroscopy. In *IEEE Proceedings of the European Solid-State Device Research Conference (ESSDERC)*. 375-378.
- Noviyanto, A., Abdullah, W., Yu, W., & Salcic, Z. (2015). Research trends in optical spectrum for honey analysis. In *2015 IEEE Asia-Pacific Signal and Information Processing Association Annual Summit and Conference (APSIPA)*. 416-425.
- Oddo, L. P., Piazza, M. G., Sabatini, A. G., & Accorti, M. (1995). Characterization of unifloral honeys. *Apidologie*, 26(6), 453-465.
- Oroian, M., & Ropciuc, S. (2018). Botanical authentication of honeys based on Raman spectra. *Journal of Food Measurement and Characterization*, 12(1), 545–554.
- Oroian, M., Ropciuc, S., & Paduret, S. (2018). Honey Adulteration Detection Using Raman Spectroscopy. *Food Analytical Methods*, 11(4), 959–968.
- Osticioli, I., Zoppi, A., & Casteilucci, E. M. (2006). Fluorescence and Raman spectra on painting materials: Reconstruction of spectra with

mathematical methods. *Journal of Raman Spectroscopy*, 37(10), 974-980.

Ouchemoukh, S., Louaileche, H., & Schweitzer, P. (2007). Physicochemical characteristics and pollen spectrum of some Algerian honeys. *Food control*, 18(1), 52-58.

Özbalci, B., Boyaci, I. H., Topcu, A., Kadilar, C., & Tamer, U. (2013). Rapid analysis of sugars in honey by processing Raman spectrum using chemometric methods and artificial neural networks. *Food Chemistry*, 136(3-4), 1444-1452.

Paradkar, M. M., & Irudayaraj, J. (2002). Discrimination and classification of beet and cane inverts in honey by FT-Raman spectroscopy. *Food Chemistry*, 76(2), 231-239.

Parri, E., Santinami, G., & Domenici, V. (2020). Front-face fluorescence of honey of different botanic origin: A case study from Tuscany (Italy). *Applied Sciences*, 10(5), 1776-1801.

Pelletier, M. J. (2003). Quantitative analysis using Raman spectrometry. *Applied spectroscopy*, 57(1), 20-42.

Peng, J., Xie, W., Jiang, J., Zhao, Z., Zhou, F., & Liu, F. (2020). Fast quantification of honey adulteration with laser-induced breakdown spectroscopy and chemometric methods. *Foods*, 9(3), 341-350.

Petersen, C. L., Chen, T. P., Ansermino, J. M., & Dumont, G. A. (2013). Design and Evaluation of a Low-Cost Smartphone Pulse Oximeter. *Sensors*, 13(12), 16882-16893

Pierna, J. A. F., Abbas, O., Dardenne, P., & Baeten, V. (2011). Discrimination of Corsican honey by FT-Raman spectroscopy and chemometrics.

Biotechnology, Agronomy and Society and Environment, 15(1), 75–84.

- Pita-Calvo, C., Guerra-Rodríguez, M. E., & Vázquez, M. (2017). Analytical methods used in the quality control of honey. *Journal of Agricultural and Food Chemistry*, 65(4), 690–703.
- Ponnuchamy, R., Bonhomme, V., Prasad, S., Das, L., Patel, P., Gaucherel, C., Pragasam, A., & Anupama, K. (2014). Honey Pollen: Using Melissopalynology to Understand Foraging Preferences of Bees in Tropical South India. *PLOS ONE*, 9(7), 101618-101629.
- Pyrzynska, K., & Biesaga, M. (2009). Analysis of phenolic acids and flavonoids in honey. *TrAC Trends in Analytical Chemistry*, 28(7), 893–902.
- Raduan, M. F., Mansor, W., Lee, K. Y., & Radzol, A. R. M. (2014a). Feature extraction of SERS spectrum of honey using Principal Component Analysis. *IEEE Conference on Biomedical Engineering and Sciences (IECBES) Conference Proceedings*, 12, 502–504.
- Raduan, M. F., Mansor, W., Lee, K. Y., & Radzol, A. R. M. (2014b). Analysis of honey using surface enhanced Raman spectroscopy. *IEEE Symposium on Industrial Electronics and Applications (ISIEA)*, 29 – 31.
- Rinnan, Å., Nørgaard, L., van den Berg, F., Thygesen, J., Bro, R., & Engelsen, S. B. (2009). Data pre-processing. *Infrared spectroscopy for food quality analysis and control*, 29-50.
- Rossmann, G. R. (2014). Optical Spectroscopy. *Reviews in Mineralogy and Geochemistry*, 78(1), 371–398.
- Rousseeuw, P. J. (1987). Silhouettes: a graphical aid to the interpretation and

- validation of cluster analysis. *Journal of computational and applied mathematics*, 20, 53-65.
- Ruoff, K., Karoui, R., Dufour, E., Luginbühl, W., Bosset, J. O., Bogdanov, S., & Amadò, R. (2005). Authentication of the botanical origin of honey by front-face fluorescence spectroscopy. A preliminary study. *Journal of Agricultural and Food Chemistry*, 53(5), 1343–1347.
- Sackey, S. S., Vowotor, M. K., Owusu, A., Mensah-Amoah, P., Tatchie, E. T., Sefa-Ntiri, B., Hood, C. O., & Atiemo, S. M. (2015). Spectroscopic Study of UV Transparency of Some Materials. *Environment and Pollution*, 4(4), 1-17.
- Salvador, L., Guijarro, M., Rubio, D., Aucatoma, B., Guillén, T., Jentzsch, P. V., Ciobotă, V., Stolker, L., Ulic, S., Vásquez, L., Garrido, P., Bravo, J., & Guerrero, L. R. (2019). Exploratory monitoring of the quality and authenticity of commercial honey in Ecuador. *Foods*, 8(3), 1–13.
- Sarle, W. S., Jain, A. K., & Dubes, R. C. (1990). Algorithms for Clustering Data. *Technometrics*, 32(2), 227 -239.
- Schulze, G., Jirasek, A., Yu, M. M. L., Lim, A., Turner, R. F. B., & Blades, M. W. (2005). Investigation of Selected Baseline Removal Techniques as Candidates for Automated Implementation. *Applied Spectroscopy*, 59(5), 545–574.
- Senior, J. M. (2009). *Optical fiber communications principles and practice* (3rd ed.). Harlow, England: Pearson Education Limited.
- Sigernes, F., Fortuna, J., Grøtte, M. E., Syrjäsuo, M., Storvold, R., & Johansen,

- T. A. (2018). Do it yourself hyperspectral imager for handheld to airborne operations. *Optics Express*, 26(5), 6021–6035.
- Sinaga, K. P., & Yang, M. S. (2020). Unsupervised K-means clustering algorithm. *IEEE access*, 8, 80716-80727.
- Smart, C., & Simpson, B. (2002). Detection of fluorescent compounds in the environment using granular activated charcoal detectors. *Environmental Geology*, 42(5), 538–545.
- Smith, E., & Dent, G. (2004). *Modern Raman Spectroscopy - A Practical Approach*. Hoboken, New Jersey, USA: John Wiley & Sons.
- Smyth, E., Syme, C. D., Blanch, E. W., Hecht, L., Vašák, M., & Barron, L. D. (2001). Solution structure of native proteins with irregular folds from Raman optical activity. *Biopolymers: Original Research on Biomolecules*, 58(2), 138-151.
- Soria, A. C., González, M., De Lorenzo, C., Martínez-Castro, I., & Sanz, J. (2004). Characterization of artisanal honeys from Madrid (Central Spain) on the basis of their melissopalynological, physicochemical and volatile composition data. *Food Chemistry*, 85(1), 121–130.
- Sowoidnich, K., & Kronfeldt, H.-D. (2012). Fluorescence Rejection by Shifted Excitation Raman Difference Spectroscopy at Multiple Wavelengths for the Investigation of Biological Samples. *ISRN Spectroscopy*, 2012, 1–11.
- Stefas, D., Gyftokostas, N., & Couris, S. (2020). Laser induced breakdown spectroscopy for elemental analysis and discrimination of honey samples. *Spectrochimica Acta Part B: Atomic Spectroscopy*, 172, 105969-105981.

- Stefas, D., Gyftokostas, N., Kourelis, P., Nanou, E., Tananaki, C., Kanelis, D., ... & Couris, S. (2022). Honey discrimination based on the bee feeding by Laser Induced Breakdown Spectroscopy. *Food Control*, *134*, 108770-108784.
- Stefas, D., Gyftokostas, N., Nanou, E., Kourelis, P., & Couris, S. (2021). Laser-induced breakdown spectroscopy: An efficient tool for food science and technology (from the analysis of martian rocks to the analysis of Olive Oil, Honey, Milk and other natural earth products). *Molecules*, *26*(16), 4981.
- Strelec, I., Brodar, L., Flanjak, I., Čačić Kenjerić, F., Kovač, T., Čačić Kenjerić, D., & Primorac, L. (2018). Characterization of Croatian Honeys by Right-Angle Fluorescence Spectroscopy and Chemometrics. *Food Analytical Methods*, *11*(3), 824-838.
- Stuart, B. H. (2004). *Infrared spectroscopy: fundamentals and applications*. Hoboken, New Jersey, USA: John Wiley & Sons.
- Šugar, J., & Bouř, P. (2016). Quantitative analysis of sugar composition in honey using 532-nm excitation Raman and Raman optical activity spectra. *Journal of Raman Spectroscopy*, *47*(11), 1298–1303.
- Svanberg, S. (2004). *Atomic and molecular spectroscopy: basic aspects and practical applications* (4th ed.). Berlin, Germany: Springer.
- Tahir, H. E., Mariod, A. A., Mahunu, G., & Xiaobo, Z. (2019). Chemical Composition, Nutritional Functions, and Antioxidant Activities of Honeys in Africa. *Journal of Apicultural Science*, *63*(2), 179-200.
- Tahir, H. E., Xiaobo, Z., Zhihua, L., Jiyong, S., Zhai, X., Wang, S., & Mariod, A. A. (2017). Rapid prediction of phenolic compounds and

- antioxidant activity of Sudanese honey using Raman and Fourier transform infrared (FT-IR) spectroscopy. *Food Chemistry*, 226, 202–211.
- Tatarkovič, M., Synytsya, A., Šťovíčková, L., Bunganič, B., Miškovičová, M., Petruželka, L., & Setnička, V. (2015). The minimizing of fluorescence background in Raman optical activity and Raman spectra of human blood plasma. *Analytical and bioanalytical chemistry*, 407, 1335-1342.
- TECA. (2022). Technologies and Practices for Small Agricultural Producers. Food Agriculture Organisation. Retrieved October 28, 2022, from <https://t-eca.apps.fao.org/teca/es/technologies/7329>.
- Tsankova, D., & Lekova, S. (2015). Botanical origin-based honey discrimination using vis-nir spectroscopy and statistical cluster analysis. *Journal of Chemical Technology and Metallurgy*, 50(5), 638-642.
- Ulloa, P. A., Guerra, R., Cavaco, A. M., da Costa, A. M. R., Figueira, A. C., & Brigas, A. F. (2013). Determination of the botanical origin of honey by sensor fusion of impedance e-tongue and optical spectroscopy. *Computers and Electronics in Agriculture*, 94, 1-11.
- Vekemans, B., Janssens, K., Vincze, L., Adams, F., & Van Espen, P. (1995). Comparison of several background compensation methods useful for evaluation of energy-dispersive X-ray fluorescence spectra. *Spectrochimica Acta Part B: Atomic Spectroscopy*, 50(2), 149-169.
- Vickers, T. J., Wambles, R. E., & Mann, C. K. (2001). Curve fitting and

- linearity: Data processing in Raman spectroscopy. *Applied Spectroscopy*, 55(4), 389-393.
- Vitha, M. F. (2018). *Spectroscopy: Principles and instrumentation*. Hoboken, New Jersey, USA: John Wiley & Sons.
- Vlaeva, I., Nikolova, K., Bodurov, I., Marudova, M., Tsankova, D., Lekova, S., ... & Yovcheva, T. (2017). Using differential scanning calorimetry, laser refractometry, electrical conductivity and spectrophotometry for discrimination of different types of Bulgarian honey. *Journal of Physics: Conference Series*. 794(1), 012034.
- Walach, J., Filzmoser, P., & Hron, K. (2018). Data normalisation and scaling: consequences for the analysis in omics sciences. In *Comprehensive Analytical Chemistry.*, 82, 165-196.
- Wei, D., Chen, S., & Liu, Q. (2015). Review of fluorescence suppression techniques in Raman spectroscopy. *Applied Spectroscopy Reviews*, 50(5), 387-406.
- Workman, D. (2020). Natural Honey Imports by Country [Webpage]. World's Top Exports. Retrieved July 25, 2021, from <https://www.world-stopexports.com/natural-honey-imports-by-country/>.
- Wu, S., Fooks, J. R., Messer, K. D., & Delaney, D. (2015). Consumer demand for local honey. *Applied Economics*, 47(41), 4377-4394.
- Ye, L., Shi, X., Wu, X., Zhang, M., Yu, Y., Li, D., & Kong, F. (2011). Dynamics of dissolved organic carbon after a cyanobacterial bloom in hypereutrophic Lake Taihu (China). *Limnologica*, 41(4), 382-388.
- Yeboah-Gyan, K., & Marfo, E. K. (1998). The colour and mineral composition of honeys produced in major vegetation areas of Ghana. *Journal*

of apicultural research, 37(2), 79-84.

Zhao, J., Bakeev, K. A., & Zhou, J. (2018). Raman spectroscopy peers through packaging. *Photonics Spectra*, 52(2), 44–49.

Zhao, J., Lui, H., McLean, D. I., & Zeng, H. (2007). Automated autofluorescence background subtraction algorithm for biomedical Raman spectroscopy. *Applied spectroscopy*, 61(11), 1225-1232.

Zhao, X., He, Y., & Bao, Y. (2011). Non-destructive identification of the botanical origin of Chinese honey using visible/short wave-near infrared spectroscopy. *Sensor Letters*, 9(3), 1055-1061.

Zhou, J., Huang, B., Yan, Z., & Bünzli, J. C. G. (2019). Emerging role of machine learning in light-matter interaction. *Light: Science & Applications 2019 8:1*, 8(1), 1–7.

APPENDICES

APPENDIX A

CHROMATOGRAM OF HMF STANDARD AND CALIBRATION REPORTS

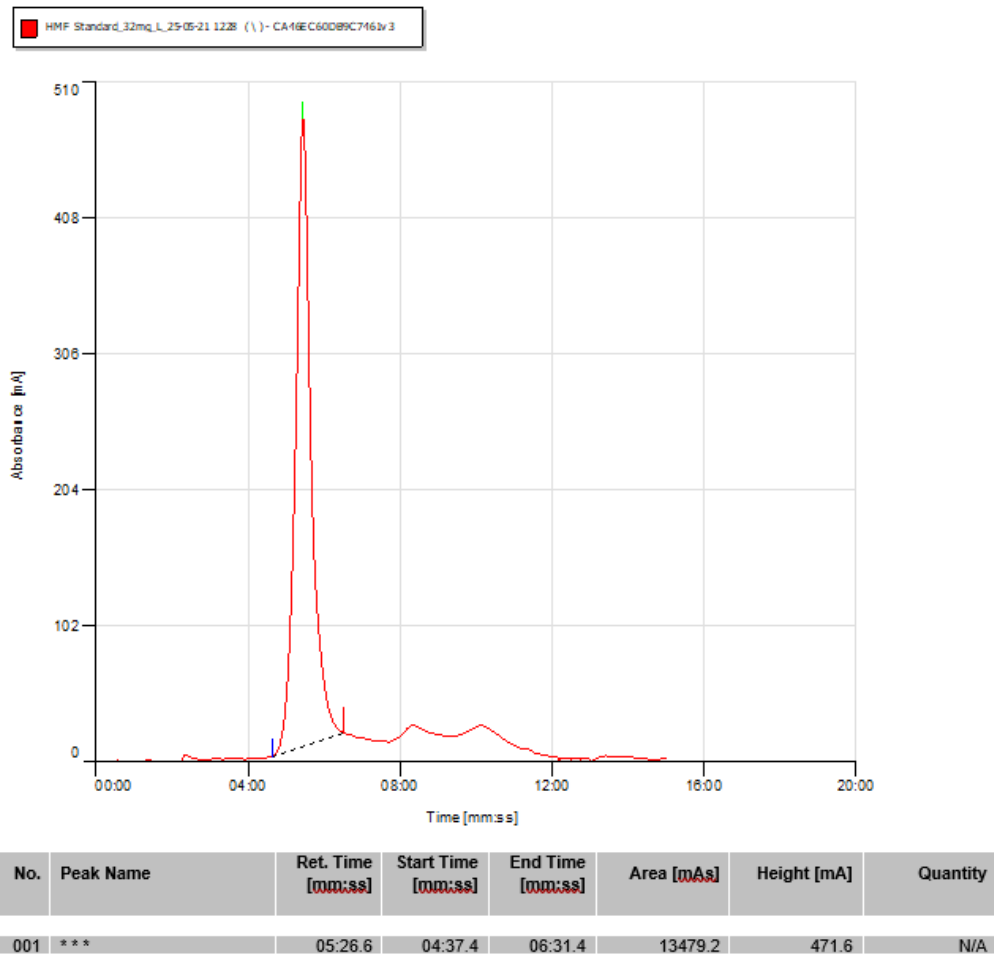


Figure 49: Chromatogram of HMF Standard

Component Calibration Report
HMF_SunFire_20210525 (\) - 32DFCDAAA67C425Ev3

Component:	HMF	Retention Time:	05:26.6	Window %:	19.830
Identify By:	Largest	Quantify By:	Area	Curve Type:	Linear
Force Origin:	Yes				

HMF_SunFire_20210525 (\) - 32DFCDAAA67C425Ev3
Component - HMF
Quantity [mg/L] = 0 + 2.37405 * Area [As]
r² = 1.000000

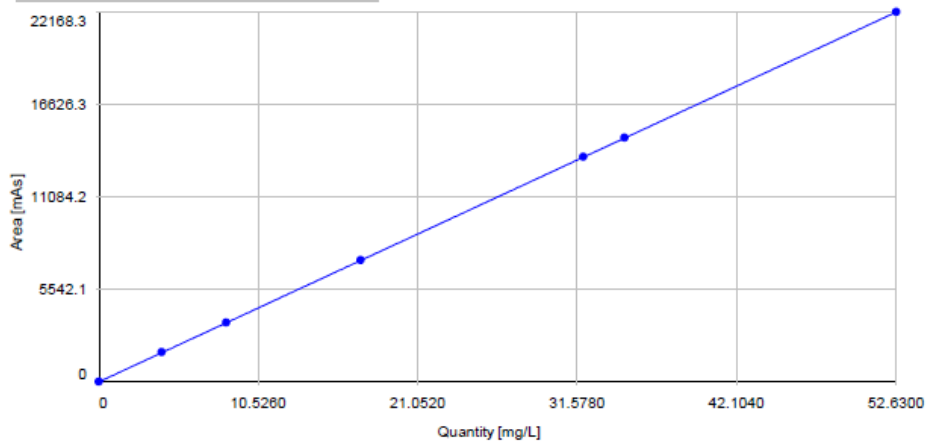


Figure 50: Calibration curve obtained for different concentrations HMF standard

APPENDIX B

HMF CHROMATOGRAM OF ALL SAMPLES

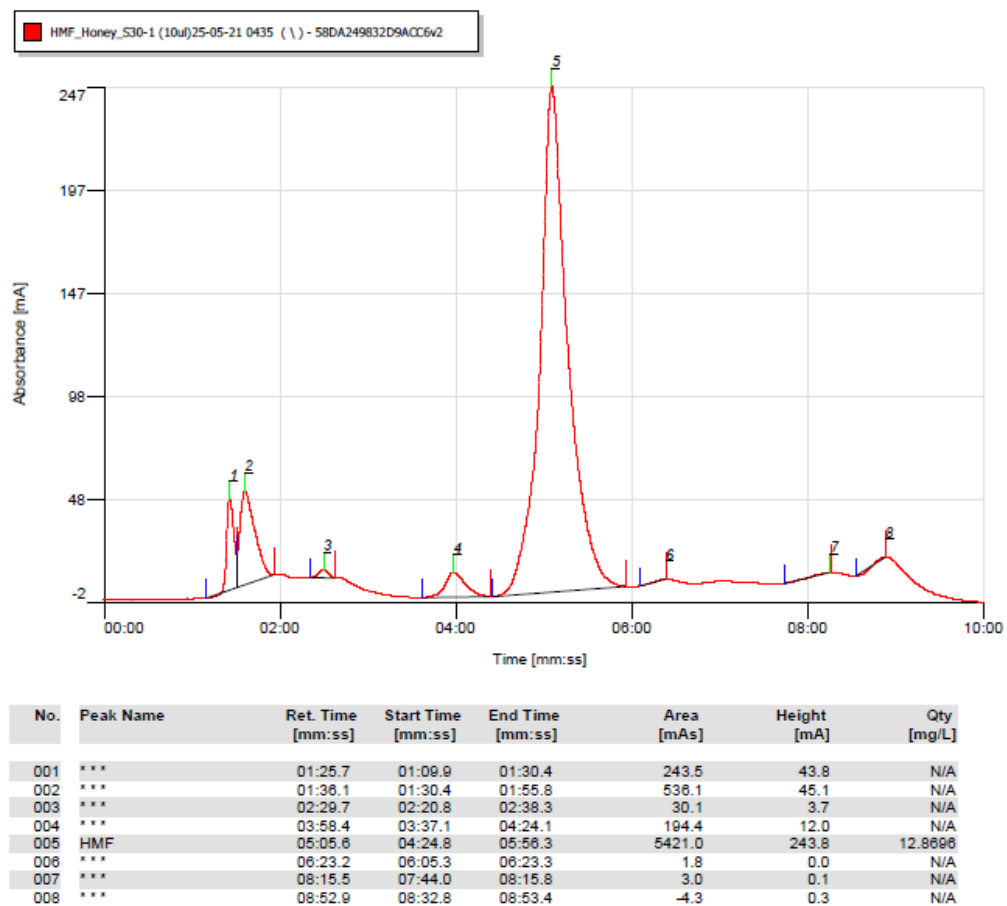


Figure 51: Chromatogram of honey sample S1 for HMF determination

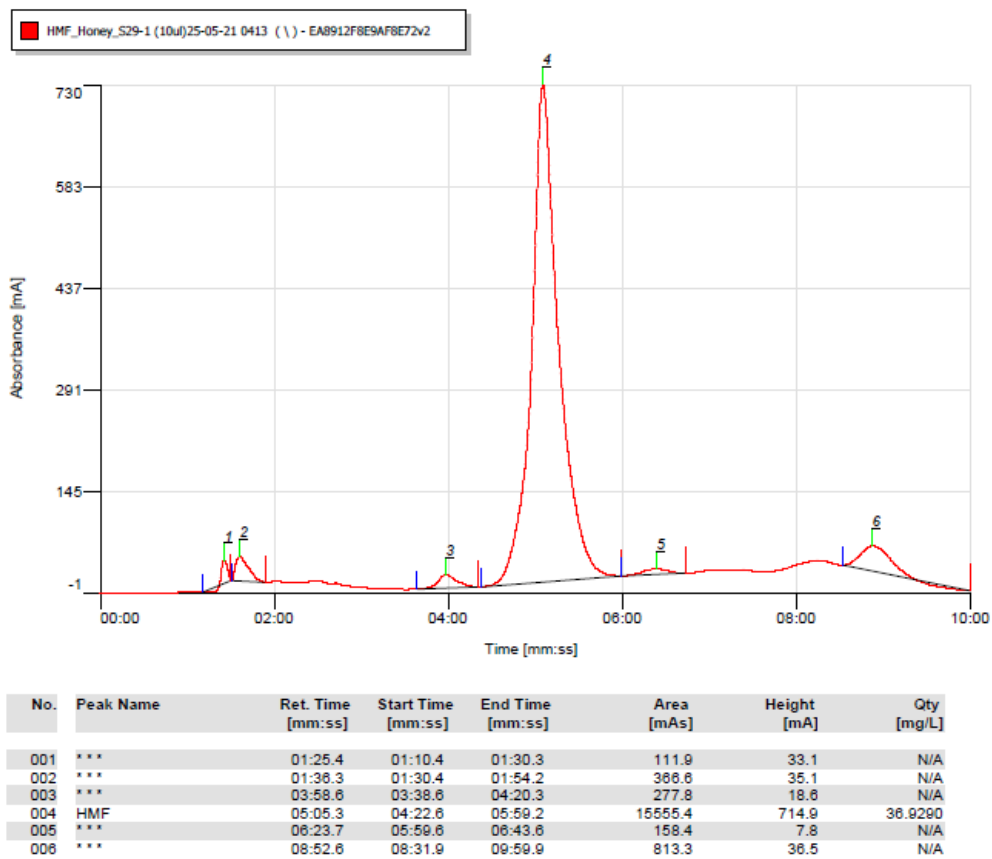


Figure 52: Chromatogram of honey sample S2 for HMF determination

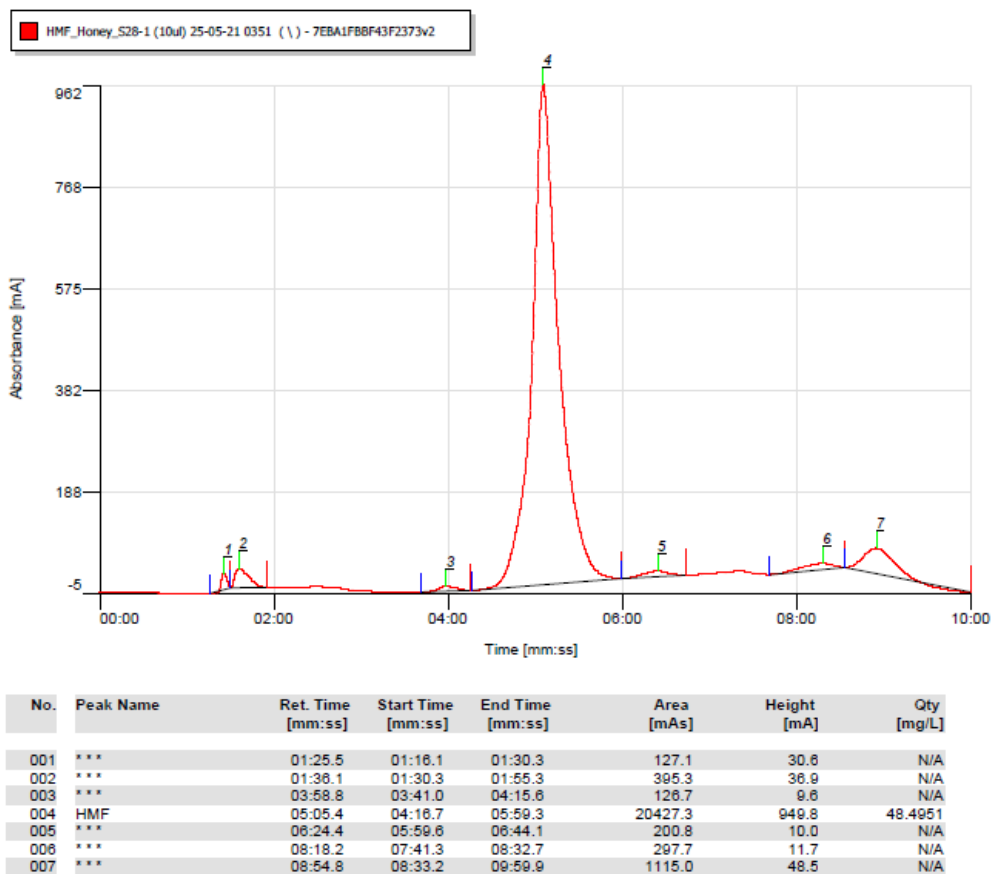


Figure 53: Chromatogram of honey sample S3 for HMF determination

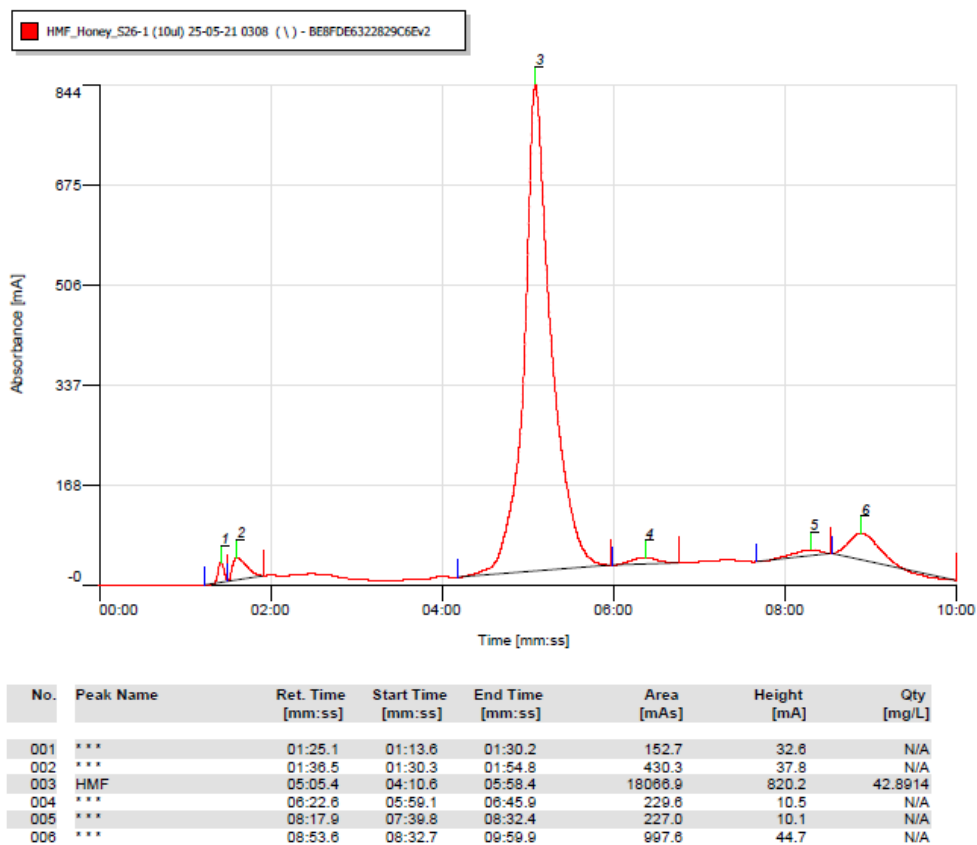


Figure 54: Chromatogram of honey sample S4 for HMF determination

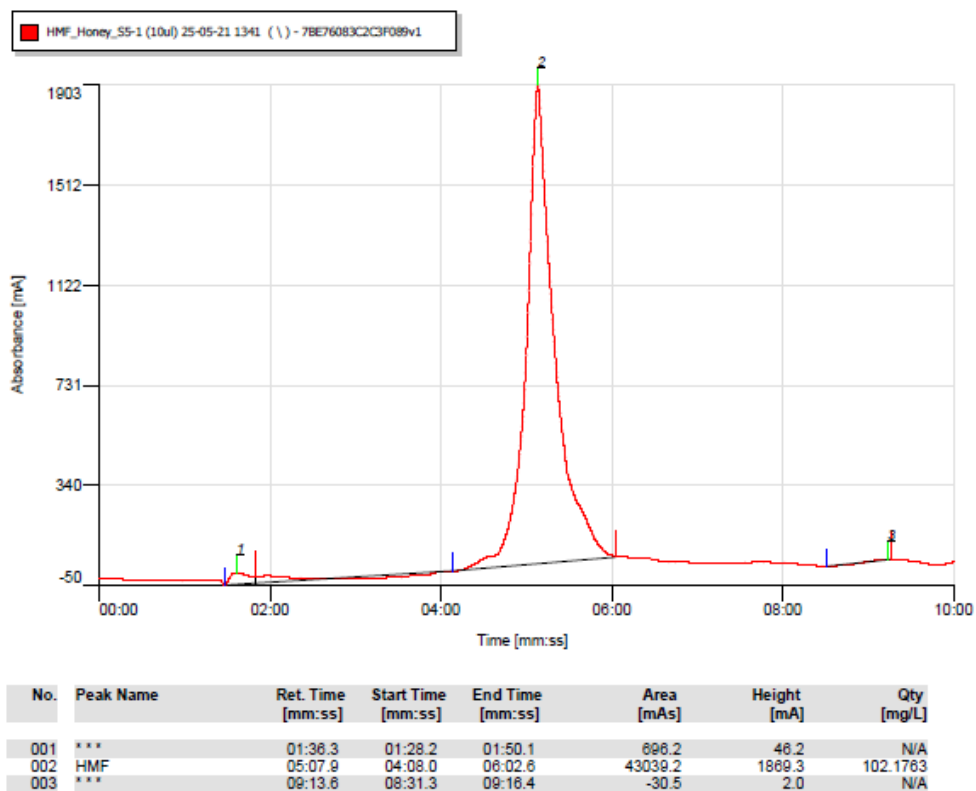


Figure 55: Chromatogram of honey sample S5 for HMF determination

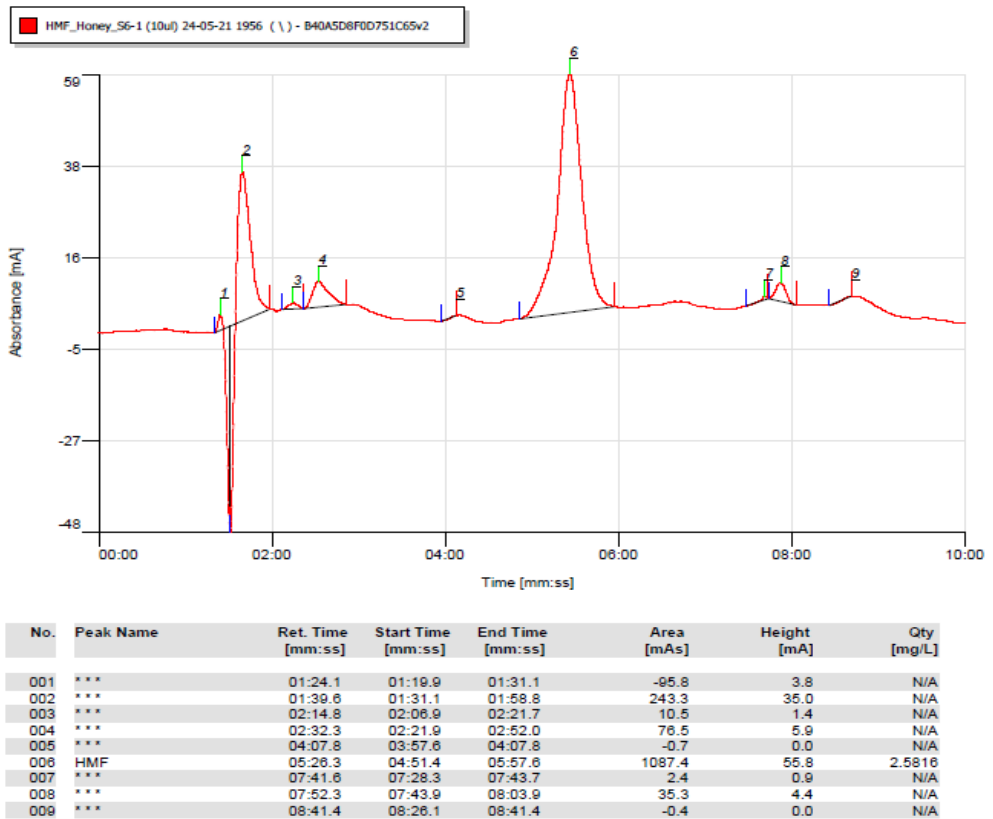


Figure 56: Chromatogram of honey sample S6 for HMF determination

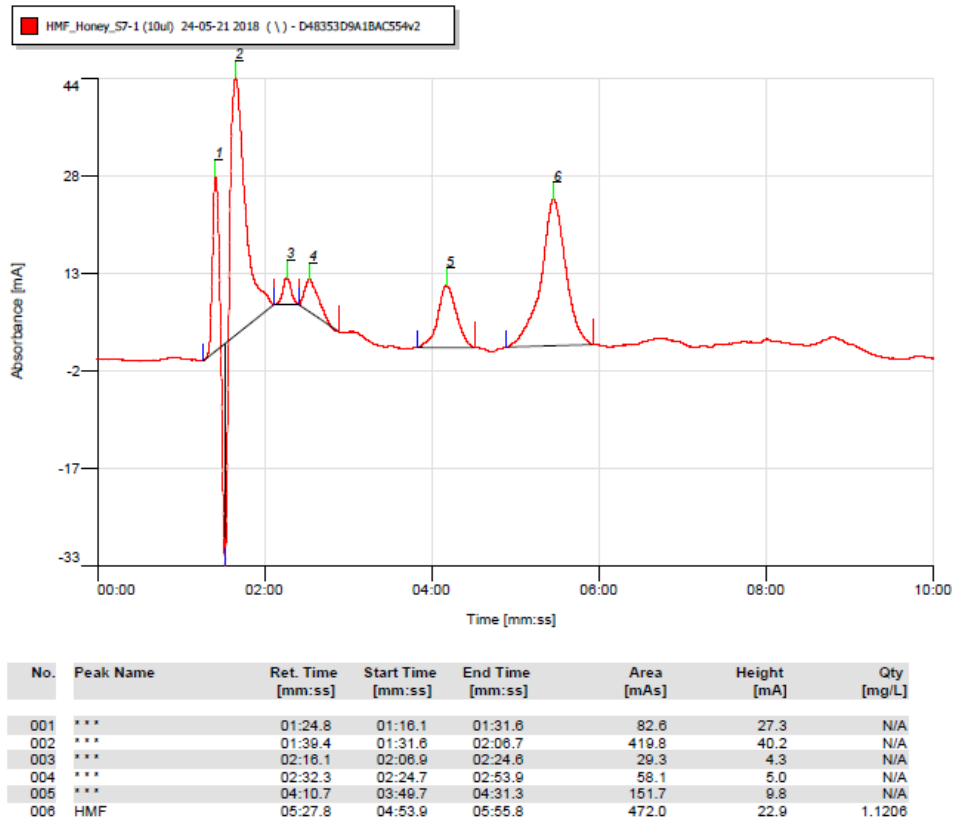


Figure 57: Chromatogram of honey sample S7 for HMF determination

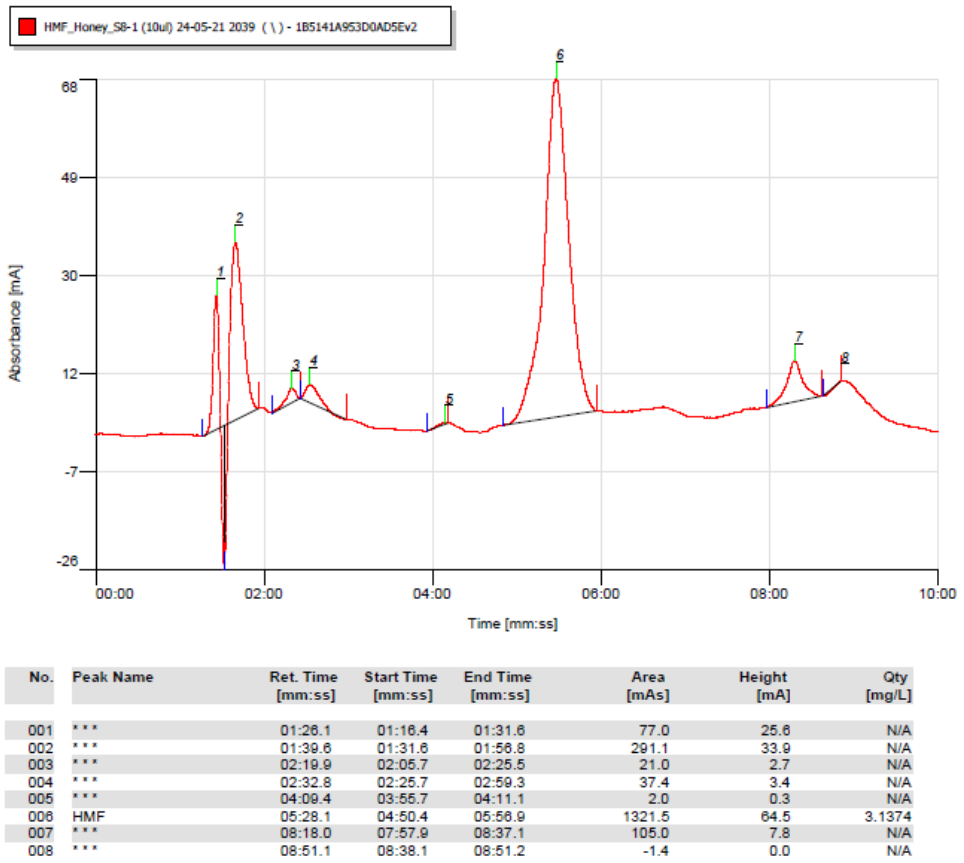


Figure 58: Chromatogram of honey sample S8 for HMF determination

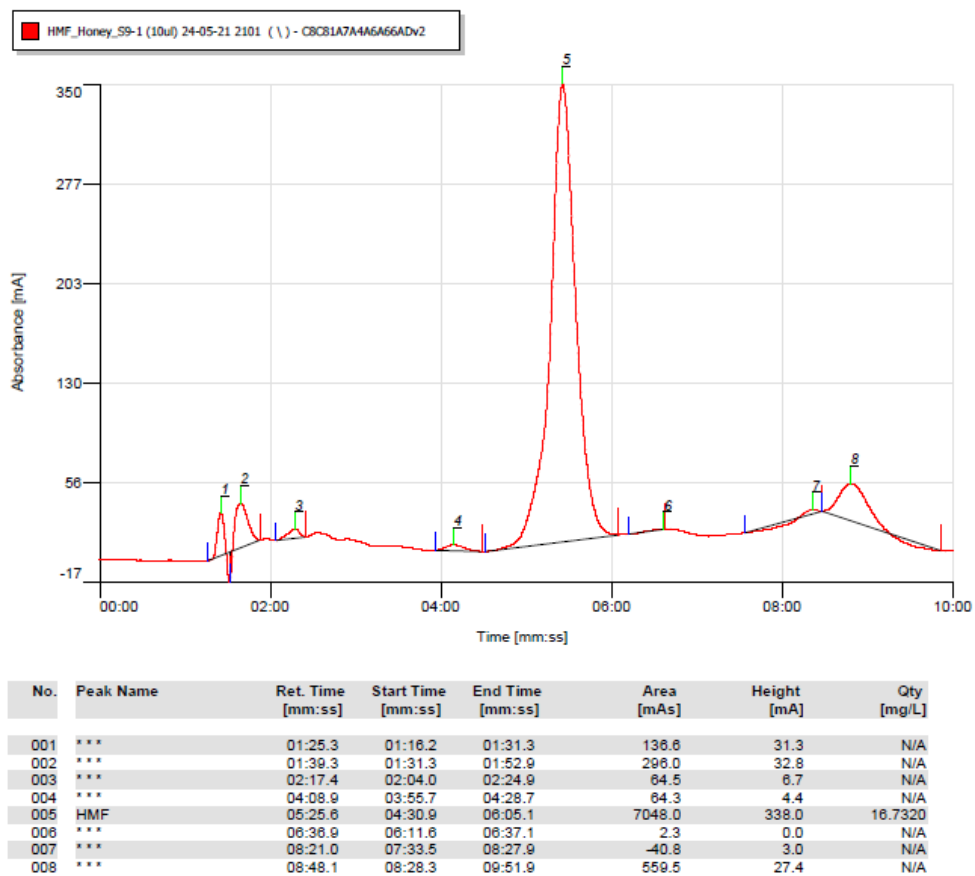


Figure 59: Chromatogram of honey sample S9 for HMF determination

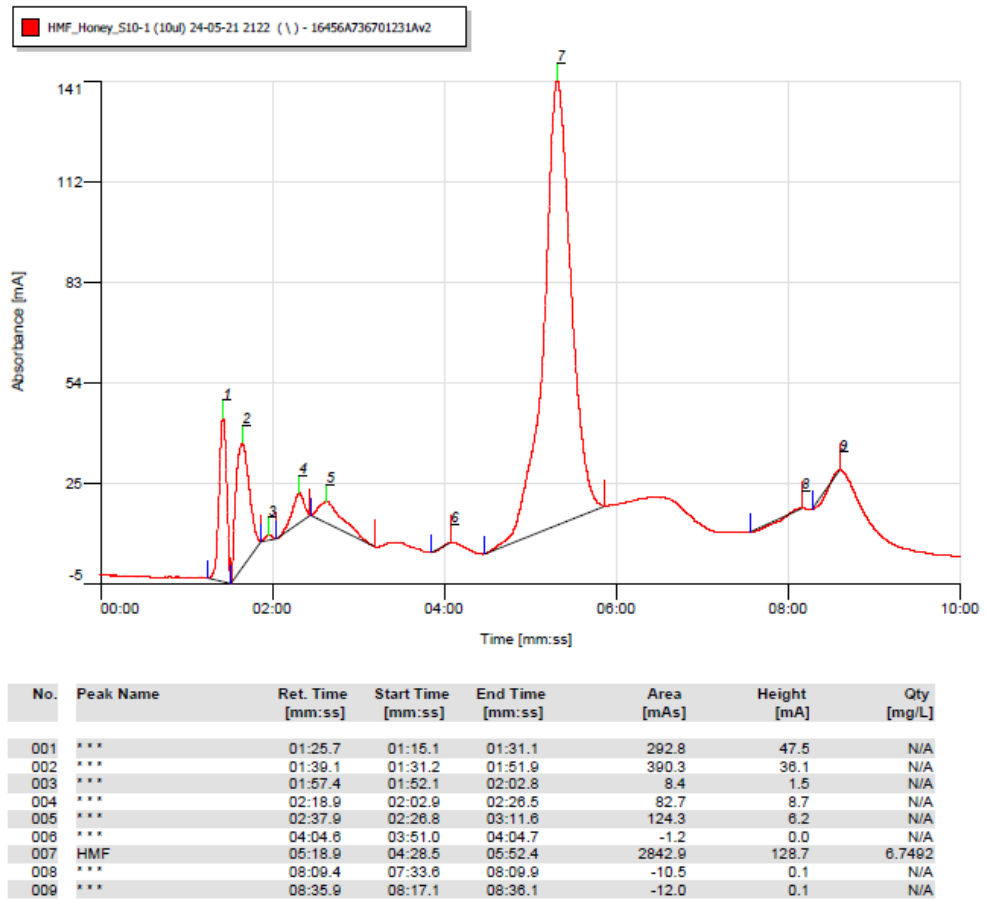


Figure 60: Chromatogram of honey sample S10 for HMF determination

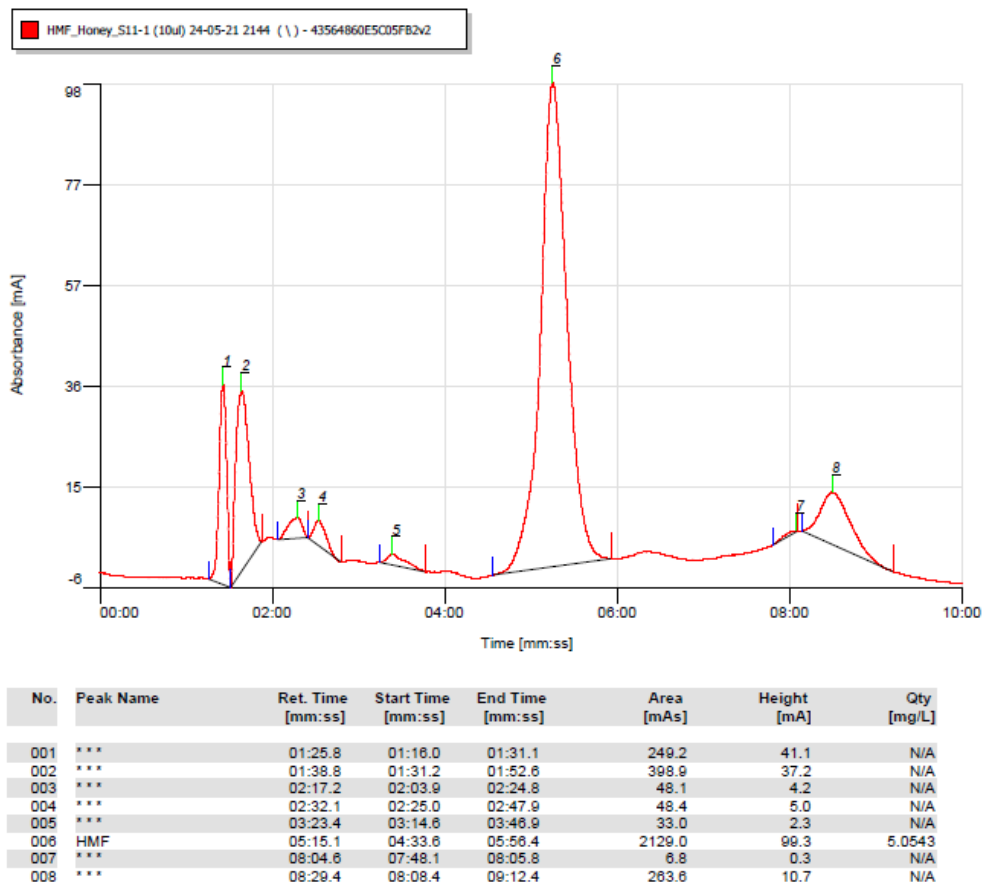


Figure 61: Chromatogram of honey sample S11 for HMF determination

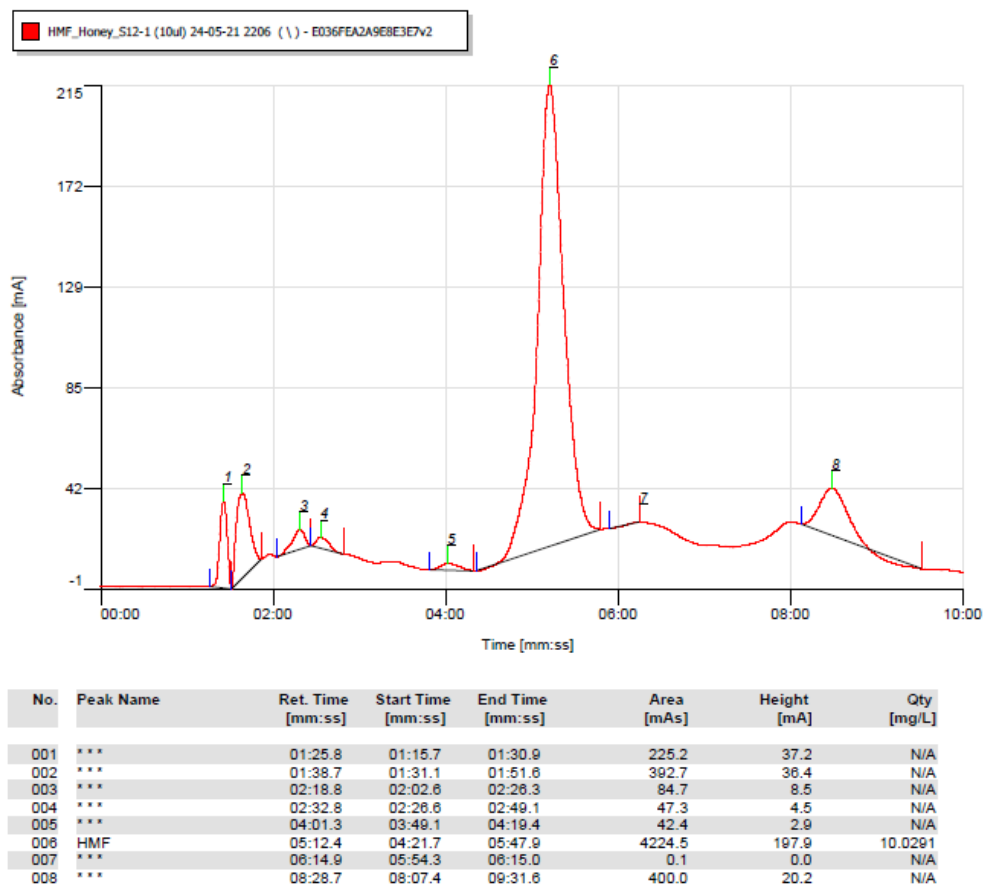


Figure 62: Chromatogram of honey sample S12 for HMF determination

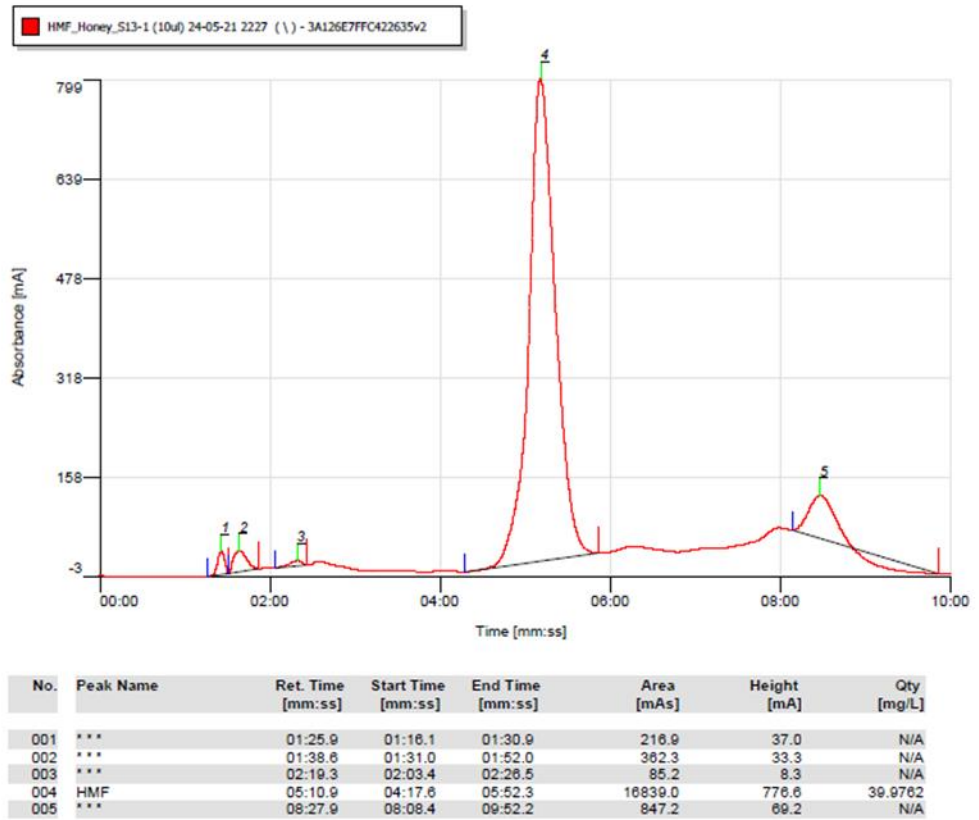


Figure 63: Chromatogram of honey sample S13 for HMF determination

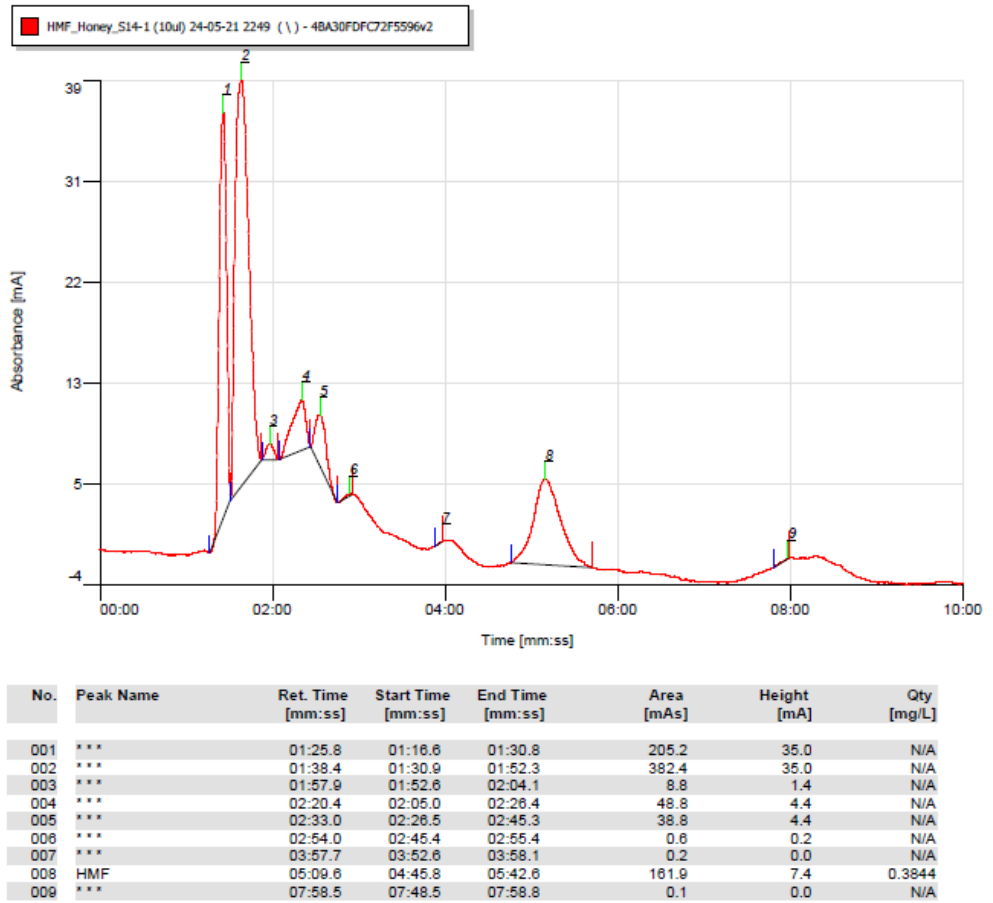


Figure 64: Chromatogram of honey sample S14 for HMF determination

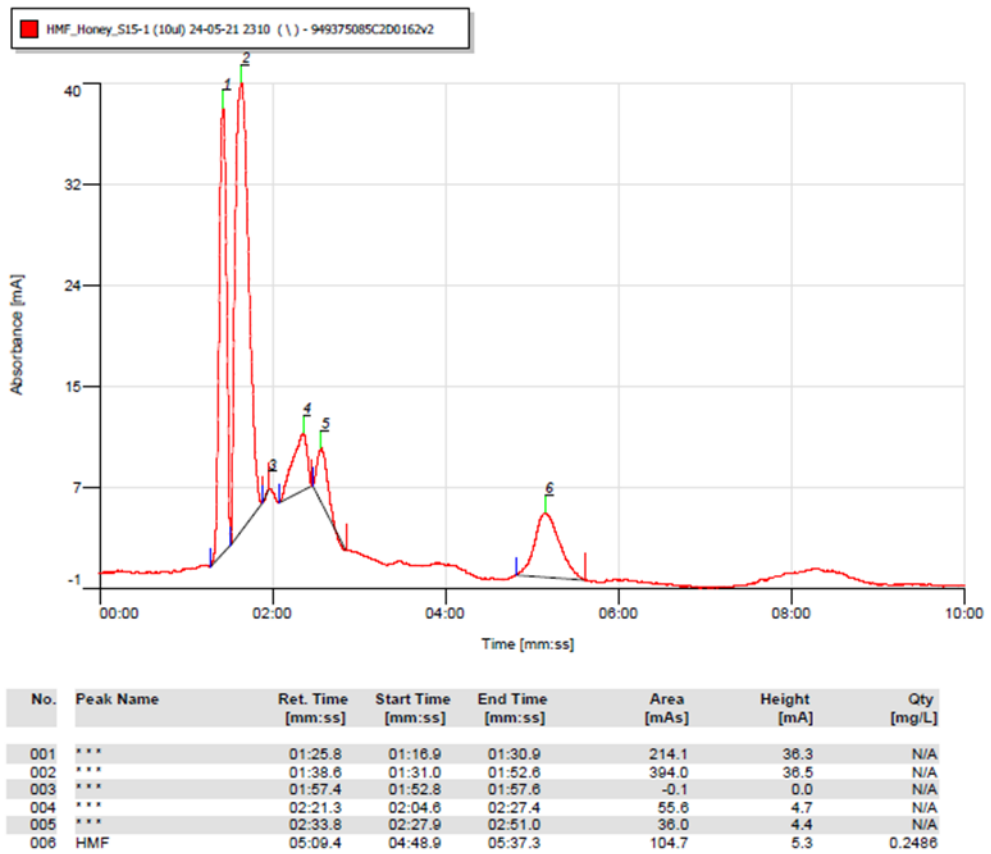


Figure 65: Chromatogram of honey sample S15 for HMF determination